Chapter 1- Cell proliferation and development

The development of a multicellular organism, from an embryo to an adult, requires the coordination of cellular growth, proliferation, and differentiation. The decision for a cell to undergo cell proliferation, that is replicate and segregate its genome into two daughter cells, should only occur in the correct developmental context. For example, cell division should only occur when a cell is the right size or when there is a signal that addditional cells are required to fulfill a differentiation program or to achieve correct organ size. Once there are enough cells it is just as important that cell proliferation should cease so differentiation can occur and overgrowth does not happen. Loss of these controls commonly result in developmental defects and tumourogenesis. Indeed, it is the study of development and cancer that has highlighted the interdependence of growth, proliferation, and differentiation regulation and how different extracellular and intracellular cues are integrated to provide specific cellular outcomes.

The control of cell proliferation occurs at many levels, although all controls must ultimately feed into the cell cycle. These controls regulate the transcription, abundance, and activity of numerous positive and negative regulators that result in either progression through or arrest of the cell cycle. Since the main outcome of the cell cycle is the irreversible segregation of the genome into daughter cells, proper regulation is critical. Consequently, cell cycle regulation is multi-tiered with many feedback loops that ensure correct progression. Our understanding of how the cell cycle is regulated has benefited greatly from the multitude of studies performed in many model systems. These studies underscore the conservation of key cell cycle regulators in all eukaryotes and highlight the need for differential and complex regulation in metazoans. Moreover,

while these studies do illustrate how much is known about cell cycle regulation, they also lay bare the holes in our understanding of how cell proliferation is coordinated with other developmental processes.

1.1 Regulation of the cell cycle in mammals

At its most basic level, the cell cycle is regulated by the actions of cyclin-dependent kinases (cdks) that are responsible for phosphorylating various substrates to bring about DNA replication (S-phase; cdk2) or mitosis (M-phase; cdk1; Figure 1.1). These cdks are themselves regulated by the binding of specific cyclins that oscillate in abundance throughout the cell cycle via carefully regulated protein synthesis and degradation. Cdks are also regulated by site specific inhibitory and activatory phosphorylation, dephosphorylation and by the binding of a number of small inhibitor proteins. Thus, both cyclins and their binding kinases are the foci of many regulatory pathways that ensure that the cell cycle only progresses when the appropriate conditions are met and events occur in the right order, i.e. mitosis follows DNA replication, and replication only occurs after a mitotic division.

1.1.1 Regulation of the G1 to S-phase transition

Entry into and progression through S-phase in mammals is controlled by cdk2 and the G1 cyclins, Cyclin E1, Cyclin E2, and Cyclin A (Figure 1.1; reviewed in Massague, 2004). The G1 to S-phase transition is also controlled by another G1 cyclin, Cyclin D, which binds cdk4 or cdk6 (Figure 1.1; reviewed in Coqueret, 2002). The expression of D type cyclins is dependent on extracellular events and they are thought to act as growth factor sensors (Sherr, 1996). Upon mitogenic stimulation, Cyclin Ds are transcriptionally upregulated and regulate the cdk4/6-mediated hyper-phosphorylation

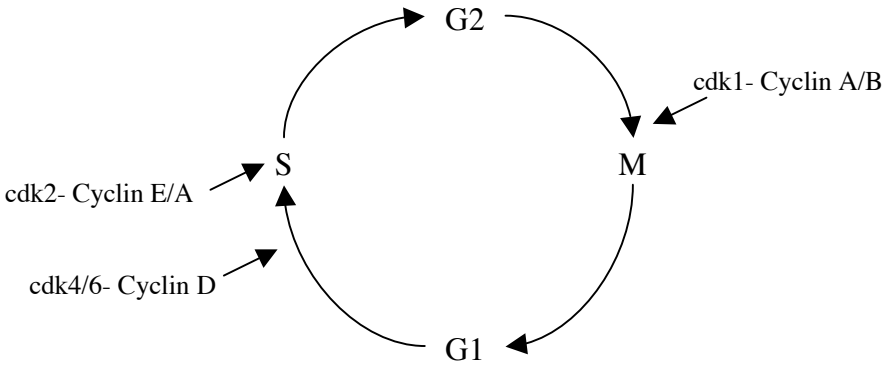

Figure 1.1 The mammalian cell cycle is controlled by cdk activity regulated by cyclin binding.

Entry into S-phase is regulated by the activity of cdk4/6 bound by Cyclin D and cdk2 bound by Cyclins A and E. Entry into M-phase is regulated by cdk1 activity bound by Cyclins A and B.

of Rb (the *retinoblastoma* gene product). Rb, and its closely related 'pocket' proteins, p107 and p130, inhibit the activity of the E2F family of transcription factors, thereby inhibiting S-phase entry (Figure 1.2). It appears that Rb is the only essential substrate for Cyclin D-cdk4/6 as cells lacking Rb do not require Cyclin D to proliferate (Lukas et al., 1994). Therefore, the only role Cyclin D plays in S-phase is to remove the inhibitory binding of Rb to E2F.

The G1-S phase regulator E2F is a heterodimer of the E2F and DP proteins. In mammals there are seven E2F genes (*E2F1-7*; de Bruin et al., 2003) and two DP genes (*DP1-2/3*; Harbour and Dean, 2000; Stevaux and Dyson, 2002; Stevens and la Thangue, 2003). In the cases of E2F1, E2F2 and E2F3, the binding of hypo-phosphorylated pocket proteins leads to their inactivation. E2F4 and E2F5 act solely as transcriptional repressors and only do so when bound by pocket proteins. E2F1-4 bind the pocket protein Rb, whereas E2F4 and E2F5 bind p107 or p130 (Harbour and Dean, 2000; Stevaux and Dyson, 2002; Stevens and la Thangue, 2003). E2F6 and E2F7 do not bind pocket proteins nor do they act as transcriptional activators. Instead they are thought to act as repressors of transcription by recruiting polycomb proteins (de Bruin et al., 2003). Thus pocket proteins can effect passive repression of E2F complexes by interfering with the ability of E2Fs to recruit transcriptional machinery. Alternatively they can actively repress E2F target genes by recruiting chromatin modifiers including histone deacetylases, SWI/SNF factors, polycomb group proteins, or methyltransferases (Harbour and Dean, 2000; Stevaux and Dyson, 2002). Since Rb plays a crucial role in repressing S-phase entry it is no surprise to find that it is commonly mutated in sporadic tumours (Sherr, 2004).

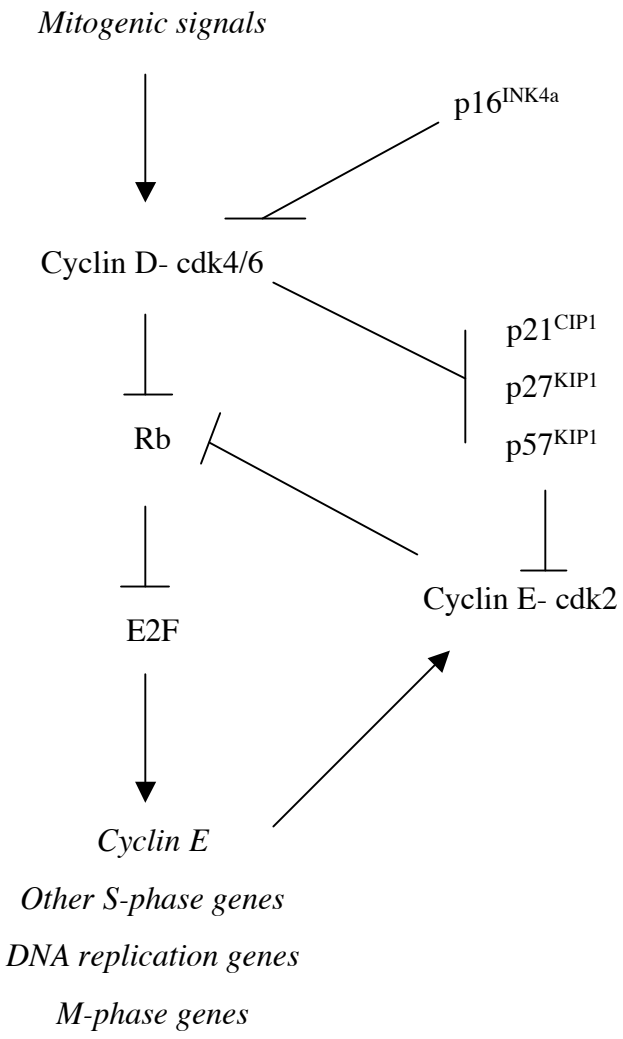

Figure 1.2 Regulation of S-phase entry in mammalian cells

Upon mitogenic signalling Cyclin D expression is upregulated. Its binding of cdk4/6 activates the cdk activity towards Rb, resulting in loss of inhibition of the transcription factor E2F. E2F is then able to transcribe many genes including *Cyclin E*. Cyclin E binds to cdk2, which further phosphorylates Rb, thus creating a positive feedback loop. Negative regulators of S-phase entry include the cdk inhibitors, $p21^{CIP1}$, $p27^{KIP1}$, and $p57^{KIP1}$ that inhibit Cyclin E-cdk2 and $p16^{INK4a}$ that inhibits cdk4/6. Cyclin D-cdk4/6 sequesters the CIP/KIP inhibitors thus relieving Cyclin E-cdk2 inhibition.

For a cell to enter S-phase the repression mediated by Rb needs to be overcome. This is achieved by the hyper-phosphorylation of Rb by Cyclin D-cdk4/6 (Figure 1.2). This results in Rb losing affinity for E2F1-3, which are then able to act as transactivators of many genes, including those needed for the initiation of S-phase, DNA replication, and mitosis (Ishida et al., 2001; Ren et al., 2002). *Cyclin E* is one of the transcriptional targets of E2F, therefore in response to Rb hyper-phosphorylation, Cyclin E protein increases in abundance at the G1-S transition. cdk2 is activated by the binding of Cyclin E and is able to phosphorylate its substrates, which include Rb. A positive feedback loop is thus established where Cyclin E-cdk2 hyper-phosphorylates Rb, causing it to release E2F, which results in increased transcription of *Cyclin E* and other E2F targets (Figure 1.2). This feedback mechanism provides the necessary amplification of signal to ensure that the cell enters a timely S-phase.

The importance of E2F and Cyclin E in inducing S-phase entry, and Rb in preventing it, is underscored by the finding that the overexpression of these proteins affects the ability of cells to enter S-phase. Overexpression of E2F or Cyclin E induces quiescent cells to enter S-phase (Johnson et al., 1993; Ohtsubo and Roberts, 1993; Resnitzky et al., 1994), thus demonstrating that these proteins are limiting for S-phase entry. In the case of E2F, its DNA binding domain is necessary, which indicates that it is the transcription of its target genes that induces S-phase (Johnson et al., 1993; Shan and Lee, 1994). Overexpression of Rb in mice results in a dwarf phenotype with primary fibroblasts showing an increased resistance to IGF-1 mediated cell proliferation (Nikitin et al., 2001). The expression of a dominant negative form of DP1 in cells also resulted in the prevention of S-phase entry (Wu et al., 1996). These findings illustrate that it is the

abundance of E2F or Cyclin E that can tip the balance in favour of cell cycle entry and therefore establishes their roles as key regulators of S-phase entry.

The overexpression data demonstrate that E2F and Cyclin E are rate limiting proteins for S-phase entry, but they do not show whether these proteins are necessary for S-phase entry. This point has been addressed by the study of knockout mice. Rb deficient mice die between days 13.5-14.5 of embryonic development (Clarke et al., 1992; Jacks et al., 1992; Lee et al., 1992) and show ectopic cell cycle entry in the CNS and the eye lens, a defect that can be suppressed by concomitant deficiency in E2F1 (Tsai et al., 1998). Consistent with expectations, mammalian E2F proteins are essential for normal proliferation and show some redundancy of function. Mice individually deficient in *E2F1*, *E2F2,* or *E2F3* are viable, but cells lacking all three proteins are not able to proliferate (Wu et al., 2001). However, each protein contributes unique functions that cannot be provided for by the others. For example, it is well established that E2F1 can induce apoptosis as well as cell proliferation and it appears to be the only E2F to do this (Bell and Ryan, 2004; La Thangue, 2003). Therefore, Rb is crucial to counteract S-phase entry induced by E2F while E2F1-3 provide necessary functions in S-phase entry.

In contrast to the E2F knockout phenotypes, mouse knockout of both Cyclin E1 and Cyclin E2 results in embryonic lethality. The primary reason this is thought to occur is because placental cells are unable to undergo endoreplication. Indeed, both Cyclin E proteins are only required for endoreplication and cell cycle entry after G0 arrest and not for normal cell cycling (Geng et al., 2003). This result is supported by the finding that knockout of cdk2 also results in viable mice and $cdk2^{-/-}$ cells are capable of normal

cell proliferation (Ortgea et al., 2003). These results show that despite Cyclin E's proposed central role in S-phase, neither Cyclin E nor cdk2 are necessary for proliferation. Therefore, there must be another protein complex that can provide the necessary function. It has been suggested that Cyclin A-cdk1 may provide this necessary function and, in support of this, Cyclin A has been found to be essential for mammalian development (Murphy et al., 1997).

In addition to Rb, a family of small cdk inhibitor proteins also act as negative regulators of S-phase. Cyclin D-cdk4/6 complexes have been shown to effect the activation of Cyclin E-cdk2 by sequestering the cdk inhibitors $p21^{WAF1/CIP1}$, $p27^{KIP1}$, and $p57^{KIP1}$, which bind to both the G1 cyclin and cdk subunits (Figure 1.2; Stevens and la Thangue, 2003). As G1 progresses, the increase in Cyclin D-cdk4/6 levels competes with Cyclin E-cdk2 for these inhibitors, titrating them away from Cyclin E-cdk2 and exposing cdk2 so it can become activated. These inhibitor proteins are also regulated by the suppression of their transcription, translation, stability, or cellular localisation upon mitogenic activation (Massague, 2004). The INK4 family of cdk inhibitors are specific for cdk4 and 6 (Figure 1.2), one of which, $p16^{INK4A}$, is a known tumour suppressor and is inactivated in cases of familial melanoma and other tumour types (Sherr, 2004). Similarly, various malignancies show haploinsufficiency for $p27^{KIP1}$ and decreased protein levels in tumours indicates a poor prognosis (Blain et al., 2003). Consistent with its role in solely regulating Cyclin D, the expression of $p16^{INK4A}$ was found to suppress glioblastoma growth *in situ* in an Rb-dependent manner (Hung et al., 2000).

1.1.2 Regulation of DNA synthesis

Once free from Rb inhibition, E2F induces the expression of genes required for DNA replication, including DNA polymerase, PCNA, Orc1, and nucleoside triphosphate synthesis genes (Ishida et al., 2001; Muller et al., 2001; Polager et al., 2002; Ren et al., 2002; Young et al., 2003). Consequently, it is clear that E2F activity is required for the initiation of S-phase. However, for DNA synthesis to occur, cdk2-Cyclin E/A activity is also required. The pre-replication complex of ORC, Cdc6/18, Cdt1, and the recruited MCM, can only recruit DNA helicases, primases and polymerases once cdk2 is activated (Kelly and Brown, 2000). A number of the pre-replication proteins become further phosphorylated by cdk2-containing complexes during DNA synthesis. This prevents re-replication from occurring by preventing the reloading of these proteins onto replication origin sites (Findeisen et al., 1999; Hua et al., 1997; Jiang et al., 1999; Petersen et al., 1999). Therefore cdk2-containing complexes are required for both the initiation of DNA synthesis and the exit from S-phase.

Cyclin A plays a crucial role in S-phase progression and completion. Not only is it involved in the regulation of DNA replication factors, but it is also required to switch off E2F mediated transcription. It achieves this by binding the transcription factor through the E2F subunit and phosphorylating the DP subunit, rendering it unable to bind DNA. In the absence of this Cyclin A-cdk2 activity, cells become arrested in S-phase and eventually apoptose (Krek et al., 1995).

1.1.3 Regulation of the G2 to M-phase transition

In mammals, the two M-phase master regulators, Cyclin A and Cyclin B, orchestrate the regulation of M-phase entry. The transcription of both cyclins A and B is activated

in part by E2F, though the abundance of Cyclin A protein occurs earlier than the abundance of Cyclin B protein (reviewed in Fung and Poon, 2005; Stevaux and Dyson, 2002). Cyclin A is also degraded earlier than Cyclin B. Cyclin A degradation occurs during the prometaphase to metaphase interval, whereas Cyclin B degradation occurs at the metaphase to anaphase transition. Both Cyclin A and B are degraded by APC/C mediated ubiquitination and subsequent recognition by the proteosome with substrate specificity of the APC/C regulated through the binding of the Cdh1 and Cdc20 subunits (see below).

While both Cyclin A and Cyclin B are required for M-phase entry it is the action of Cyclin B-cdk1 that results in the morphological changes seen in cells when they enter M-phase and, as such, this complex was first known as the mitosis-promoting factor (MPF). Prior to M-phase, the MPF is held inactive through inhibitory phosphorylation by the Wee1 and Myt1 kinases on Thr 14 and Tyr 15 of cdk1 (Figure 1.3). Upon entry into M-phase these inhibitory phosphates are removed by the activity of the phosphatases Cdc25B and Cdc25C (Figure 1.3; Karlsson et al., 1999). Since the entry into M-phase results in the irreversible segregation of the genome, the activity of the Wee1 and Myt1 kinases and the Cdc25 phosphatases are tightly regulated.

Cdc25B is regulated in part by its subcellular localisation (Figure 1.3). The binding of a 14-3-3 dimer to different binding sites on Cdc25B either hides or exposes the nuclear localisation signal (NLS) or nuclear export signal (NES) of Cdc25B. Therefore, the nuclear or cytoplasmic localisation of Cdc25B is dependent upon which phosphorylated

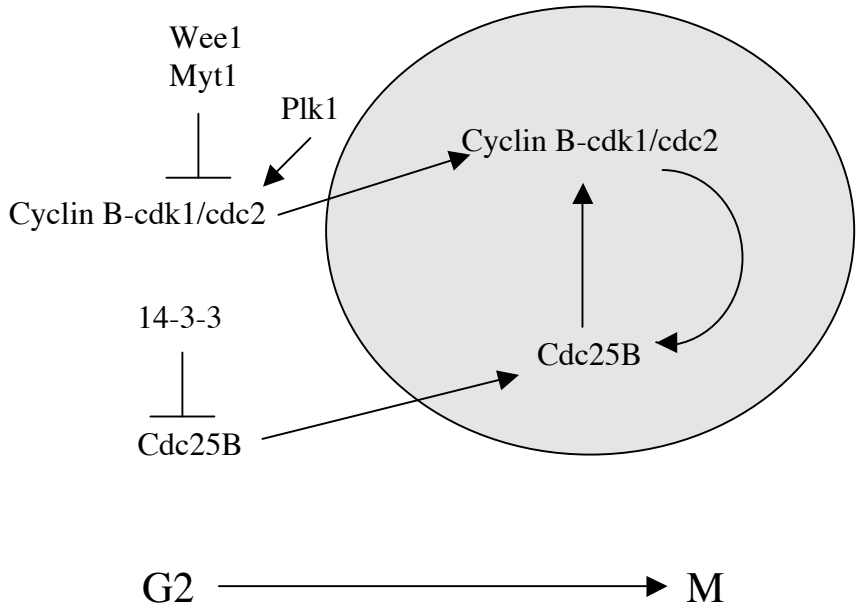

Figure 1.3 Regulation of M-phase entry

During G2 Cyclin B- cdk1 is held inactive by inhibitory phosphorylation by Wee1 and Myt1 and localisation in the cytoplasm. Cdc25 is held inactive by cytoplasmic localisation caused by 14-3-3 binding. At the M–phase transition both Cyclin B-cdk1 and Cdc25 localise to the nucleus (grey circle) due to phosphorylation of Cyclin B by Plk1 and of Cdc25 by cdk2, respectively. In the nucleus Cdc25 can remove the inhibitory phosphates on cdk1, thereby activating it.

sites the 14-3-3 dimer is bound. The bound 14-3-3 dimer also forms an intramolecular bridge, which serves to block the active site of Cdc25B (Giles et al., 2003). In order to activate Cdc25, 14-3-3 binding is removed through the action of cdk2, which allows protein phosphatase to access and dephosphorylate the inhibitory sites (Margolis et al., 2003). Once the inhibitory phosphates on Cdc25 are removed, Cdc25 is able to activate cdk1 by removing the inhibitory phosphates on Thr 14 and Tyr 15. Cyclin B-cdk1 is then able to further activate Cdc25 and thus set up a positive feedback loop to ensure efficient Cyclin B-cdk1 activation.

Nuclear localisation plays a further role in regulating M-phase entry by preventing Cyclin B from accumulating in the nucleus during interphase. Cyclin B can shuttle between the nucleus and the cytoplasm at all stages of the cell cycle. However, in interphase nuclear export is greatly favoured over import, resulting in a net cytoplasmic localisation (Figure 1.3; Hagting et al., 1998). The phosphorylation of Cyclin B by Polo like kinase 1 (Plk1) in prophase prevents this nuclear export and therefore Cyclin B accumulates in the nucleus and mitotic entry can occur (Toyoshima-Morimoto et al., 2001).

One of the key roles of Cyclin A-cdk2/cdk1 is to prevent the degradation of Cyclin B prior to anaphase. It achieves this by phosphorylating Cdh1, which is one of the activating subunits of APC/C. This phosphorylation prevents Cdh1 from associating with the APC/C (Lukas et al., 1999). In its place, another APC/C activating subunit, Cdc20, is able to bind (Figure 1.4 A). However, the APC/C^{CDC20} can only become active after several subunits are phosphorylated by both Cyclin B-cdk1 and Polo-like

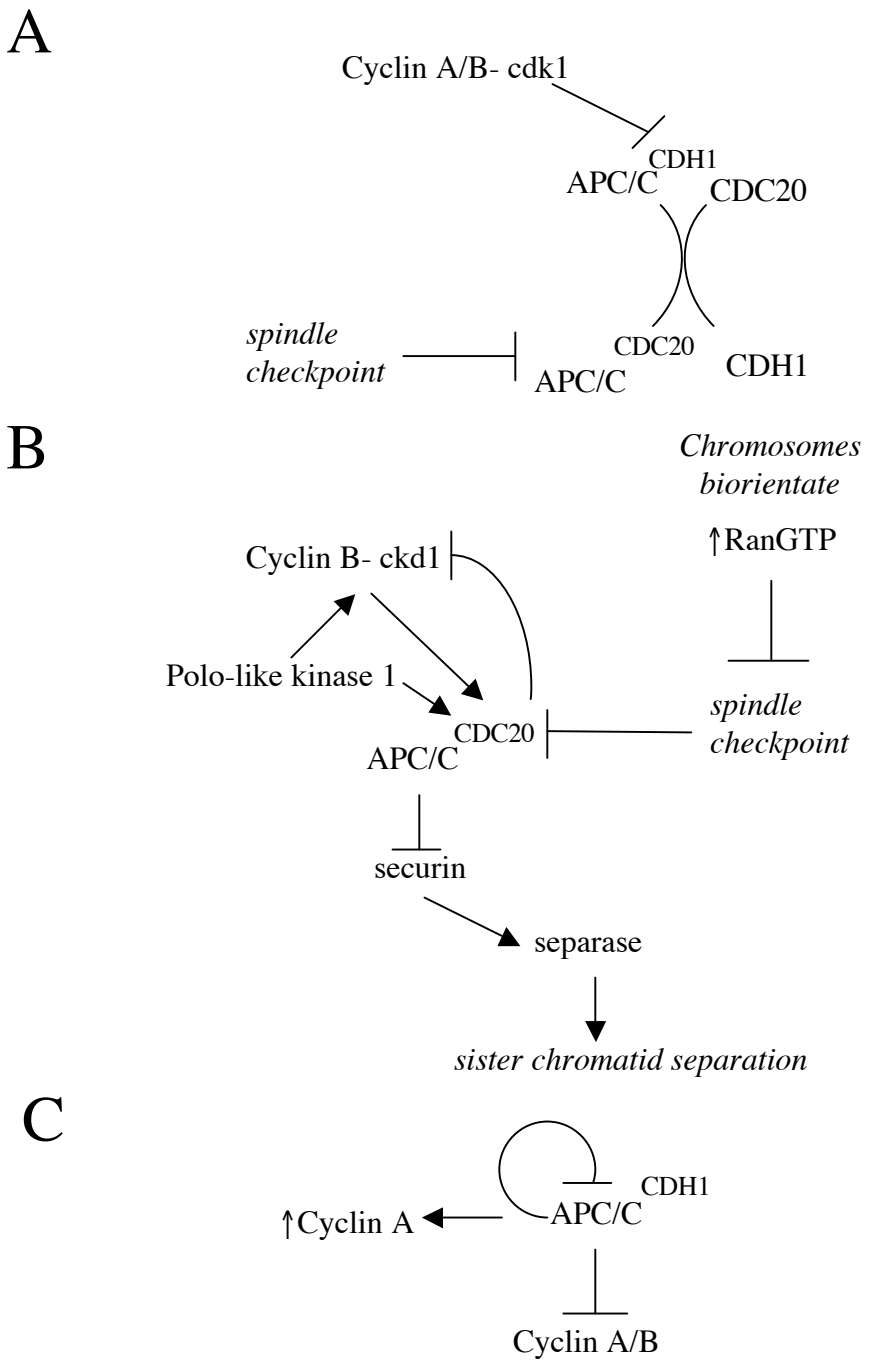

Figure 1.4 Regulation of APC/C activation

(**A**) During metaphase the APC/C is held inactive by inhibitory phosphorylation of the CDH1 subunit by cyclin A/B-cdk1, which causes it to no longer bind APC/C. This allows CDC20 to bind the APC/C instead. Activation of CDC20 is inhibited by the spindle checkpoint. (**B**) At the metaphase to anaphase transition, inhibition of CDC20 by the spindle checkpoint is lost due to proper biorientation of the chromosomes on the spindle and possible increase in RanGTP levels. CDC20 is also activated by Cyclin B-cdk1 and Polo-like kinase 1. (**C**) In telophase and G1 the activated APC/C degrades Cyclins A and B. Once these substrates run out the APC/C degrades its own UBCH10 subunit, inactivating itself. This then allows Cyclin A levels to rise again leading into the next S-phase.

kinase (Figure 1.4 B; Golan et al., 2002; Kramer et al., 2000). Cyclin B-cdk1 also phosphorylates Cdh1, thus keeping it inactivate until mitosis is completed. Therefore, Cyclin B remains stable until Cdc20 is activated at the metaphase to anaphase transition (Figure 1.4 A and B), after which it is rapidly degraded.

The activation of APC/C^{CDC20} by MPF not only results in the degradation of the MPF itself through Cyclin B degradation, but is also required for the onset of anaphase and the exit of mitosis. This is achieved by the ubiquitination and proteolysis of securin, an inhibitor of a protein called separase that, once activated, cleaves cohesion (a protein complex that holds sister chromatids together after DNA replication until anaphase) therefore allowing sister chromatids to separate (Figure 1.4 B; Uhlmann, 2003). Once Cyclin B is degraded, the inhibition of Cdh1 is lost and Cdh1 is able to rebind APC/C (Figure 1.4 C). APC/C^{CDH1} degrades Cdc20 and is able to remain active throughout G1. cdk activity is low under these condition, which allows the reloading of pre-replication complexes onto DNA in preparation for the next S-phase (see above). APC/C^{CDH1} activity is downregulated at G1-S by autoubiquitination of its UBCH10 subunit after other G1 substrates have been degraded, thus allowing the accumulation of Cyclin A in the next S-phase (Figure 1.4 C; Rape and Kirschner, 2004).

While Cyclin A/B-cdk1 are the master regulators of M-phase entry and exit, at least two other kinases are required for regulation of the mitotic machinery, polo-like kinase 1 (Plk1) and aurora kinase. These kinases play key roles during prophase, metaphase, anaphase and cytokinesis. Plk1 phosphorylates and activates both Cyclin B-cdk1 and the APC/C complex. Like Cyclin B, Plk1's phosphorylation and activation of APC/C has been shown to lead to Plk1's subsequent ubiquitination and phosphorylation at the

end of mitosis in yeast (Charles et al., 1998). It appears that Plk1 binds proteins through its polo-box domain that recognises phospho-serines and threonines generated by cdks or mitogen activated protein kinases (MAPK, see below; Lowery et al., 2004). Indeed, the phosphorylation of Cyclin B by Plk1 is enhanced by prior phosphorylation by MAPK (Yuan et al., 2002).

During the cell cycle, Plk1 localises to centrosomes and spindle poles during interphase, prophase, and metaphase and then to the spindle midbody in anaphase and teleophase (Golsteyn et al., 1995). Likewise, Cyclin B is partially localised to the spindle and condensed chromosomes during metaphase (Pines and Hunter, 1991). These localisation patterns implicate these two proteins in regulating spindle dynamics by phosphorylating proteins found at the centrosomes, on spindles, and the kinetochores, the majority of which are unknown.

Aurora kinases are also required for the correct regulation of many events during mitosis (reviewed in Ducat and Zheng, 2004; Meraldi et al., 2004). Aurora-A localises to centrosomes in interphase and to spindle poles and spindle microtubules in early mitosis. Consistent with its localisation, Aurora-A mainly functions in centrosome maturation and spindle assembly. In contrast, Aurora-B is a chromosomal passenger protein, complexing with INCENP, Survivin, and Borealin/Dasra and localising to kinetochores until anaphase where it then localises to the spindle midbody. Aurora-B functions in kinetochore assembly and bipolar attachment, the spindle checkpoint, and cytokinesis. Consistent with their essential roles in driving progression through M-phase both Plk1 and Aurora kinases have been implicated in tumourogenesis (Keen and Taylor, 2004; Liu and Erikson, 2003; Meraldi et al., 2004).

1.1.4 Cell cycle checkpoints

Orderly progression through the cell cycle requires a multitude of positive regulators as discussed above. Just as importantly, negative regulators are required to ensure that the phases occur in the right order and that if a problem is encountered the cell can arrest in order to remedy it. This ability to detect and fix errors is called checkpoint activation. It allows cells to monitor cell cycle progression and is essential to prevent inappropriate cell proliferation and genetic instability. Checkpoint activation involves sensing and signalling pathways feeding into negative regulators of the cell cycle, causing them to hold the respective cyclins/cdk complexes inactive, until the defect has been corrected. There are two main kinds of checkpoints, one that responds to damaged or incompletely replicated DNA and one that responds to incorrect spindle formation and chromosome alignment. Checkpoints that respond to damaged or incompletely replicated DNA allow cell cycle arrest to occur at either G1/S, during S-phase, or at the G2/M transition and have many components in common.

DNA damage and cell cycle checkpoints

The G1/S, the intra-S, and the G2/M checkpoints all utilise the same sensing and signalling pathways of the ATM/ATR and Chk1/Chk2 cassettes to respond to various insults upon the cell's DNA. The downstream effects of these three pathways are very similar. The checkpoint signalling cascade results in the inhibition of Cyclin-cdk complexes and their activating phosphatases, thereby preventing entry into the next stage of the cell cycle. Therefore, no matter which stage a particular cell is at when DNA damage occurs, the signalling response will result in cell cycle arrest before the

damage can be transformed into a devastating event through attempts at replicating or segregating the damaged DNA.

The ability of cells to sense that they have DNA damage is primarily due to the action of the ATM/ATR sensing and signalling pathway. ATM and ATR are closely related PI(3)K-like kinases that are involved in the recognition and signalling of ionising radiation-induced DNA damage and unreplicated DNA, respectively (Kastan and Bartek, 2004). ATM is dispensable in cells, but patients with germline mutations in ATM suffer from the inherited disorder, ataxia telangiectasia, and have an increased disposition to cancer (Shiloh and Kastan, 2001). In contrast, ATR is essential for normal growth, which suggests that it has a critical function within the normal cell cycle, possibly in the progression of DNA replication forks (Shechter et al., 2004).

ATM and ATR, together with a complex comprised Mre11, Rad50 and Nbs (MRN), signal to the checkpoint kinases Chk1 and Chk2 and to p53 (Figure 1.5) to bring about cell cycle arrest. These proteins bring about a global phosphorylation (Chk1 and Chk2) and transcription (p53) response to counter cell proliferation until the stress has been dealt with. If the damage is too high or remains unresolved for too long, p53 is also able to bring about an apoptotic response.

The Chk1 phosphorylation response results in the inhibition of Cdc25, thereby allowing accumulation of inhibitory phosphates on cdks, which results in a rapid cell cycle arrest in response to DNA damage. p53 is also a target of Chk1 and Chk2 (Craig et al., 2003). One of the key p53 transcriptional targets is the cdk2 inhibitor $p21^{CIP1}$, thereby G1 arrest occurs through the inactivation of Cyclin E-cdk2 and subsequent activation of RB

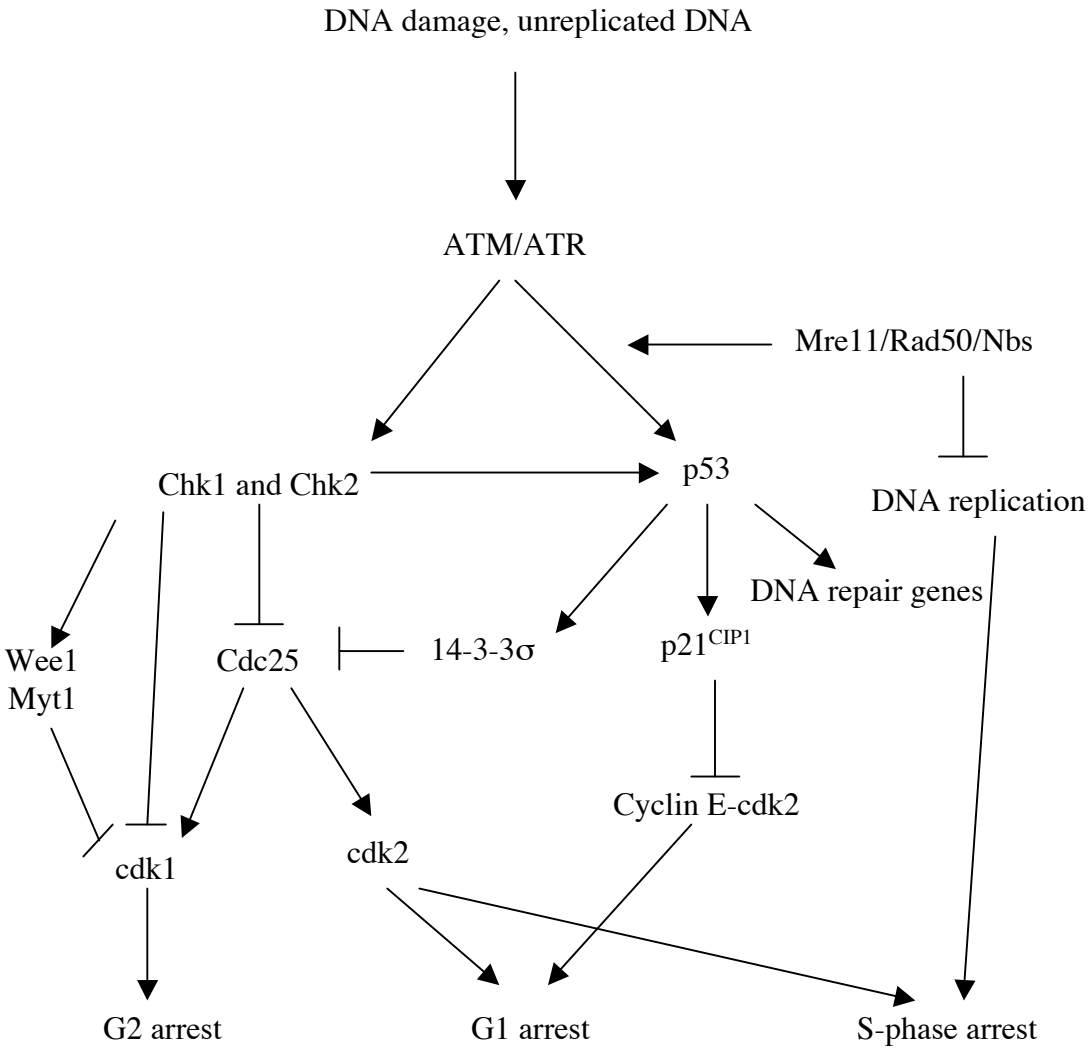

Figure 1.5 Activation of cell cycle checkpoints in response to DNA damage or unreplicated DNA.

The ATM/ATR signalling pathway is activated in response to DNA damage or unreplicated DNA. ATM/ATR phosphorylate Chk1 and Chk2 and p53. Chk1 and Chk2 phosphorylate Cdc25B, Wee1, Myt1 and cdk1 to prevent entry into M-phase. Phosphorylation of Cdc25A prevents entry into S-phase. p53 activation results in a transcriptional response including the upregulation of $p21^{CIP1}$ which inhibits Cyclin E-cdk2 activity (preventing S-phase entry), and 14-3-3σ which binds phosphorylated Cdc25B and sequesters it in the nucleus (preventing M-phase entry). S-phase is arrested due to the actions of the MRN complex possibly interfering with the replication machinery and through inactivation of cdk2 activity which is required for replication machinery recruitment to pre-replication complexes.

(Kastan and Bartek, 2004). Consequently, activation of Chk1, Chk2, and p53 results in the cell cycle arrest at both G1-S and G2-M (Figure 1.5). While the p53-mediated response seems to mainly affect a G1/S arrest it can also upregulate proteins required for the G2/M arrest. The p53-mediated pathway takes longer to respond and while it can result in a reversible arrest, it is also the pathway that generates a prolonged arrest resulting in either senescence (permanent arrest) or apoptosis (Kastan and Bartek, 2004).

The p53 pathway is also induced in the presence of high mitogenic signalling. In mammals, the INK4a locus encodes another protein, ARF, on the opposite strand. The ARF protein activates p53 by binding and sequestering a negative regulator of p53, Mdm2 (Sherr, 2004). Transcription of both INK4a and AFR is responsive to heightened mitogenic signalling such as from oncogenic Ras, E2F, and Myc. Therefore, both Rb and p53 are activated and cell proliferation is arrested when the signals to enter S-phase increase beyond a certain threshold (Massague, 2004; Serrano et al., 1997).

The Chk proteins not only act in G1/S and G2/M but can also bring about arrest at the intra-S checkpoint. This checkpoint is dependent on Chk inhibition of Cdc25, which results in inhibition of cdk2 activation (Figure 1.5). In the absence of cdk2 activity, DNA replication does not occur because DNA helicases and polymerases cannot be recruited to replication origins (see above). This checkpoint is also dependent on the activities of ATM-activated Nbs, BRCA1, and FANCD2 in a way that is not fully understood at this point. One way in which Nbs may induce the checkpoint is by inhibiting replication complexes. Nbs is able to interact with PCNA throughout S-phase and with E2F at sites of origin replication (Maser et al., 2001; Wang et al., 2000a). The

intra-S-phase checkpoint is also important in responding to stalled or collapsed replication forks, which in the latter can result in the formation of a DNA double strand break (Figure 1.5; Michel et al., 1997). Activation of the intra-S-phase checkpoint plays an important role in ensuring that DNA replication is completed properly before the cell progresses into mitosis.

The G2/M DNA damage checkpoint is able to arrest the cells prior to mitosis in response to DNA damage or unreplicated DNA. The main targets of this checkpoint are the mitotic activators cdk1 and Cdc25 (Figure 1.5; Kastan and Bartek, 2004; Nyberg et al., 2002). cdk1 is phosphorylated on inhibitory residues by the checkpoint kinases Wee1 and Myt (Donzelli and Draetta, 2003) as well as through the ATM/ATR, Chk1/Chk2 pathway (Kastan and Bartek, 2004). This checkpoint also results in the sequestration of Cdc25 in the cytoplasm by 14-3-3 binding to sites phosphorylated by Chk1 or Chk2, thereby preventing it from entering the nucleus and activating cdk1 (Lee et al., 2001). One 14-3-3 isoform, 14-3-3σ, is transcriptionally upregulated by p53 and is required to sequester both Cyclin B and cdk1 in the cytoplasm (Figure 1.5; Chan et al., 1999). In the absence of 14-3-3σ, cells are able to enter G2 arrest in the presence of DNA damage, but fail to maintain this arrest. Since 14-3-3σ cannot sequester them in the cytoplasm, Cyclin B and cdk1 enter the nucleus and the cells undergo mitotic catastrophe. Another 14-3-3 isoform, 14-3-3β, also aids in preventing M-phase entry by binding Wee1 following Chk1 phosphorylation, which enhances the stability and activity of Wee1 (Lee et al., 2001; Wang et al., 2000b). Another way Chk1 and Chk2 may also prevent M-phase entry is by the inhibitory phosphorylation of Polo-like kinase 1 (Nyberg et al., 2002).

The DNA damage checkpoint results in a global activation of many negative cell cycle regulators and inhibition of positive regulators through the activation of two similar signalling pathways, the Chk1/Chk2 and the p53 pathways. Since only a small number of signalling proteins result in the activation of a large number of effectors, loss of one or two of the effectors can be tolerated due to redundancy in the system and the cell would still arrest effectively. By this same token, it can be understood why loss of p53, Chk1, or Chk2 occurs in over half of tumours of diverse origins (Sherr, 2004), since this would inactivate the G1/S, G2/M and intra-S-phase checkpoints in just one hit.

The spindle checkpoint

Many cancers show chromosomal instability (aneuploidy), which underscores the importance of the spindle checkpoint and the coordination of cytokinesis with mitotic exit in preventing tumourogenesis. Unlike checkpoints that respond to defects in DNA, the spindle checkpoint responds to defects in spindle formation and kinetochore-microtubule attachments. The principal checkpoint machinery consists of Bub1, BubR1, Bub3, Mps1, Aurora B, Mad1, Mad2, CENP-E and the target is the Cdc20 subunit of the APC/C (Kramer et al., 2000; Vanoosthuyse and Hardwick, 2005). Aurora B kinase is also thought to function is regulating the kinetochore-microtubule attachment by sensing the lack of tension across the sister kinetochores, which occurs only upon bipolar attachment (Ducat and Zheng, 2004; Tan et al., 2005).

When the spindle checkpoint is activated by signals from chromosomes that are not bi–orientated, the activity of the Cdc20 subunit is inhibited and therefore it is unable to activate APC/C. Thus, cells in metaphase are prevented from commencing sister chromatid separation, exit from mitosis, and cytokinesis until the spindle checkpoint is satisfied (Figure 1.4 B).

The Ran pathway, which has an established role in spindle assembly, also appears to have a role in the spindle checkpoint (Arnaoutov and Dasso, 2003). High levels of RanGTP can result in override of the spindle checkpoint, which results in the loss of checkpoint regulators, including Mad2, CENP-E, Bub1 and Bub3, from the kinetochores. In low RanGTP conditions these regulators remain on the kinetochores. In cells in which the checkpoint has not been activated by microtubule depolymerising drugs, the Ran activating GEF, RCC1 localises to chromosomes at the onset of anaphase. It has been hypothesised that high RanGTP at the kinetochores may be the signal to switch off the checkpoint (Figure 1.4 B; Harel and Forbes, 2004) but how this achieved at present is unknown.

1.2 Mitogenic signalling and the control of cell proliferation

Since proper development requires the coordination of cell proliferation with cell growth and differentiation, it is no surprise that the same signalling pathways that control patterning and differentiation also control growth and proliferation. In mammalian cells, signalling through the Wnt, Hedgehog, PI-3 kinase, and Ras pathways can lead to an upregulation of cell proliferation, whereas TGFβ signalling results in a downregulation (Sherr, 2004). In the *Drosophila* eye imaginal disc, Notch is the primary S-phase inducer in the second mitotic wave with Ras and Hedgehog signalling playing a lesser role in positively regulating S-phase entry, whereas Wg and Dpp act negatively (Brumby et al., 2004).

1.2.1 The Ras signalling pathway

Many mitogenic factors act through receptor tyrosine kinases (RTKs) to activate the Ras signalling pathway and, as such, this pathway plays a central role in activating G1-S progression. This central role is underscored by the finding that Ras is a potent oncogene, where mutations in Ras, which serve to make it constitutively active, can drive cells into the cell cycle in the absence of any external signal. Mutations that result in the upregulation of this pathway are found in approximately 30% of human cancers (Chang et al., 2003), which highlights the importance this pathway plays in linking external cues with the initiation of cell proliferation.

Ras signalling in normal cells involves the binding of a ligand to an RTK, which sets off a signalling cascade resulting in a specific transcriptional outcome (Figure 1.6). Ligand binding to the receptor induces receptor dimerisation and autophosphorylation of the cytoplasmic domains of the receptor. These phosphates form docking sites for the adaptor proteins Grb2 and Shc, which recruit Ras to the plasma membrane, where it is activated by GTP loading by Sos. The conformation of Ras changes when bound by GTP, creating binding sites for its downstream effectors. Ras is deactivated by its own GTPase activity stimulated by p120 and neurofibromin. Thus the regulation of the guanidine nucleotide binding state of Ras acts as a molecular switch modulating downstream signalling events.

One pathway downstream of Ras is the Raf/MEK/MAPK cassette (Figure 1.6). Recruitment of Raf to activated Ras at the plasma membrane is in part due to 14-3-3 proteins binding to Raf. 14-3-3 binding holds Raf inactive in resting cells (Figure 1.6A), but it is also required for Raf's activation and recycling back to the cytosol (Roy

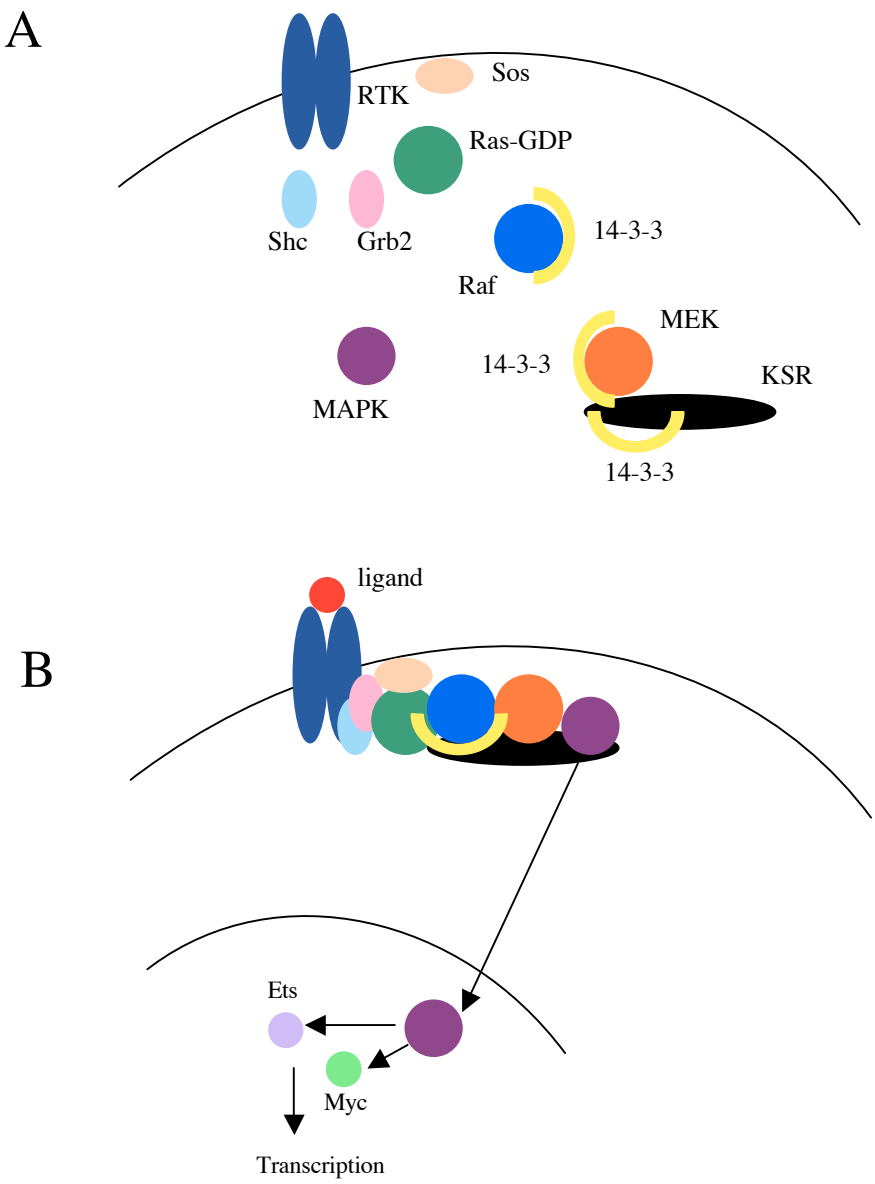

Figure 1.6 The Ras signalling pathway.

(**A**) In resting cells most components of the Ras pathway are found in the cytosol. Raf, MEK and KSR are bound by 14-3-3 proteins which act to keep them inactive. All the proteins are labelled and the same colours are used in B. (**B**) Upon binding of ligand to the receptor tyrosine kinase (RTK), the receptor becomes activated and binds the adaptor proteins Shc and Grb2. They recruit Ras to the plasma membrane where it becomes activated by its guanidine-exchange factor, Sos. Activated Ras then recruits Raf to the plasma membrane and phosphorylates it. Raf still binds 14-3-3 but in a different conformation which exposes its catalytic site. KSR and MEK are recruited to the membrane, where Raf can activate MEK by phosphorylation. MEK in turn activates the recruited MAPK by phosphorylation. Once activated MAPK can translocate into the nucleus where it phosphorylates and activates transcripton factors including Ets and Myc. These then induce the transcription of genes involved in cell proliferation, cell cycle arrest, or differentiation. The phosphorylated residues are not shown for clarity.

et al., 1998; Thorson et al., 1998; Tzivion et al., 1998). MEK is recruited to the plasma membrane by the scaffold protein KSR, which it binds constitutively (Figure 1.6 A). MEK is activated by Raf and in turn activates MAPK, which is only recruited to KSR when KSR is at the membrane (Figure 1.6 B; Cacace et al., 1999). Once activated, MAPK translocates into the nucleus where it is able to phosphorylate its downstream transcription factors (Figure 1.6 B). MEK and KSR are also bound by 14-3-3 proteins (Figure 1.6 A; Cacace et al., 1999; Fanger et al., 1998; Ory et al., 2003). For KSR to be recruited to the plasma membrane, the binding by 14-3-3 needs to be disrupted, possibly by Ras, and the phospho-binding site dephosphorylated by protein phosphatase 2A. In *Drosophila,* the two 14-3-3 isoforms, 14-3-3ζ and 14-3-3ε act genetically downstream of Ras in the signalling pathway. 14-3-3ζ acts downstream of Ras and 14-3-3ε acts parallel to, or downstream of Raf (Chang and Rubin, 1997; Kockel et al., 1997). Since Raf, MEK and MAPK activation occurs at the plasma membrane, possibly in a complex, these findings indicate that 14-3-3 proteins are components of this complex or regulate its formation, both in mammals and in flies. The overexpression of 14-3-3ζ can activate the Tor-RTK signalling pathway in the absence of Tor receptor, but this requires the presence of Raf and Ras (Li et al., 1997), thus indicating that 14-3-3 proteins play a general role in RTK/Ras signalling.

1.2.2 Ras signalling effects on cell proliferation, cell growth and differentiation

Ras signalling induces cell proliferation through the activation of the transcription targets Ets and Myc (Chang et al., 2003; Massague, 2004). Myc is able to induce the transcription of *Cyclin D* and *E2F1-3* and suppress the transcription of cdk inhibitors (Sears and Nevins, 2002), thereby inducing entry into S-phase. In contrast to mammalian cells, in *Drosophila* Ras signalling promotes growth (Halfar et al., 2001;

Prober and Edgar, 2000). In the wing, increased Ras signalling results in an upregulation of Myc and together both proteins can affect an upregulation of Cyclin E protein through post-transcriptional means. This results in an acceleration of G1-S progression but as there is no concomitant upregulation of the *Drosophila* Cdc25 homologue (encoded by *string*), there is no acceleration through G2-M and no overall change in proliferation rates due to an increase in G2 length (Prober and Edgar, 2000). However, in haemocytes, activated Ras can stimulate overproliferation, which indicates that at least in these cells Ras signalling can activate expression of genes required for both S- and M-phase (Asha et al., 2003). Therefore, cell specific differences determine how a cell responds to Ras, and presumably other types of signalling.

Ras signalling has also been shown to inhibit cell cycle progression in some cell types, which indicates further cell specific differences in responding to Ras signalling. Extensive Ras signalling due to oncogenic mutations results in the transcriptional upregulation of negative regulators of the cell cycle, such as p53, $p21^{CIP1}$ and $p16^{INK4a}$ (Chang et al., 2003; Lowe et al., 2004; Massague, 2004). In mammals, therefore, for oncogenic Ras to transform cells, mutations in the p53 or Rb pathways are required to overcome the Ras-induced cell cycle arrest. This is supported by the finding that in cells lacking p53 or p16, proliferation occurs in the presence of oncogenic Ras (Serrano et al., 1997). Expression of other members of the signalling pathway, including Raf, can also result in proliferative or arrest outcomes. It is thought that the switch between the two opposing outcomes relies on the strength of the signal and its affect on $p21^{CIP1}$ expression. At low signalling levels, low levels of $p21^{CIP1}$ expression are induced and this protein binds to Cyclin D-cdk4/6, allowing Cyclin E-cdk2 to induce S-phase. However, at higher signalling levels, high levels of $p21^{CIP1}$ are produced, which acts to

inhibit Cyclin E-cdk2 (Woods et al., 1997). A similar situation may explain the different effects that Ras signalling has in developmental outcomes in *Drosophila*. Low levels of Ras expression in the developing eye permit cell growth and survival and differentiation of the R8 photoreceptor cell. On the other hand, high levels of Ras signalling are required for differentiation of the photoreceptor cells R1 through R7 (Halfar et al., 2001). Therefore, specific cell types can regulate the strength of this signalling pathway to provide specific cellular outcomes.

It is possible that the negative effects of Ras signalling may be used to halt or exit the cell cycle to allow for differentiation to occur. In mammals, the Ras signalling pathway has important roles in the differentiation of neuronal, adipocytic, and myeloid cells, sometimes accompanied by growth arrest (Crespo and Leon, 2000). In *Drosophila,* Ras signalling is required for the differentiation of wing veins, photoreceptor cells, and for terminal structures in the embryo. It is also required for the specification of muscle, cardiac, and neuronal precursors (Carmena et al., 2002; de Celis, 2003; Schnorr and Berg, 1996; Sundaram, 2005). Therefore, the Ras signalling pathway may be a key regulator of integrating cell proliferation, cell growth, and differentiation and further investigation of its roles are crucial to the understanding of metazoan development.

1.3 Control of cell proliferation during development in *Drosophila*

The broad mechanisms of cell cycle control and signalling are conserved in all metazoans, including *Drosophila*. However, some of the details are different between vertebrate and invertebrate systems. There are a smaller number of homologues in flies than in mammalian systems, indicating that there is likely to be less functional redundancy. In *Drosophila* one, or possibly two, proteins provide all the functions

required in contrast to the large number usually found in mammalian genomes. This makes the study of these functions easier and therefore *Drosophila* has been a valuable model in understanding cell proliferation. Furthermore, since cell proliferation can be studied *in situ,* the role that developmental control plays in cell proliferation regulation is currently more clearly understood in the *Drosophila* model than in vertebrates.

1.3.1 Differences in the cell cycle regulation between *Drosophila* and mammals

In *Drosophila*, there are only two known E2F homologues, E2f1 and E2f2. E2f1 acts as a transcriptional activator, whereas E2f2 acts as a repressor (Cayirlioglu et al., 2001; Frolov et al., 2001). The *Drosophila* genome encodes only one Dp homologue (Royzman et al., 1997) and two Rb homologues, Rbf1 and Rbf2. Rbf1 can bind and suppress both E2f homologues, whereas Rbf2 only binds E2f2 (Stevaux et al., 2002). As in mammals, Cyclin E also acts upstream and as a target of E2F (Duronio et al., 1998) but, unlike in mammals, it is essential for normal development and appears to be the only G1 cyclin that is involved in the S–phase transition. Unlike in mammals, *Drosophila* Cyclin D-cdk4 complexes appear to only have roles in regulating cell growth and do not regulate proliferation (Datar et al., 2000; Meyer et al., 2000). In addition, *Drosophila* appears to lack INK inhibitors and contains only one known Kip/Cip homologue, *dacapo*, which does not bind Cyclin D-cdk4 (Meyer et al., 2000). Therefore, in *Drosophila*, the key positive regulators of S-phase entry are E2f1 and Cyclin E.

The conservation of M-phase regulators is also quite strong between humans and *Drosophila*. Cyclin A, Cyclin B, and Cyclin B3 regulate M-phase entry and progression by binding to cdc2 (cdk1). Similar to the situation in mammals, Cyclin A is necessary

for normal development (Lehner and O'Farrell, 1989), whereas loss of Cyclin B or Cyclin B3 results in viable flies. However, in *Drosophila*, loss of both type B cyclins results in lethality (Jacobs et al., 1998; Knoblich and Lehner, 1993). In contrast, both Cyclin Bs are required individually for proper fertility and even though Cyclin B is not essential for development it is required for normal formation of the mitotic spindle. In the absence of both B type cyclins, entry into mitosis is delayed and spindle formation is strongly impaired. Reflecting its role in spindle function, Cyclin B localises to the spindle in metaphase, whereas Cyclin A localises to the chromosomes (Stiffler et al., 1999). Unlike in mammalian cells, Cyclin A does not bind cdk2 in *Drosophila* and is unlikely to play any roles in S-phase (Knoblich et al., 1994). Unlike mammalian systems, where it appears that Cyclin B is the key regulator of M-phase entry, in *Drosophila* efficient entry and progression through M-phase requires the activity of all three cyclins, Cyclin A, Cyclin B, and Cyclin B3, though it can still occur in the absence of one of the proteins.

1.3.2 Adaptation of the cell cycle during development

The developmental pattern of cell proliferation is well known in *Drosophila* and it is easy to study perturbations within the cell cycle *in situ*. As a result, the developmental requirements for regulation of G1-S phase and G2-M phase can be examined in cell types that utilise the canonical cell cycle (comprising G1, S, G2, and M phases) or those that use variations on the theme (reviewed in Lee and Orr-Weaver, 2003). There are numerous examples of different cell cycles occurring throughout *Drosophila* development (Figure 1.7). In syncytial embryos, cells cycle rapidly between S- and M-phase with no intervening gap phases (Figure 1.7 A). In later embryogenesis and during larval life, as well as in the nurse and follicle cells of the ovary, cells endocycle (S and

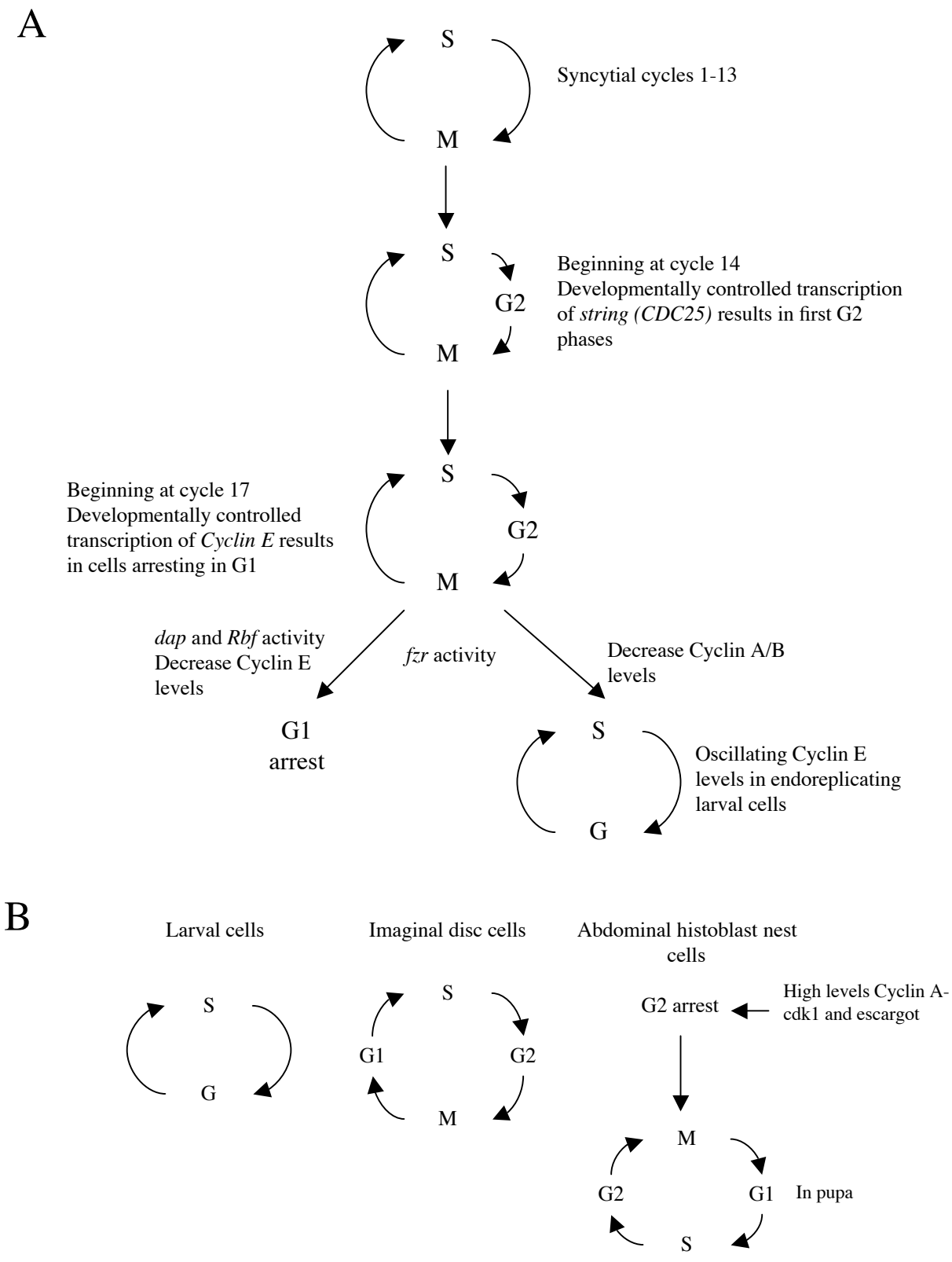
A
S
M
Syncytial cycles 1-13
S
G2
M
Beginning at cycle 14
Developmentally controlled transcription of *string (CDC25)* results in first G2 phases
Beginning at cycle 17
Developmentally controlled transcription of *Cyclin E* results in cells arresting in G1
S
G2
M
dap and *Rbf* activity
Decrease Cyclin E levels
fzr activity
Decrease Cyclin A/B levels
G1
arrest
S
G
Oscillating Cyclin E levels in endoreplicating larval cells
B
Larval cells
Imaginal disc cells
Abdominal histoblast nest cells
S
G
S
G1
G2
M
G2 arrest
High levels Cyclin A-cdk1 and escargot
M
G2
G1
S
In pupa

C

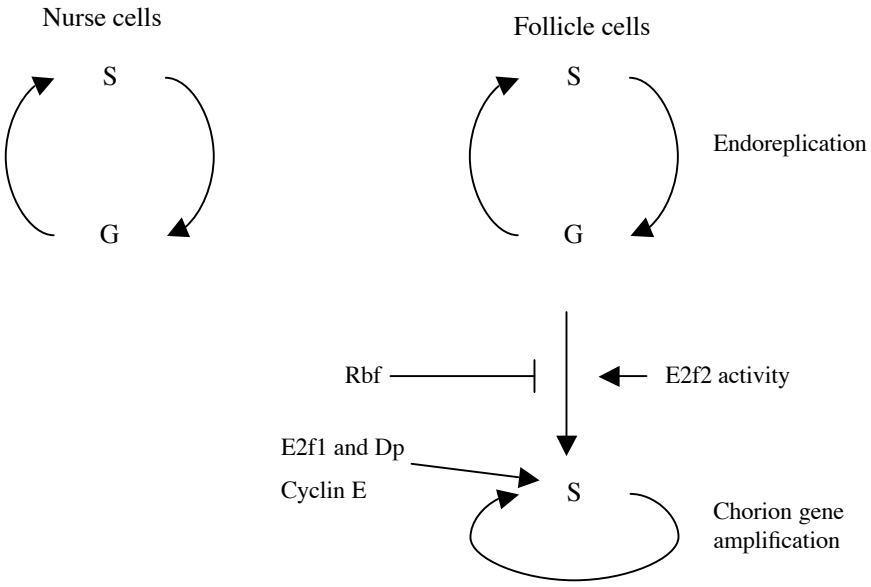

Figure 1.7 Cycle variations throughout *Drosophila* development.

(**A**) Embryonic development begins with rapid syncytial divisions of alternating S- and M-phases. The developmentally controlled expression of *string* results in the establishment of G2 in cycle 14. In cycle 17 developmental control of Cyclin E occurs, introducing the first G1. At this time some cells enter a G1 arrest due to decrease in Cyclin E levels and expression of *dap* and *fzr*. *fzr* is required for endoreplication by degrading Cyclins A and B. Oscillation of Cyclin E levels is also required for endoreplication. (**B**) During the larval stages larval cells continue to grow due to endoreplication. Imaginal discs cells proliferate through the cannonical cell cycle. Cells of the abdominal histoblast nests remain arrested in G2 during the larval stages due to the activities of Cyclin A- cdk1 and escargot. They reenter the cell cycle during pupariation. (**C**) During oogenesis nurse cell endoreplicate. Follicle cells undergo three cycles of endoreplication, then nested S-phase where the chorion genes are amplified. This switch requires E2f2 and is inhibited from occuring prematurely by Rbf. Both endocycles and gene amplification require E2f1, Dp and Cyclin E. Adapted from Vidwans and Su (2001).

G phases with no M phases; Figure 1.7 A and B). Follicle cells also undergo gene amplification, which is a form of nested S-phases acting on specific genomic regions (Figure 1.7 C). During larval life cells that will become the adult tissues, the imaginal discs, undergo the canonical cell cycle, whereas those that will form the adult abdomen, the histoblast nests, arrest in G2 until pupariation, after which they proliferate (Figure 1.7 B).

1.3.3 Developmental control of the cell cycle

In *Drosophila* the first cell cycle that is controlled developmentally is embryonic cycle 14. At this stage maternal *string* contribution is degraded and mitosis can only occur in spatial and temporal domains caused by developmentally regulated *string* transcription (Figure 1.7 A; Edgar and O'Farrell, 1990). G1 phases first occur slightly later in development when zygotic transcription of *Cyclin E* is required for entry into S-phase of cycle 17 (Figure 1.7 A; Knoblich et al., 1994). Both *string* and *Cyclin E* contain complex promoter and enhancer sequences (Edgar et al., 1994; Jones et al., 2000), indicating that they are under strict developmental control.

The developmental role of cell cycle regulators is readily examined by genetic analyses in *Drosophila*. *E2f1* and *Dp* are both essential for normal development in flies. Loss of *E2f1* function results in a reduction in transcription of both *PCNA* and *RNR2* but the effects on S-phase are dependent on the allele. *E2f1*$^{-}$ alleles examined by Duronio et al. (1995) result in prevention of S-phase entry at embryonic cycle 17 and lethality during embryogenesis, whereas *E2f1*$^{-}$ alleles examined by Royzman et al. (1997) allow embryonic S-phases to occur with lethality occuring at the larval to pupal boundary. These latter alleles also caused slow larval growth and the formation of melanotic

pseudotumours. *Dp* mutants die mainly as pupae, although some develop into pharate adults that struggle to eclose (Royzman et al., 1997). Some pupae demonstrate pseudotumour formation as well as abdominal defects (Royzman et al., 1997). It appears that the defects in growth in *E2f1* mutants are due to an increase in E2f2 activity since loss of this gene can suppress these defects (Frolov et al., 2001). These data, therefore, show that correct control of S-phase entry is important for correct development.

Negative regulators of the cell cycle are also required during development to either effect cell cycle exit or to arrest the cells to allow for morphological changes or commitment to differentiation. *Rbf* is required for maintaining the normal arrest that occurs in the embryonic epidermis following cycle 16 (Figure 1.7 A). In its absence, ectopic PCNA expression and an extra S-phase occur (Du and Dyson, 1999). As only one extra S-phase occurs there must be other gene products that ensure that cell cycle arrest occurs. One of these genes is *dacapo (dap)*, the *Drosophila* $p21^{CIP1}$ homologue. Similar to *Rbf* mutant phenotypes, loss of *dap* causes cells to undergo an extra cell cycle when they should be arrested in G1 (Figure 1.7 A). This occurs in the embryonic epidermis, PNS and CNS (de Nooij et al., 1996). The *fizzy-related (fzr)* gene, the homologue of Chd1, is also required for cell cycle exit in embryos, highlighting the role it plays in downregulating cyclins in G1 (Sigrist and Lehner, 1997). *fzr* is also required for endoreplication (Figure 1.7 A; see below). While cell cycle exit is dependent upon these negative regulators, it is also dependent on the downregulation of positive regulators. For example, Cyclin E transcript levels decrease leading into cell cycle exit (Knoblich et al., 1994; Richardson et al., 1993).

Arrrest of the cell cycle is required for morphogenesis to occur. One example is the delay in mitosis of mitotic domain 10 of embryos to allow for gastrulation to occur. In these cells *string* mRNA is expressed yet mitosis is halted. This delay is in part dependent on *tribbles*. In the absence of *tribbles*, cells in mitotic domain 10 overproliferate and gastrulation does not occur properly (Grosshans and Weischaus, 2000; Mata et al., 2000; Seher and Leptin, 2000), thus highlighting the need for coordination of cell proliferation and morphogenesis.

Similarly, in the developing eye imaginal disc, cell proliferation and differentiation are coordinated in the morphogenetic furrow, a constriction of cells that moves posterior to anterior through the disc (Dickson and Hafen, 1993). Cells become arrested in the furrow in part by the combined negative actions of *dpp*, *dap,* and *roughex (rux)*, an inhibitor of Cyclin A (Avedisov et al., 2000; Horsfield et al., 1998). Upon exiting the furrow, some cells, known as the proneural cluster, are committed to differentiate. The remaining cells undergo a synchronous cell cycle, which is in part under the control of signalling pathways. The expression of Cyclin E in the furrow, which drives the synchronous S-phase posterior to the furrow, is due to Hedgehog-induced, Ci-dependent transcription (Duman-Scheel et al., 2002). Differentiation of the proneural cluster activates EGFR signalling in cells posterior to the synchronous S-phase. This leads to increased *string* expression and entry into a synchronous M-phase (Baker and Yu, 2001).

1.3.4 The control of endoreplication and gene amplification

Two variations on the canonical cell cycle that have been well studied in *Drosophila* are endocycles and gene amplification. Both variations involve the re-replication of

DNA in the absence of a prior M-phase and, as such, illustrate how cells regulate the interdependence of S- and M- phases and how this may be overcome. Endocycles occur in the gut, salivary gland, almost all larval cells (indeed, this is the means by which larvae grow), and in the follicle and nurse cells during oogenesis.

The positive regulation of endocycles requires the presence and oscillation of Cyclin E protein (Knoblich et al, 1994; Lilly and Spradling, 1996). Importantly, in the absence of M-phase in these cells, the reduction of Cyclin E levels during the gap phase is required for pre-replication complexes to form and load onto DNA, an event that cannot occur in high cdk activity (see above). The reduction in cdk activity, and therefore resetting of the competence for DNA synthesis, is likely to be due to *fzr* activity, which has been shown to be required for the transition to the first few cycles of endoreplication (Sigrist and Lehner, 1997).

The negative regulation of endocycles requires the activities of Cyclin A and cdc2, which may be regulated by *escargot* (Hayashi, 1996). This regulation is most clearly seen in the abdominal histoblast nests where the cells remain arrested in G2 throughout larval life (Figure 1.7 B). In the absence of these negative regulators, cells enter an endocycle program, possibly allowed by the low level of Cyclin E-cdk2 activity present at G2 (Sauer et al., 1995). This results in abdominal defects due to insufficient cell numbers for normal proliferation and differentiation to occur (Hayashi et al., 1993). Therefore, for an endocycle to occur the cell needs to be reset in a G1 state without a previous mitosis occuring. This results in initial low cdk activity, particularly cdk1 (cdc2), which allows for reloading of the pre-replication complex and the subsequent increase in Cyclin E-cdk2 levels. How this resetting is achieved is not well understood.

While the resetting of the G1 state is mainly unknown, the initiation of the S-phases during endoreplication and gene amplification is better understood. Like in other cell cycles, the E2f-Dp-Rbf pathway plays a major role in the regulation of endoreplication and gene amplification in nurse and follicle cells (Figure 1.7 C). Mutants of genes in this pathway display female sterility due to formation of eggs with abnormal chorion thickness and dorsal appendage development (Bosco et al., 2001; Frolov et al., 2001; Myster et al., 2000; Royzman et al., 2002). During oogenesis, endoreplication and gene amplification provide the nurse and follicle cells with sufficient gene copies to generate the large amount of RNA and protein required by the oocyte and to make enough chorion protein for the eggshell, respectively. In nurse cells E2f1 and Dp are required for the polyteny- polyploid switch (Royzman et al., 2002) and Dp is needed to prevent an extra mitotic division in the germ cells (Myster et al., 2000). In controlling chorion gene amplification Dp and E2f1 are required to restrict the activity of Orc2 to gene amplification regions (Royzman et al., 1999) and E2f2 promotes the switch between endoreplication and gene amplification (Cayirlioglu et al., 2001). Rbf is required to prevent premature amplification and in its absence follicle cells are able to undergo an extra S-phase (Bosco et al., 2001). These effects on endoreplication and gene amplification seem to be independent of the role of E2F as a transcriptional activator. Cyclin E is required to positively regulate gene amplification and to prevent inappropriate firing at other origins (Calvi et al., 1998). Therefore, in regulating the key S-phase regulatory pathways, the nurse and follicle cells can ensure that enough RNA and protein is generated for proper egg and early embryonic development.

1.4 Identification of novel regulators of cell proliferation

From the detailed introduction above it is clear that the current literature contains a lot of detail regarding cell cycle progression and control. Much is also understood about the proteins involved in cell signalling and how these signals are transduced. However, while it is known that cell signalling can regulate the cell cycle, how these two cellular processes interact is still largely unknown, particularly in the context of development. Furthermore, it is still to a great extent unknown how signalling pathways are fine tuned to result in such different outcomes as cell proliferation or differentiation. If it is dependent on signal strength, as discussed above, then what senses the difference in signal strength and how is the signal fine-tuned to result in different cellular outcomes? It is also unclear what other cellular processes impinge upon a cell's decision to undergo proliferation. Data emerging from genetic screens and microarrays indicate that regulators of cell cycle entry interact with or cause the expression of a number of genes from such disparate cellular processes such as protein trafficking, cell adhesion, biosynthesis, cell signalling, and hox genes (Brumby et al., 2004; Ishida et al., 2001; Young et al., 2003). Therefore, it is likely that many important regulators of cell proliferation are still waiting to be identified and characterised.

1.4.1 Novel regulators of cell proliferation uncovered in genome projects

The recent sequencing of the human genome and many model organisms has provided a wealth of genetic and genomic information. Included in these data is the identification of many previously unknown and uncharacterised genes. It is expected that amongst these new genes will be important regulators of cell proliferation, some acting directly, some indirectly. So how can they be identified? Some of these genes have been assigned a function in regulating cell proliferation (or another role) due to conservation

of sequence within the encoded protein that is suggestive of a particular function or protein family. However, for many genes, function cannot be assigned based on protein sequence alone. For these genes, comparative expression profiling with known cell proliferation regulators by microarray analysis or proteomics, systematic RNAi looking for defects in cell proliferation, or physical association with known regulators may be required to identify novel regulators of cell proliferation.

1.4.2 Identification of *deflated* as a novel cell proliferation regulator in *Drosophila*

One gene that has been identified as a putative regulator of cell proliferation is the *Drosophila* gene, CG18176 (*deflated*). This gene was annotated in the genome project as having an unknown function. Homologues are found in genomes of all multicellular organisms examined to date, but are absent from yeast and fungal genomes (Table1.1). The identification of *deflated* as a putative novel cell proliferation regulator came from a study by Stuart et al. (2003). In this study, over 3182 microarray experiments from *S. cerevisiae*, *C. elegans, D. melanogaster,* and *H. sapiens* were analysed. Genes were grouped into 'metagenes', which were defined as the best-hit reciprocal orthologue from each of the four species and assessed for correlation of co-expression. These analyses allowed for an assessment of conservation of co-expression across the evolutionary distances between the four species with the hypothesis that genes displaying evolutionary conserved co-expression had a high probability of being involved in the same biological processes. In the analysis by Stuart et al., *deflated* was assigned the metagene 4869 and was found to have a high level of co-expression with the S-phase regulator *Dp* and the DNA synthesis gene *Ctf4*. Therefore, it is very likely that *deflated* plays a role in regulating cell proliferation.

Table 1.1 DEFLATED orthologues identified in multicellular organisms

Species	**Protein name**[†]	**Accession number**[§]
Drosophila melanogaster	DEFLATED, CG18176 protein product	NP 648352
Apis mellifera	Similar to RIKEN cDNA 5930412E23	XP 396796
Anopheles gambiae	ENSANGP00000011390	XP 317927
Danio rerio	DKFZP434B168 protein homologue	NP 775374
Galluls gallus	Similar to DKFZP434B168 protein	NP 001006399
Mus musculus	RIKEN cDNA 5930412E23	NP 848747
Homo sapiens	C1orf73 protein, DKFZP434B168	NP 056249
Rattus norvegicus	Similar to RIKEN cDNA 5930412E23	XP 223075
Pan troglodytes	Similar to DKFZP434B168 protein	XP 514179
Canis familaris	Similar to DKFZP434B168 protein	XP 547398
Tetraodon nigraviridis	Unamed protein product	CAG 01530
Dictyostelium discoideum	Hypothetical protein DDB0186028	XP 638520
Caenorhabditis elegans	Putative protein of bilateral origin 2L877, D1043.1	NP 496477
Caenorhabdidtis briggsae	Hypothetical protein CBG02853	CAE 59469
Schistosoma japonicum	unknown	AAX 3059
Arabidopsis thaliana	Hypothetical protein F18F4.160	NP 193739

[†] All DEFLATED orthologues have been identified through genome or EST projects. Where two names exist, both have been listed.

[§] The accession number refers to the protein sequence (including those used in the homology alignment in Figure 4.1) from the NCBI Entrez Protein database.

1.5 Thesis overview

The investigations described in this thesis were aimed at addressing the hypothesis that *deflated* plays a role in the regulation of cell proliferation. Using various genetic and cellular approaches, the role that *deflated* plays in development, cell proliferation, and cell signalling were examined. Mutant alleles were generated (Chapter 3), which allowed for an in depth phenotypic characterisation of several of these alleles (Chapter 4). The expression pattern and predicted protein domains and motifs were also examined (Chapter 4). These analyses were performed to understand the role of *deflated* in development and whether it was consistent with a role in cell proliferation. Genetic interactions of *deflated* with cell proliferation and cell signalling alleles were assessed to find to which genetic pathway(s) *deflated* belong and to further understand its role (Chapter 5). The Ras signalling pathway was examined in detail to further elucidate the role of *deflated* in cell signalling and cell proliferation (Chapter 6). From the data generated in this study a model can be postulated on how *deflated* may contribute to the regulation of cell proliferation (Chapter 7).

Chapter 2- Materials and Methods

Materials

2.1 Chemical reagents

Reagents were all of analytical grade and obtained from Amresco, Lancaster, Merck, MP Biomedicals, Research Organics, Scientifix, Sigma, and Spectrum. All water was deionised and autoclaved before use.

2.2 Commonly used solutions

TE:	10mM Tris-HCl, pH 7.5, 1mM EDTA
TAE:	40mM Tris, 20mM acetate, 2mM EDTA, pH 8.1
PBS:	140mM NaCl, 3mM KCl, 2mM KH_2PO_4 and 10mM Na_2HPO_4 (purchased as 10X pack from Amresco)
PBTx:	1xPBS, 0.1% Trion X-100
PBTw:	1xPBS, 0.1% Tween 20
20x SSC:	3M NaCl, 0.3M sodium citrate
3/5M NaOAc:	3M Na^+, 5M OAc^-, pH 5.2
IAC:	25:24:1 phenol:chloroform:isoamyl alcohol

Solutions and buffers were prepared as described in Sambrook and Russel, (2001) unless otherwise specified. Additional solutions specific to particular techniques are described within the methods below.

2.3 Bacterial media

Luria Broth (LB): 1% tryptone, 0.5% yeast extract, 1% NaCl, pH 7

LB plates: LB plus 1.5% agar

2.4 Bacterial strains

E. coli DH12S cells (genotype: *80dlacZM15Δ mcrA Δ(mrr-hsdRMS-mcrBC) araD139 Δ(ara, leu)7697 ΔlacX74 galU galK rpsL (StrR) nupG recA1/F′ proAB+ lacIqZΔM15;* Invitrogen) were used in all cloning experiments.

2.5 DNA restriction and modification enzymes

Restriction enzymes were obtained from New England Biolabs or Promega and used according to the suppliers' specifications. DNA modifying enzymes were obtained from the following suppliers; T4 DNA ligase (Promega), Shrimp Alkaline Phosphatase (Promega), RNase (Sigma), Taq Polymerase (Biotech), Pfu Turbo DNA polymerase (Stratagene), and Rnasin® ribonulease inhibitor (Promega).

2.6 Oligonucleotide primers

Custom oligonucleotides were synthesised by Proligo (Table 2.1).

2.7 Plasmids

pOT2-*deflated* (Berkely Drosophila Genome Project EST GH11567)

pALX190 (gift from Alex Andrianopolous, Univ. of Melbourne)

pUAST (Brand and Perrimon, 1993)

pUASP (Rorth, 1998)

pπ25.7wc (Spradling, 1986)

Table 2.1 List of the oligonucleotide primers and their sequences used in this study

Oligo name	Sequence 5' to 3'	Experiment
806-NBSgscreena	TTAACTATGGCTTGGAATACGCCTACA	2.14.1
807-NBSgscreenb	ATTGTGTACCAATTCCAAGGAGCAGTT	2.14.1
808-NBSgscreenc	ATCTGCGATAAATGTGAGTGAGGAAAC	2.14.1
809-NBSgscreend	GTAGGGGAATGTCACAATCGGCTTAT	2.14.1
810-NBSgscreene	TTTGGTCTTCCGTGTTATGTGCTTACT	2.14.1
811-NBSgscreenf	GCTTGTTCACAGAATCCTCAAGAGAAG	2.14.1
812-NBSgscreeng	ATTTGGCCAGGGATCTGAAAAACTT	2.14.1
459-PF2	CGACGGGACCACCTTATGTTAT	2.14.1
759-NBS-G2	TACCGGTACTAGTACTCACAGTGTGAATTGTGCC	2.14.2
752-P-left1	GCATGTCCGTGGGGTTTGAATTAAC	2.14.3
828-P-right1	CGTCCGCAGACAACCTTTCCTC	2.14.2
829-P-left2	CTGTCTCACTCAGACTCAATACGACACTCAG	2.14.2, 2.14.3
854-deflfT7	TAATACGACTCACTATAGGCTGCTCCTGATTCCCGTGT	2.21.1
855-deflrT7	TAATACGACTCACTATAGGTGCGGTGGAAAAGGCGTACT	2.21.1
856-deflf	GCTGCTCCTGATTCCCGTGT	2.21.1
857-deflr	TGCGGTGGAAAAGGCGTACT	2.21.1
A015-deflCtermstart	ATCTGCGGTACCTGTGAGTGAGGAAACCTG	2.16.2
A016-deflCtermstop	CCCCCAAGCTTATAAACCTCCTCGTCTGTCCC	2.16.2
A054-deflseq1	CCCACCAGCGTTCGTGATGAC	2.15
A055-deflseq2	CGCCCAAGGTGCGCAGGAGGAG	2.15
A056-deflseq3	CGCTTCATCAGCGGAATTAGAGG	2.15
A096-deflseq3new	CTCGCAGGCTGGCCAGCGCTTGC	2.15
A057-deflseq4	GCGGTGGCGGCGTGATTAGCTG	2.15
A097-deflseq5	GCCACCGAACCCGTGAATGTCC	2.15
A075-deflS653E1	CCTGCGAGCTGGCGAGTCGCCCCAGCATCC	2.16.3
A076-deflS653E2	GGATGCTGGGGCGACTCGCCAGCTCGCAGG	2.16.3
A079-deflS653A1	CTGCGAGCTGGCGCCTCGCCCCAGCATC	2.16.3
A080-deflS653A2	GATGCTGGGGCGAGGCGCCAGCTCGCAG	2.16.3

2.8 Antibodies

2.8.1 Primary antibodies

Anti-GFP (rabbit): Molecular Probes (IgG fraction) used at 1:200 on tissues.

Anti-BrdU (mouse): Pharmigen, Becton Dickson (clone 3D4) used at 1:20 on tissues.

Anti-phospho-histone H3 (rabbit): Upstate Biotechnology (catalogue number 06-570) used at 1:1000 on tissues.

Anti-di-phosphorylated MAPK (mouse monoclonal): Sigma (clone MAPK-YT) used at 1:50 on tissues.

2.8.2 Secondary Antibodies

Goat anti-rabbit Alexa Fluor® 488 (Molecular Probes) used at 1:200 on tissues.

Goat anti-mouse Alexa Fluor® 488 (Molecular Probes) used at 1:200 on tissues.

Goat anti-mouse Alexa Fluor® 546 (Molecular Probes) used at 1:200 on tissues.

2.9 *Drosophila* stocks and maintenance

Flies were kept on standard cornmeal-treacle media at 25°C, unless otherwise indicated. A list of *Drosophila* stocks and from where they were obtained is given in Table 2.2.

Methods

2.10 DNA extraction

2.10.1 Extracting plasmids from bacteria (minipreps)

Plasmid DNA was purified following the Promega WizardPrep protocol. A 2ml culture was grown overnight at 37°C with shaking. Cells were harvested by centrifugation at 8,000 rpm for 2 min and resuspended in 200µl of Solution I (50mM Tris-HCl pH 7.5,

Table 2.2 List of the *Drosophila* stocks used in this study.

Stock	Obtained from
w[1118]	G. Hime
w[1118]; P{w[+mC]=EP}EP3301	BL #17111
w; CyO/If; MKRS/TM6B	G. Hime
y[1] w[*]; CyO H{w[+mC]=P Delta2-3}HoP2.1/ Bc[1] Egfr[E1]	BL #2078
w[*];; Dr[1]/ TMS P{ry[+t7.2]=Delta2-3}99B	BL #1610
w;; TM3 Sb[1]/TM6B p[Xp] Tb[1]	BL #1765
ru[1] h[1] th[1] st[1] p[p] cu[1] sr[1] ca[1]/ TM3	G, Hime
nanosGal4 p{w[+mC] Scer\GAL4[nos.UTRT:Hsim\VP16]=GAL4::VP16-nosUTR}	P. Rorth
MS1096Gal4 P{GawB}Bx[MS1096]	G. Hime
armadilloGal4 P{GAL4-arm.S}	G. Hime
eyelessGal4 P{Scer\GAL4[ey.PB]w[+mC]=GAL4-ey.B}	R. Saint
sevenlessGal4 P{sevEP-GAL4.B}	G. Hime
GMRGal4 P{GAL4-GMR.S}	G. Hime
SdGal4; If/CyO P{GawB}sd[SG29.1]	G. Hime
spalt majorGal4	G. Hime
escargotGal4	G. Hime
T1096Gal4	G. Hime
dup[a1]/CyO	BL #7275
dup[a3]/CyO	BL #7276
y[1] w[67c23]; P{w[+mC]=lacW}dup[k03308]/CyO	BL #10530
dpp[hr92] cn[1] bw[1]/SM6a	BL #2069
cn[1] P{ry[+t7.2]=PZ}dpp[10638]/CyO; ry[506]	BL #12379
ru[1] h[1] th[1] st[1] cu[1] sr[1] e[s] stg[4] ca[1]/TM3, Sb[1] Ser[1]	BL #2500
w[1118]; P{w[+mC]=UAS-stg.N}16	BL #4777
ry[506] P{ry[+t7.2]=PZ}stg[01235]/TM3, ry[RK] Sb[1] Ser[1]	BL #11525
y[1] w[*]; P{w[+mC]=lacW}14-3-3epsilon[j2B10]/TM3, Sb[1]	BL #12142
P{ry[+t7.2]=PZ}14-3-3zeta[07103] cn[1]/CyO; ry[506]	BL #12335
w[*]; CycA[C8LR1]/TM3, Sb[1] P{w[+mC]=35UZ}2	BL #6627
P{ry[+t7.2]=PZ}CycA[03946] ry[506]/TM3, ry[RK] Sb[1] Ser[1]	BL #11616
w[*]; P{w[+mC]=UAS-Cdk4-myc}II.1	BL #6631
y[1] w[67c23]; P{w[+mC]=lacW}Cdk4[k06503]/CyO	BL #10629
w[*]; P{w[+mC]=UAS-Cdk1-myc}III.1	BL #6638
w[*]; cdc2[B47] cn[1] bw[1]/CyO, P{ry[+t7.2]=ftz/lacB}E3	BL #6643
w[*]; E2f2[76Q1] cn[1] bw[1]/CyO, P{ry[+t7.2]=ftz/lacB}E3	BL #7436
y[1] w[67c23]; P{w[+mC]=lacW}smt3[k06307]/CyO	BL #10419
y[1] w[67c23]; P{w[+mC]=lacW}CycE[k05007]/CyO	BL #10384
P{ry[+t7.2]=PZ}CycE[05206] cn[1]/ CyO; ry[506]	BL #11396

y[1] w[*]; P{w[+mC]=UAS-CycE.L]ML1	BL #4781
ry[506] P{ry[+t7.2]=PZ}E2f[07172]/TM3, ry[RK] Sb[1] Ser[1]	BL #11717
b[1] Dp[49Fk-1] c[1]/SM5	BL #5553
y[1]; P{y[+mDint2] w[BR.E.BR]=SUPor-P}Dref[KG09294]/CyO; ry[506]	BL #15178
cn[1] bw[1] Kr[1]/SM6a, bw[k1]	BL #3494
cn[1] thr[1] bw[1] sp[1]/ CyO	BL #3262
w[1]; wee[DS1] cn [1]/ CyO P{w[+mC]=ActGFP}JMR1	BL #3499
w[1]; wee[ES1] cn [1]/CyO P{w[+mC]=ActGFP}JMR1	BL #5833
w[*]; P{w[+mC]=UAS-CycA.W}II.2	BL #6633
w[1118]; P{w[+mC]=UAS-E2f.N}3B P{w[+mC]=UAS-Dp}1-4b	BL #4770
al[1] b[1] lat[1] c[1] sp[1]/ CyO sp[*]	BL #5570
CyO SevRas[V12]	G. Hime
SevGal4 UASrl[SEM]/TM6B	G. Hime
aur[87Ac-3]/ MRKS	BL #6188
b[1] Orc5[2] elA[1] rd[s] pr[1] cn[1]/ CyO	BL #3593
fzy[1] cn[1] bw[1] sp[1]/ CyO	BL #2492
nkd e/FLP MKRS	G. Hime
cact[4] pr[1]/ CyO P{ry[+t]=elav-lacZ.H]YH2*	BL #564
SevRas[V12]	G. Hime

10mM EDTA, 100µg/ml Rnase A). Cells were lysed by the addition of 200µl of Solution II (0.2M NaOH, 1% SDS) and proteins and chromosomal DNA were precipitated by 200µl of Solution III (1.25M potassium acetate, 7.14% glacial acetic acid). The precipitate was pelleted by centrifugation at 14,000 rpm for 10 min and the supernatant was added to 1ml of celite slurry (2.3% diatomaceous earth in 7M guanidine hydrochloride). The solution was pulled through a Promega Wizard® minicolumn by a vacuum manifold. The column was washed (200mM NaCl, 20mM Tris-HCl pH 7.5, 5mM EDTA, 50% ethanol) and then placed in an 1.5ml microfuge tube and centrifuged to remove any excess ethanol. The plasmid DNA was eluted with 60µl of TE.

2.10.2 Extracting plasmids from bacteria (midi and maxi preps)

Plasmids were extracted from 25ml or 100ml bacterial cultures using QIAGEN midi and maxi prep kits, respectively, according to manufacturer's specifications. The purified DNA was resuspended in 300µl or 1ml of TE, respectively.

2.10.3 Single fly genomic DNA extraction (for use in single fly PCR)

DNA was extracted from single flies for subsequent PCR analysis as described by Gloor et al., (1993). Single flies were frozen in a 0.5ml microfuge tube and then homogenised on ice using the tip of a yellow micropippette tip containing 50µl of Extraction Buffer (10mM Tris-Cl pH8.2, 1mM EDTA, 25mM NaCl + 200µg/ml Proteinase K) prior to expelling any liquid. Once homogenised the extraction buffer was expelled into the tube. The homogenate was incubated at room temperature to lyse the cells for 30 min and then at 95°C for 2 min to denature the proteinase K. 1µl of the crude extract was used as template DNA in each PCR reaction.

2.10.4 Quick genomic DNA extraction

Genomic DNA was rapidly extracted as described by Huang et al., (2000). Approximately 30 flies were collected in a 1.5ml microfuge tube and frozen at -20ºC. Flies were homogenised using a pestle in 200µl of Buffer A (100mM TrisCl pH 7.5, 100mM EDTA, 100mM NaCl, 0.5% SDS). A further 200µl of Buffer A was added and the slurry was incubated at 65°C for 30 min. 800µl of cold Buffer B (100ml 5M potassium acetate, 250ml 6M lithium chloride) was added and then incubated on ice for between 10 min and a few hours. The solution was centrifuged at 12,000 rpm for 15 min at room temperature. 1ml of the supernatant was transferred to a new microfuge tube, if any of the precipitate was transferred the sample was centrifuged again. 600µl of isopropanol was then added to precipitate the DNA. DNA was recovered by centrifugation at 12,000 rpm for 15 min at room temperature. The pellet was washed with 70% ethanol, air dried, and resuspended in 150µl TE.

2.10.5 Lifton genomic DNA extraction

High quality genomic DNA was extracted from flies according to the method described by Bender et al., (1983). Approximately 100 flies were place into an microfuge tube and frozen at -20ºC. The flies were homogenised in 50µl of fresh Lifton solution (0.2M sucrose, 0.05M EDTA, 0.5% SDS, 100mM Tris pH 9) using a pestle. Once homogenised, a further 400µl of Lifton solution was added and the solution was incubated at 65°C for 30 min. 100µl of 3/5M NaOAc was added and incubated on ice for 60 min. The solution was centrifuged at 10,000 rpm for 10 min at 4°C. The supernatant was divided into two clean microfuge tubes and the DNA was extracted by successive phenol, phenol: IAC (1:1) and IAC extractions. 1µl of RNase (10mg/ml) was added and incubated at 37°C for 15 min. To precipitate the DNA an equal volume

of room temperature ethanol was added, mixed, and incubated at room temperature for 5 min. The DNA precipitate was pelleted by centrifugation at 8000 rpm for 15 min at room temperature and the pellet was washed with 70% ethanol, air dried, and resuspended in 30µl of TE.

2.11 Electrophoresis

DNA electrophoresis was performed using 1-2% agarose gels in 1x TAE buffer at 100V for 45 min. Lambda DNA digested with *HindIII* or *HindIII*/*EcoR1* (Promega) was used as a size marker. DNA was visualised by the addition of ethidium bromide to the gel when cast (0.04µg/ml gel).

2.12 DNA manipulation

2.12.1 Ligation of DNA

The concentration and size of DNA to be ligated were estimated by ethidium bromide fluorescence following gel electrophoresis. Ligations were set up with a 3:1 or 9:1 ratio of insert to vector according to the supplier's directions (Promega) and incubated at 10°C overnight.

2.12.2 Ethanol precipitation

DNA was precipitated by the addition of 1/10th volume of 3/5M NaOAc and twice the volume of cold 100% ethanol, followed by incubation on ice or at –20ºC for at least half an hour. The precipitate was centrifuged at 4°C for 30 min and then washed with cold 70% ethanol. The pellet was air dried and then resuspended in an appropriate volume of TE.

2.12.3 Agarose gel extraction

DNA was extracted for agarose gels using the MinElute Gel Extraction kit (QIAGEN) according to manufacturer's instructions.

2.13 Bacterial transformation

2.13.1 Preparation of chemically competent bacterial cells

A single colony of DH12S cells was used to inoculate a 5ml LB starter culture that was grown at 37°C overnight. This starter culture was added to 500ml of LB and incubated until the OD_{600nm} was between 0.6 and 0.8. The culture was chilled on ice for at least 30 min and then the cells were harvested by centrifugation at 4°C for 10 min. The cells were resuspended in 50ml 0.1M cold $CaCl_2$, incubated on ice for 30 min and centrifuged again. The cells were resuspended in 5ml of cold 15% glycerol in 0.1M $CaCl_2$, aliquoted in 150µl lots and stored at -80°C until needed.

2.13.2 Bacterial transformation

Chemically competent bacterial cells were transformed with 5µl of ligation mix and incubated on ice for 30 min. The cells were heat shocked at 37°C for 2 min, then allowed to recover on ice for 5 min. 1ml of LB was added and then incubated at 37°C for 40 min to allow for expression of antibiotic resistance. Cells were harvested and then resuspended in 100µl of LB and aliquoted onto LB plates with the appropriate antibiotic (ampicillin at 75µg/ml or chlorophenicol at 50µg/ml). The plates were then incubated at 37°C overnight.

2.14 Polymerase Chain Reaction (PCR)

All PCR reactions were carried out on an Eppendorf Mastercycler personal or BioRad iCycler thermocycler. Reactions either used *Taq* polymerase (Biotech) or *Pfu* Turbo® (Stratagene). See Table 2.1 for primer sequences.

2.14.1 Multiplex PCR for detecting mobilised P-elements

In the multiplex PCR reactions performed to identify local P-element transposition, DNA from single fly preps were pooled into groups of five and 1µl of the DNA mix was used in each PCR reaction. When confirmation of the genotype of a particular fly was required, 1µl of its DNA was used in a separate reaction.

Reaction constituents:

dH_2O	8.93µl
5x PCR dye	4µl
10x *Taq* buffer	2µl
$MgCl_2$ (25mM)	2µl
dNTPs (2mM)	1µl
Primer mix 806-812 (equal amounts each of 50µM stock)	0.7µl
Primer PF2	0.17µl
Template (pools of 5 or single preps)	1µl
Taq polymerase	0.2µl

Cycling conditions: 1x 94ºC for 3 min, 30x (94ºC for 20 sec, 65ºC for 10 sec, 72ºC for 2 min), 1x 72ºC for 10 min.

For single primer tests, only 0.1µl of that primer was used in place of the primer mixture and the water volume was adjusted accordingly. PF2 was also used individually in a separate reaction to test if there were two P-elements situated close together on the chromosome and the volume of water was adjusted accordingly.

2.14.2 Generation of PCR templates for sequencing of P-element insertion sites

To map the orientation of each P-element insertion and to generate a template for the sequencing reaction to map the exact site of insertion, DNA from each P-element mobilised line was used in the following reaction:

Reaction constituents:

dH_2O	9.6µl
5x PCR dye	4µl
10x *Taq* buffer	2µl
$MgCl_2$ (25mM)	2µl
dNTPs (2mM)	1µl
primers 806-812, used individually (50µM) or 759-NBS-G2	0.1µl
primer 828 or 829 (50µM)	0.1µl
template (single fly preps)	1µl
Taq polymerase	0.2µl

The cycling conditions were the same as above (Section 2.14.1).

2.14.3 Inverse PCR

To generate template to sequence some of the P-element insertion sites, DNA was extracted using the quick genomic DNA extraction method (Section 2.10.4) and used in the following protocol, which is modified from Huang et al., (2000). 10µl of the DNA preparation was digested with *Msp1* in a total volume of 25µl. 10µl of the DNA digest was ligated in a reaction volume of 400µl, which favours intramolecular ligation. Ligation reactions were then ethanol precipitated and resuspended in 100µl of dH_2O.

PCR reaction constituents:

10x *Taq* buffer	5µl
$MgCl_2$ (25mM)	5µl
dNTPs (2mM)	4µl
primer 752	0.2µl
primer 829	0.2µl
Taq polymerase	0.4µl
Resuspended ligated DNA	10µl
dH_2O	25.2µl

Cycling conditions: 1x 94º for 3 min, 35x (94ºC for 20 sec, 60ºC for 10 sec, 72ºC for 2 min), 1x 72ºC for 10 min. Following inverse PCR amplification, PCR products were separated by gel electrophoresis, excised, purified by gel extraction, and sequenced directly.

2.15 Automated DNA sequencing

PCR products and generated plasmid constructs were sequenced using the ET sequencing mix (Amersham). For PCR product templates, 10ng of DNA per 100 bp was used in each reaction. For plasmid sequencing, 100-300ng of midi or maxi prep plasmid DNA was used per reaction. A 4μl aliquot of ET mix and 0.1μM of primer was used per reaction and subjected to the following cycling conditions: 35x (95ºC for 20 sec, 50ºC for 15 sec, 60ºC for 3 min). Sequencing reactions were ethanol precipitated and sent off for analysis by 96 capillary MegaBACE (Amersham) performed by the Advanced Analytical Centre, James Cook University, Townsville.

2.16 Generation of plasmid constructs used in this study

2.16.1 UAS-*deflated* cDNA

The *deflated* cDNA (3.2 kb) was excised from pOT2 by the restriction enzymes *EcoR1* and *Xho1* and subcloned into pUAST cut with these same enzymes.

2.16.2 UAS-*deflated::GFP*

The *deflated* cDNA was used in a PCR reaction to generate a product that contained a *Kpn1* site 5′ and a *HindIII* site 3′, the latter also designed to abolish the TAA stop codon. This fragment was cloned into pALX190 so that the GFP coding region was fused in frame at the 3′ end of the *deflated* cDNA. The *deflated* cDNA and GFP coding

regions were then excised using the restriction enzymes *Kpn1* and *Xba1* and subcloned into both pUAST and pUASP via these same sites.

PCR reaction constituents:

H_2O	12.7µl
10x *Taq* buffer	2µl
$MgCl_2$ (25mM)	2µl
dNTPs (2mM)	2µl
primer A015 (50µM)	0.2µl
primer A016 (50µM)	0.2µl
Taq polymerase	0.4µl
pOT2-*deflated* (0.3µg)	0.5µl

Cycling conditions: 1x 94ºC for 2 min, 5x (94ºC for 10 sec, 55ºC for 15 sec, 72ºC for 2.5 min), 25x (94ºC for 10 sec, 60ºC for 15 sec, 72ºC for 2.5 min), 1x 72ºC for 10 min.

2.16.3 UAS-*deflated*^{S653A} and UAS-*deflated*^{S653E}

The pOT2-*deflated* cDNA construct was used as template for site-directed mutagenesis using *Pfu* Turbo® polymerase and the quick change protocol (Stratagene). The oligonucleotide primers used were generated with the aid of The Primer Generator (http://www.med.jhu.edu/medcenter/primer/primer.cgi).

Site-directed mutagenesis reaction constituents:

10x *Pfu* buffer	5µl
pOT2-*deflated* DNA(50ng)	2.2µl
primer A075 or A079	0.27µl or 0.29µl (for 125ng primer)
primer A076 or A078	0.27µl or 0.29µl (for 125ng primer)
dNTPs (2mM)	1µl
dH_2O	40.26µl or 40.22µl
Pfu Turbo	1µl

Cycling conditions: 1x 95ºC 1 min, 16x (95ºC 30 sec, 65ºC for 30 sec, 68ºC 11 min). 30% of each site-directed mutagenesis reaction (15µl) was electrophoresed and if an amplified product was observed then the remainder was digested with 1µl of *Dpn1* to

degrade the template DNA. 10µl was then used to transform bacterial cells and the resulting transformants were tested for mutagenised plasmid by restriction enzyme digest with *BseR1*, since the introduced mutations were designed to abolish this site at position 2006 of the cDNA. Plasmids carrying the desired S653A and S653E mutations were excised from pOT2 by digestion with *EcoR1* and *Xba1* and subcloned into pUAST using these same restriction enzyme sites.

2.17 *Drosophila* transformation

2.17.1 Injection of embryos

Microinjections were performed with 1mm thin walled capillaries (Clark Capillaries) that had been pulled to a fine point using a Narishige PC-10 needle puller as previously described (Spradling, 1986). The capillaries were back-filled with DNA solution and then mounted on a micromanipulator. The volume of DNA solution injected per embryo was controlled by an Eppendorf Femptoject microinjector. w^{1118} embryos of < 20 min old were microinjected in their posterior end with a solution containing the P–element plasmid of interest and a Δ2-3 helper plasmid resuspended in injection buffer (5mM KCl, 0.1mM PO_4, pH 7.8) to a final concentration of 150µg/µl and 100µg/µl, respectively.

2.17.2 Selection of transformants

Injected embryos were allowed to develop to first instar larvae in a humid chamber for 24 hr. Hatched larvae were collected and put into vials containing standard cornmeal-treacle media supplemented with instant *Drosophila* medium (Sigma). G_0 adults that subsequently eclosed were backcrossed to w^{1118} flies. Germline transformants in the G_1 progeny were selected due to coloured eyes caused by expression of the w^+ allele on the

P-element vector. P-element insertions were mapped to a chromosome by segregation analysis using the w^{-}/w^{-}; *CyO*/*If*; *TM6B*/*MKRS* stock.

2.18 Assessment of lethality period of homozygous *deflated* mutant individuals

Eggs from $defl^{-}$/*TM6B(α-IT::GFP)* parents were collected on grape juice agar (1.5%) plates overnight at 25°C. The eggs were transferred to fresh grape juice agar plates and arrayed in a grid. Small amounts of yeast paste were provided on the edges of the plate. The new plates were incubated at 25°C for 24 hr and the number of larvae that had hatched were counted and scored for GFP fluorescence. The larvae were placed on a fresh plate with yeast paste and incubated for a further 24 hr. This was continued every 24 hr until no homozygous individuals (those that were tubby and lacked GFP fluorescence) remained alive.

2.19 Examination of chorion and dorsal appendage formation in eggs

Eggs laid by transheterozygote or cDNA-rescued homozygous *deflated* mothers were collected on grape juice agar (1.5%) plates. Eggs were picked off the plate with a pair of forceps and washed in a drop of PBS, then placed in a clean drop of PBS for photography.

2.20 Collection of *Drosophila* embryos

Embryos were collected on grape juice agar (1.5%) plates for indicated time periods. Embryos were washed off the plates with distilled water into nylon mesh collection baskets, washed with embryo Rinse Solution (0.7% NaCl and 0.1% Triton X-100) and then dechorionated in 50% bleach for 2 min. The embryos were washed again in Rinse Solution and then transferred to a microfuge tube.

2.21 Whole mount RNA *in situ* hybridisation of embryos

2.21.1 Generation of riboprobe template

To generate the sense and antisense templates for riboprobe synthesis, DNA to exon 1 of *deflated* was generated by PCR using primers 854 and 856 and 855 and 857 and the following reaction:

H_2O	28.8µl
Taq buffer (10x)	4µl
$MgCl_2$ (25mM)	3.5µl
dNTPs (2mM)	2µl
reverse primer 856 or 857 (50µM)	0.4µl
forward primer 854 or 856 (50µM)	0.4µl
template (*w1118* genomic DNA)	0.5µl
Taq polymerase	0.4µl

Cycling: 1x 94ºC for 3 min, 30x (94ºC for 20 sec, 60ºC for 10 sec, 72º for 1 min), 1x 72ºC for 2 min. The resulting ~800 bp PCR fragments were separated by gel electrophoresis, excised, and purified by gel extraction.

2.21.2 Generation of DIG labelled riboprobe

All solutions used in the following steps were treated with DEPC to prevent RNase contamination. The yield of purified sense and antisense templates was quantified by ethidium fluorescence following gel electrophoresis and approximately 100ng was used in each labelling reaction. DIG (Roche) labelled riboprobes were generated in the following reaction by incubation at 37°C for 2 hr:

deflated rT7 and fT7 template	104 ng
10X DIG labelling mix	2 µl
T7 RNA polymerase transcription buffer	2µl
T7 RNA polymerase	2µl
Rnasin® RNase inhibitor	1µl
H_2O	11µl

The resulting DIG labelled riboprobes were precipitated with 2.5µl of 4M LiCl and 75µl prechilled 100% ethanol and stored overnight at -20°C. The probes were pelleted by centrifugation for 15 min at 4°C and washed in 70% ethanol and centrifuged again for 5 min. The dried pellet was resuspended in 100µl formamide to minimise degradation and stored at -80°C.

2.21.3 Testing of DIG labelled riboprobes by dot blot

DIG labelled riboprobes were serially diluted 10^{-1}, 10^{-2}, and 10^{-3} in H_2O. 1µl of undiluted and 1µl each dilution was added to 5µl of 5x SSC and heated at 80°C for 5 min. The samples were cooled on ice and centrifuged. 1µl of each dilution was spotted on nitrocellulose Hybond C (Amersham) and baked between blotting paper for 30 min at 80°C. The filter was then wetted with 2x SSC and washed twice in PBTw for 5 min each. The filter was blocked in PBTw for 30 min and incubated with 0.2µl of anti-DIG-alkaline phosphatase antibody (Roche) per ml of PBTw for 60 min. Filters were washed with PBTw (four times, 15 min each), then with DIG staining buffer (100mM NaCl, 50mM $MgCl_2$, 100mM Tris pH 9.5, 0.1% Tween 20) twice for 5 min. Nitrocellulose membranes were developed in 1ml of DIG staining buffer with 20µl NBT/BCIP solution (50x conc. 18.75mg/ml NBT and 9.4 mg/ml BCIP; Roche). After adequate colour developement the blot was washed several times in PBTw. The relative concentrations of the sense and antisense probes were determined by eye.

2.21.4 *In situ* hybridisation to embryos

Embryos were collected for 24 hr and treated as in Section 2.20. They were fixed in a 1:1 solution of 3.7% paraformaldehyde (in PBS): heptane for 30 min. After removal of the paraformaldehyde, the embryos were devitenillised by the addition of an equal

volume of methanol and shaken vigourously for 30 sec. Both the heptane and methanol were removed and the embryos washed three times in methanol to remove all traces of heptane. The embryos were then washed three more times in ethanol and then either stored under ethanol at -20°C or used immediately. Before use, embryos were rinsed twice in 100% ethanol, then once in ethanol: xylene (1:1). Embryos were then soaked in 100% xylene for 90 min to reduce background, then rinsed in xylene: ethanol (1:1), then several times in 100% ethanol. Following this, embryos were rinsed once in methanol, then in methanol: PBTw (1:1). They were fixed again in 3.7% paraformaldehyde in PBTw for 20 min and rinsed three times in PBTw. The embryos were split between two tubes and digested with 4μg/ml non-predigested Proteinase K (Sigma) at 37°C for 3 or 5 min. The protease digestion was stopped by quickly rinsing in PBTw twice. The embryos were fixed again in 3.7% paraformaldehyde in PBTw for 20 min. They were washed five times in PBTw for at least 5 min per wash. Embryos were split between another two tubes, in order to have test (anti-sense probe) and control (sense probe) tubes. The embryos were rinsed in a 1:1 solution of PBTw: prehybe solution (50% deionised formamide, 5x SSC, 50μg/ml heparin, 0.1% Tween 20) and then prehybed in 100% hybe solution (prehybe solution plus 100μg/ml herring sperm DNA) for at least 1 hr at 55°C. Hybridisation occurred at 55°C overnight in 100μl of hybe solution with equal amounts of sense and antisense riboprobe denatured at 80°C for 10 min added to control and test tubes, respectively. The hybe solution was drawn off with a finely drawn out Pasteur pipette. All washes were then done at 55°C with pre-warmed solutions. The embryos were washed for 20 min in prehybe solution, followed by 20 min in 1:1 prehybe solution: PBTw, and five times for 20 min in PBTw. The washed embryos were incubated in 1:2000 dilution of anti-DIG-alkaline phosphatase antibody in PBTw for 1 hr to detect DIG-labelled riboprobes. The embryos

were then washed in PBTw four times for 20 min. Embryos were transferred to plastic tissue culture wells in order to observe the colour change more readily under a dissecting microscope. The embryos were rinsed three times for 5 min with 1ml DIG staining buffer. To the third 1ml wash, 20µl of NBT/BCIP was added and the colour was allowed to develop in the dark. Once sufficient colour development had occurred, the reaction was stopped by rinsing the embryos in 20mM EPTA in PBTw. Five min washes were then performed at least ten times. Embryos were left in 80% glycerol, 20mM EPTA in PBS overnight and then were mounted on slides using double sided tape as a bridge between the slide and the coverslip to prevent flattening of the embryos.

2.22 Examination of imaginal discs from third instar larvae

Third instar larvae were cut in half, the front half was turned inside out and most of the fat removed. These carcasses were fixed for 60 min in 3.7% paraformaldehyde in PBS. Imaginal discs were dissected away from the remaining material and mounted in 80% glycerol in PBS for photography.

2.23 Antibody detection of larval tissues

All manipulations involving larval tissues were carried out in cut-off microfuge tube lids. Second or third instar larvae were roughly dissected in PBS by cutting in half and turning inside out before being fixed in 3.7% paraformaldehyde in PBS for 60 min. Following fixation, discs or brains were dissected completely in PBS. Alternatively, the brains and discs were dissected fresh and then fixed in 3.7% paraformaldehyde in PBS for 30 min. The tissues were washed a few times in PBS and then a few times in PBTx. They were incubated for 30 min in Wash Solution (0.2% BSA, 0.1% Triton X-100 in

PBS) and then blocked for 1 hr in Block Solution (1% BSA, 0.3% Triton X-100, 10% goat serum in PBS). Incubation of the primary antibody(ies) at appropriate concentrations was performed in block solution at 10ºC overnight. The tissues were washed twice rapidly with Wash Solution then washed over a 2 hr period with regular changes of solution. The secondary antibody(ies) were incubated for 1hr at room temp. Material was again rapidly washed twice, then washed at regular intervals over a 2 hr period and then left in wash solution at room temperature overnight. The tissues were mounted in a few drops of 80% glycerol in PBS for imaging by confocal microscopy.

2.24 BrdU labelling and detection of larval tissues

BrdU labelling of S-phase cells was performed essentially as described by Royzman et al., (1997). Desired larval tissues were dissected cleanly in PBS and placed into a cut-off microfuge tube lid containing Schneider Insect Cell Media (Sigma). If a number of dissections were to be performed, the lid(s) were kept on ice until all material had been collected. The lids were removed from the ice and BrdU was added at a final concentration of 1mg/ml and material was incubated at room temperature for 30 min (eye imaginal discs) or 1hr (second instar brains). The BrdU containing media was removed and the tissues were washed rapidly three times in PBS. They were then fixed in 3.7% paraformaldeyde in PBS for 30 min, then washed in PBS. Washed material was incubated in PBTx for up to 30 min then denatured in 2M HCl in PBTx for 70 min. The denatured tissue was again rapidly washed twice with PBTx, then washed for about 1hr, changing the solution about every 15 min. After this the material was processed as for normal antibody staining (Section 2.23) using a 1:20 dilution of the anti-BrdU antibody (Pharmigen).

2.25 Preparation of *Drosophila* for scanning electron microscopy

Adult flies were dehydrated by passing through a series of acetone: H_2O solutions (25% acetone for 2 hr, 50% acetone overnight, 75% acetone overnight and 100% acetone) with gentle agitation. They remained in 100% acetone until they were mounted. The acetone was allowed to evaporate off and the flies were mounted, using a stereomicroscope, onto adhesive circles on metal stubs. Samples were then sputter-coated in platinum five or six times before being imaged.

2.26 Preparation and mounting of wings

Flies were stored in wing dissection solution (50% ethanol: 50% lactic acid) at least overnight prior to mounting. The wings were dissected and mounted in wing dissection solution under a coverslip and imaged immediately.

2.27 Microscopy

Light micrographs were taken on an Olympus BX51 microscope or Olympus SZ60 dissecting microscope equipped with an Olympus DP50 digital camera. Fluorescent images were taken on a BioRad 2000 laser scanning confocal microscope with Lasersharp 2000 (ver. 5) software. Scanning electron micrographs were taken on a Joel JSM 5410LV scanning electron microscope with "SemAfore" software. All images were processed by ImagePro and Graphics Converter.

Chapter 3- Generation and molecular analysis of mutant alleles of *deflated*

3.1 Introduction

deflated (CG18176) is found on chromosome 3L in a gene rich region in polytene band 67C5 (Figure 3.1). It is flanked by *nbs* (the homologue of the NBS DNA repair gene, see Section 1.1.4) and another uncharacterised gene CG18177, a putative acetyltransferase. Attempts to generate germline mutations of *nbs* resulted in the additional recovery of mutations in *deflated*. These alleles were generated using a P-element, EP(3)3301, which is inserted 276 bp downstream of *deflated,* as the mutagen. This P-element insertion was generated during a genome disruption screen by the BDGP Project Members (2000) and does not cause any observable phenotypes.

Two approaches were used to generate *nbs* and *deflated* alleles, P-element mobilisation and P-element induced male recombination. When mobilised, P-elements frequently jump locally (Golic, 1994; Tower et al., 1993; Zhang and Spradling, 1993), so the first approach aimed to take advantage of this property through local mobilisation and insertion into the *nbs* and *deflated* coding regions. The second approach takes advantage of the fact that P-elements can induce apparent recombination in *Drosophila* males (which normally do not undergo meiotic recombination) due to formation of a double strand break at the site of the P-element. In repairing this break against its homologue the chromosomes can in effect 'recombine'. Two thirds of recombined chromosomes show a chromosomal rearrangement of either a duplication or a deletion at the site of the P-element (Preston and Engels, 1996; Preston et al., 1996). Thus, this second approach aimed at generating *nbs* and *deflated* alleles by causing chromosomal

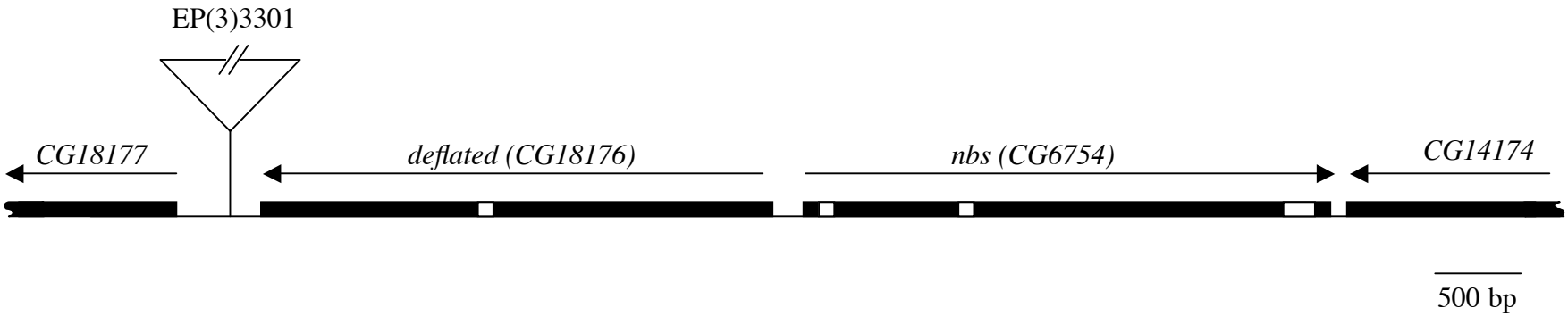

Figure 3.1 The *deflated* genomic locus.

The exon/intron structure of *deflated* and surrounding genes is shown. Black boxes represent exons and white boxes represent introns. Arrows indicate the direction of transcription. *deflated* is found on chromosome 3L at 67C. It is flanked by the genes *nbs* and *CG18177*. The presence of a P-element inserted approximately 270 bp downstream from *deflated*, EP(3)3301, enabled the generation of *deflated* alleles by P-element mutagenesis.

deletions originating at the P-element insertion site into the *nbs* and *deflated* coding regions.

3.2 Generation of alleles by P-element mobilisation

3.2.1 Inducing P-element mobilisation

To mobilise the *EP(3)3301* element, flies of this line were crossed to flies that contained the *Δ2-3 transposase* (Figure 3.2; Robertson et al., 1988). Flies containing both the *EP(3)3301* element and the *Δ2-3 transposase* were backcrossed to w^{1118} flies. As mobilisation of the P-element occurs in the germ line of these flies, backcrossing resulted in the independent segregation of the *Δ2-3 transposase* and the potentially mobilised P-element, thereby stabilising the P-element in a population of the progeny. Offspring of this cross (that still retained the P-element as indicated by expression of the dominant eye colour marker, *white*) were mated singly, as mobilisation events could potentially differ between individuals. Flies that contained a darker eye than the *EP(3)3301* flies were crossed preferentially because darker eyes are considered indicative of mobilisation of the P-element, either due to new local chromosomal effects on expression or, as is commonly seen for local transpositions, two copies of the P-element being in close proximity (Golic, 1994; Timakov et al., 2002; Tower et al., 1993). The parental sex and rearing temperatures were noted as it has been observed that P-element insertions and mobilisations can vary in the two germlines and with temperature (Timakov et al., 2002; Zhang and Spradling, 1993). Once F3 larvae were present, the F2 parental fly, containing the putative mobilised P-element, was frozen prior to DNA extraction and subsequent identification of a mobilised P-element using PCR (see Section 3.2.2). Lines that were identified as containing a mobilised event of

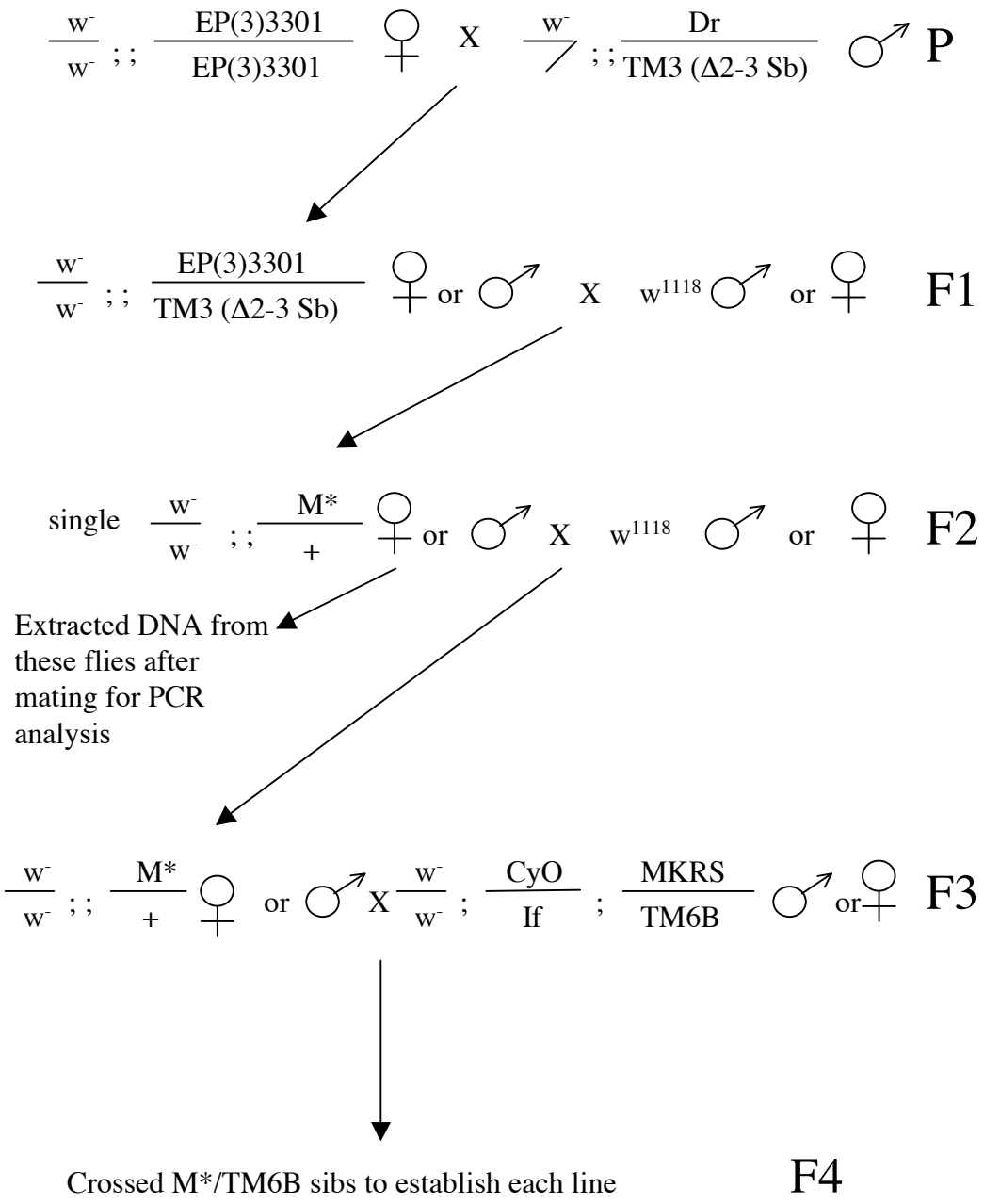

Figure 3.2 The genetic cross to mobilise the P-element in EP(3)3301.

Homozygous flies containing the EP P-element 276 bp downstream of *deflated* were crossed to flies containing Δ2-3 transposase (P). In the F1 generation stubble flies (TM3) were crossed to w^{1118} for both transposition to occur in the germline and to segregate Δ2-3 from the mobilised element (M*). In the F2 generation single flies containing potential mobilised elements (M*) were crossed to w^{1118} and once mated were tested by multiplex PCR for mobilisation into the *nbs* and *deflated* genomic region. Offspring of those F2 flies that had an insert of interest were crossed to a multiple balancer stock(F3) in order to set up a balanced stock from the F4.

interest were established as balanced heterozygous lines over the *TM6B* balancer (Lindsley and Zimm, 1992) by crossing F4 flies of the appropriate genotype.

3.2.2 A multiplex PCR screen was used to identify mobilised P-elements

A multiplex PCR screen that could differentiate between mobilised and non-mobilised elements was designed to identify P-element mobilisations into the *nbs* and *deflated* genomic region (Figure 3.3). In the multiplex PCR, screen seven genomic primers (a-g) and a primer that can bind to the inverted repeat ends of the P-element (PF2) were used (Table 2.1). The screen was designed so that non-mobilised elements would generate a PCR product of just under 1.5 kb produced by priming between the genomic primer a and the PF2 primer of the P-element arm (Figure 3.3 A). In contrast, mobilised elements would generate PCR products 1 kb or less in size due to the other genomic primers being complementary to genomic sequence spaced 1 kb or less apart. A hypothetical example given in Figure 3.3 B shows the P-element mobilised into the coding region of *nbs* and the subsequent PCR product generated is approximately 740 bp in size due to priming between genomic primer e and PF2. PCR conditions were optimised prior to commencement of the screen to ensure that all the primers would produce a product under the same conditions and within the same reaction (Section 2.14.1) and that one chromosome in ten (the equivalent of one chromosome in one out of five flies having a mobilised element) could be detected (data not shown).

If a product of < 1 kb was produced, the DNA from each of the five flies was used in separate reactions to identify which fly carried the mobilisation. Figure 3.4 A shows a representative gel demonstrating the initial identification of a mobilised element, which was subsequently found to be present in the line MCEP. To map individual mobilised

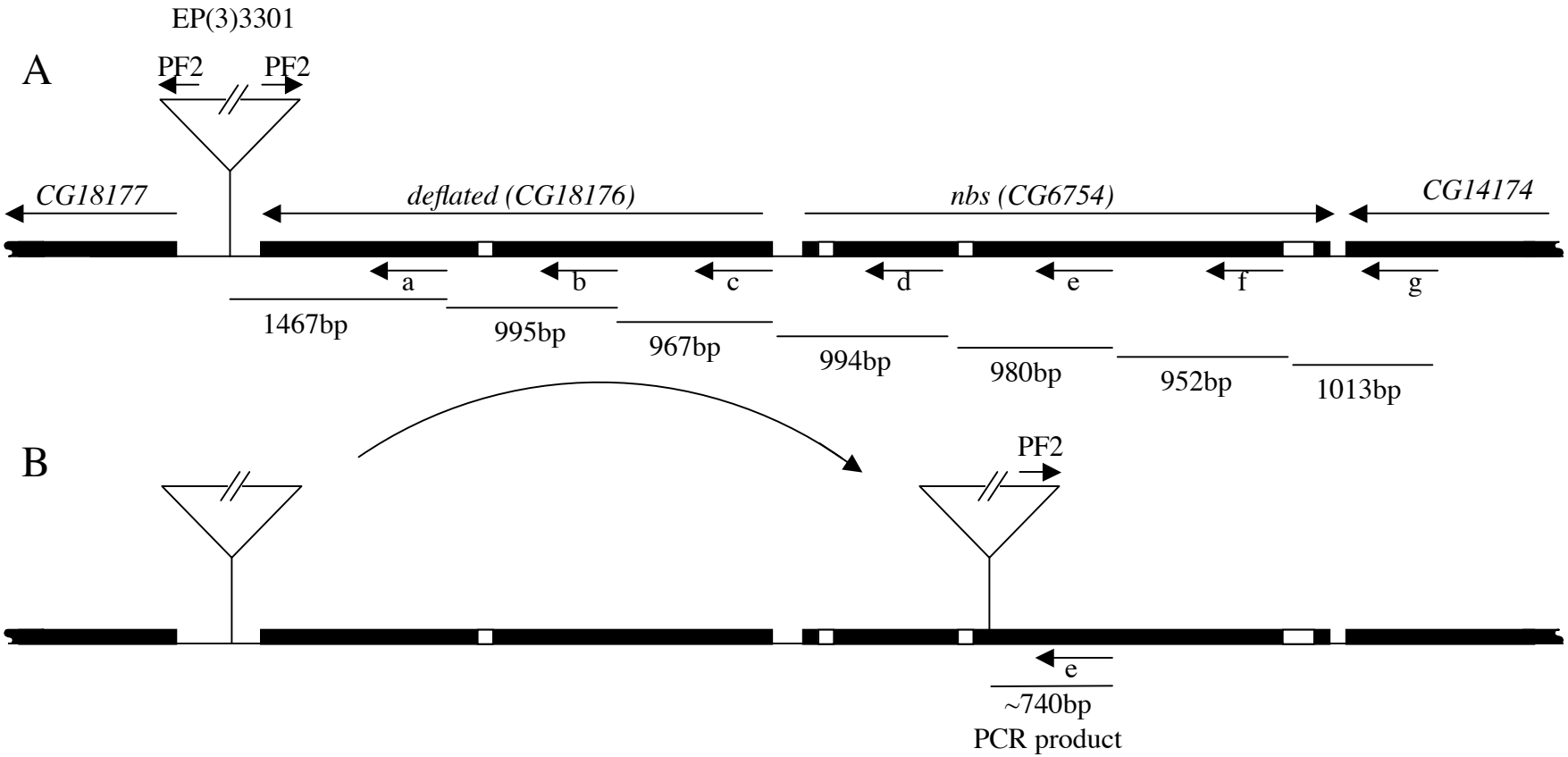

Figure 3.3 Multiplex PCR strategy employed to identify P-element mobilisations into the *nbs* and *deflated* genomic region.

(A) Mobilisation of the 11 kb P-element insert EP(3)3301 from 276 bp downstream of the *deflated* coding region can be detected by multiplex PCR. Oligonucleotide primer a was designed to generate a 1.5 kb product with the P-element specific primer PF2 if the P-element fails to mobilise and primers b-g were designed to generate a product of >1 kb if the P-element mobilised locally. **(B)** In the hypothetical example given, the mobilised element inserts into the *nbs* coding region. The resulting PCR product between PF2 and primer e ~740 bp in size.

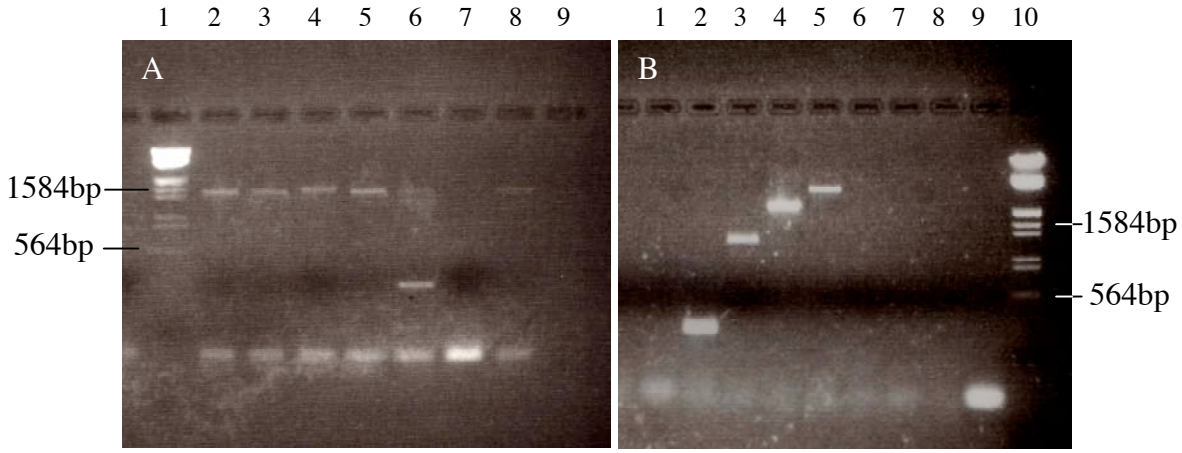

Figure 3.4 Identification of mobilised P-elements by multiplex PCR.

(**A**) PCR products generated from multiplex reactions containing DNA template consisting of pools of genomic DNA from 5 flies were separated by gel electrophoresis (2% agarose gel in TAE; λ *HindIII*/ *EcoRI* marker lane 1). Lanes 2-5 show non mobilised P-elements as the PCR products are ~1.5 kb in size. Lane 6 indicated the presence of a mobilised P-element within the pool of DNA by the presence of an additional product of ~300 bp. Examination of the DNA from each of the five flies in separate reactions allowed identification of this transposition to have occurred in line MCEP. Lane 7 contains DNA from a w^{1118} fly and serves as a negative control. Lane 8 contains DNA from EP(3)3301 and serves as a positive control. (**B**) Each of the genomic primers (a-g) were used in separate PCR reactions with MCEP genomic DNA as the template in order to roughly map the insertion site (lanes 1-7). The PCR products were separated by gel electrophoresis (1.5% agarose gel in TAE) with the marker λ *HindIII*/*EcoR1* (lane 10). Reactions using PF2 primer only and MCEP template (lane 8) and a w^{1118} template using all eight genomic primers (lane 9) are also shown. The absence of a product in the reaction containing primer a (lane 1) and the ~300 bp product using primer b (lane 2) revealed that the P-element in MCEP is inserted ~300 bp upstream of the primer b binding site, which is in the *deflated* coding region.

elements, the genomic primers were used individually in separate PCR reactions and therefore the presence and size of a product using a particular primer enabled an estimate of the insertion site (Figure 3.4 B). The PF2 primer was also used on its own to check for any mobilisations that resulted in two P-elements close enough to each other to generate a PCR product. In all mobilisation events identified no products were generated using primer PF2 alone. For MCEP, a product of approximately 300 bp was generated using genomic primer b, so the insertion could be mapped to approximately 300 bp upstream of primer b which is within the coding region of *deflated* (Figure 3.3 A).

3.2.3 P-element mobilisation generated 27 local transpositions

Using the approach just described, a total of 2309 flies were screened (with approximately 20% of screened flies showing discernibly darker eyes) and 20 local transpositions were identified based on a change in the size of PCR product. Upon rough mapping it was found that five transpositions (MAJL, MBEZ, MCEP, MBSM and MATX) had inserted into *deflated* but none into *nbs*. To isolate further alleles, two of these mobilised P-elements (MCEP and MBSM) were used as the starting element for another round of mobilisations as they were the closest to the *nbs* coding region. A further seven mobilised elements were recovered out of 1325 flies tested (with approximately 5% having darker eyes). Five P-elements had inserted into *deflated* (EPACA, SMZN, SMAHC, SMVU, SMWV) but none had inserted into *nbs*. The remainder of the mobilised P-elements mapped very close to the original EP(3)3301 insertion site.

The mobilisation events recovered were roughly divided in half having a darker eye phenotype and the other with a similar eye colour to flies containing the original insert (Table 3.1). However, most transpositions that resulted in a similar eye colour to the *EP(3)3301* insert had inserted into the original site. Therefore darker eye colour was more indicative of a desired mobilisation event (defined as a jump into sequence other than in the original insertion site; 9/14 with darker eyes, compared to 3/13 with the original eye colour). The male germline generated more of these desired mobilisation events (10/18, compared to 2/9 for females). This may reflect the slightly higher proportion of darker eyed flies tested from male parents (0.175 to 0.125), but this difference does not account for the difference in desired mobilisation events between male and female germlines. Temperature had a major effect on transpositions in the female germline as none were recovered from flies raised at 29°C. The effects of temperature on the transpositions in the male germline were not as striking but more desired mobilisation events were recovered from males raised at 29°C (6/8, compared to 4/10 at 25°C).

3.3 Generation of an *nbs* and *deflated* deletion by P-element induced male recombination

The second approach to generate alleles of *nbs* and/or *deflated* was P-element induced male recombination using the MCEP insertion as the starting element. Two steps were required to identify male recombination events and associated deletions. The first step was to induce the recombination event between the P-element-containing chromosome and its homologue, which contained a number of recessive alleles scattered along its length (Figure 3.5). As a result, the recombined chromosome contained recessive

Table 3.1 Summary of germline source and rearing temperature for each mobilisation recovered.

	Male 25°C	Female 25°C	Male 29°C	Female 29°C
Darker eye colour	MAJL[†] MATX MBEZ MBEY MCEE MDEV	MDEK EPKQ EPKR	MABN MBEP MBEV MBCL MCEV	none
Same eye colour	SMVU SMWV SMZN EPACA	MCGW MCHT MCIP MCPR MCOR SMAHC	MBJO MBSM MCEP	none
Total darker eyes tested (proportion)	291 (0.2)	103 (0.1)	76 (0.15)	45 (0.15)
Total tested	1420	931	501	300

[†] Coloured text indicates which of the complementation groups each line belongs to. For further details see Figure 3.8.

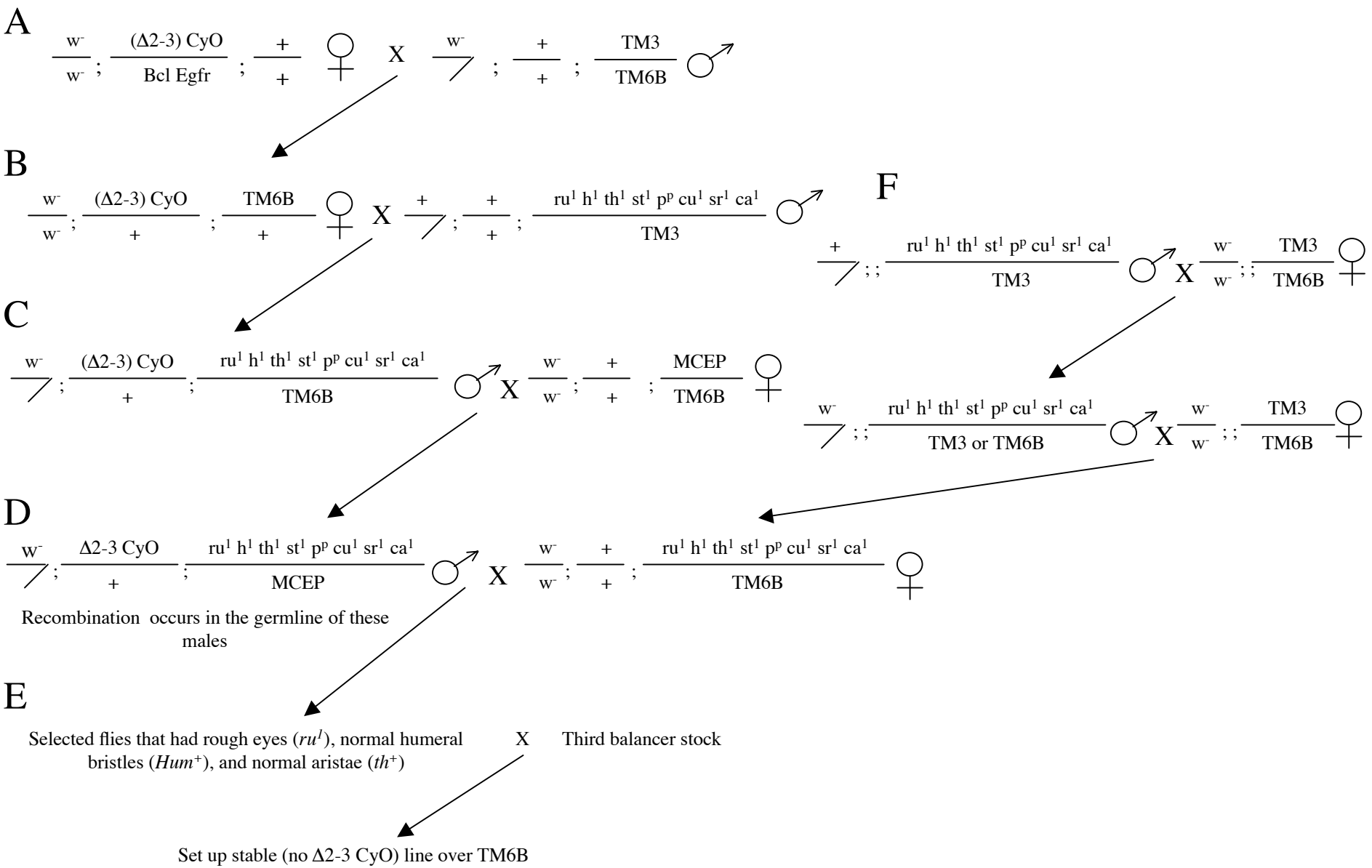
A
w- / w- ; (Δ2-3) CyO / Bcl Egfr ; + / + ♀ X w- / ♂ ; + / + ; TM3 / TM6B ♂
B
w- / w- ; (Δ2-3) CyO / + ; TM6B / + ♀ X + / ♂ ; + / + ; ru1 h1 th1 st1 pp cu1 sr1 ca1 / TM3 ♂
C
w- / ♂ ; (Δ2-3) CyO / + ; ru1 h1 th1 st1 pp cu1 sr1 ca1 / TM6B ♂ X w- / w- ; + / + ; MCEP / TM6B ♀
D
w- / ♂ ; Δ2-3 CyO / + ; ru1 h1 th1 st1 pp cu1 sr1 ca1 / MCEP ♂ X w- / w- ; + / + ; ru1 h1 th1 st1 pp cu1 sr1 ca1 / TM6B ♀
Recombination occurs in the germline of these males
E
Selected flies that had rough eyes (ru1), normal humeral bristles (Hum+), and normal aristae (th+)
X
Third balancer stock
Set up stable (no Δ2-3 CyO) line over TM6B
F
+ / ♂ ; ; ru1 h1 th1 st1 pp cu1 sr1 ca1 / TM3 ♂ X w- / w- ; ; TM3 / TM6B ♀
w- / ♂ ; ; ru1 h1 th1 st1 pp cu1 sr1 ca1 / TM3 or TM6B ♂ X w- / w- ; ; TM3 / TM6B ♀

Figure 3.5 The genetic cross used to generate deletions via P-element induced male recombination

(**A**) A Δ2-3 transposase source present on a CyO balancer chromosome was crossed to a third balancer stock. (**B**) A multiply marker third chromosome was then crossed into the fly with the Δ2-3 transposase source. The two different third balancer chromosomes were used to be able to distinguish between the wild type and the recessively marked chromosome. (**C**) The chromosome carrying the MCEP insertion was crossed into the background of Δ2-3 and multiply marked chromosome. (**D**) Males containing the multiply marked chromosome over the MCEP insertion and the Δ2-3 were crossed to females that contain the same multiply marked chromosome over the balancer TM6B. P-element induced male recombination occurs in the germline of these males. (**E**) Identification of desired recombination events was revealed by the presence of rough eyes *(ru*$^{-}$*),* but normal aristalae (*th*$^{+}$) in flies containing the recombined chromosome over the multiply-marked chromosome (identified by absence of humeral bristles (TM6B)). Flies containing recombination events were crossed to a third balancer stock to establish it as a heterozygous balanced stock over TM6B. (**F**) Females needed to be generated that contained the multiply marked third chromosome over TM6B and a white eye allele on the X, so that the presence of the P-element could be identified in the flies containing recombination events in E.

markers, either proximal or distal to the P-element, which would enable its identification when it was backcrossed to the multiply-marked chromosome.

Since recombination can occur at either end of the P-element but the associated deletions occur unidirectionally (Preston and Engles, 1996; Preston et al., 1996), only half of the recombination events were selected for. This was achieved by selecting chromosomes that contain the recessive markers on the same side of the P-element as the gene of interest. Therefore, in this particular case, the MCEP insertion is proximal to the transcription start sites of *deflated* and *nbs* (Figure 3.6). Therefore recessive markers that are distal are selected for. On the multiply-marked chromosome used, *hairy* (*h*) and *roughoid* (*ru*) are distal to *deflated* and *nbs* and therefore would also be involved in the recombination event. *roughoid* was chosen as the marker as it was easiest to score. On the other hand, *thread* (*th*) is proximal to the MCEP insertion so will be selected against. Flies that had rough eyes (*roughoid*$^{-}$) but were wild type for *thread* and for the balancer marker *Humeral* were taken and mated to a third balancer stock prior to molecular testing as putative deletion-containing chromosomes.

To test the recombined chromosomes for deletions of the DNA distal to the MCEP insertion site, the same multiplex PCR approach used to test for mobilisations was employed, since the P-element remains intact (Section 3.2.2). Using this approach, 2985 flies were examined and a total of 14 distal recombination events were observed. One of these (D1) produced a PCR product using genomic primer e and the PF2 primer, indicating a breakpoint in the *nbs* coding region and a deletion of both the transcription start sites of *nbs* and *deflated* (Figure 3.8 and 3.9).

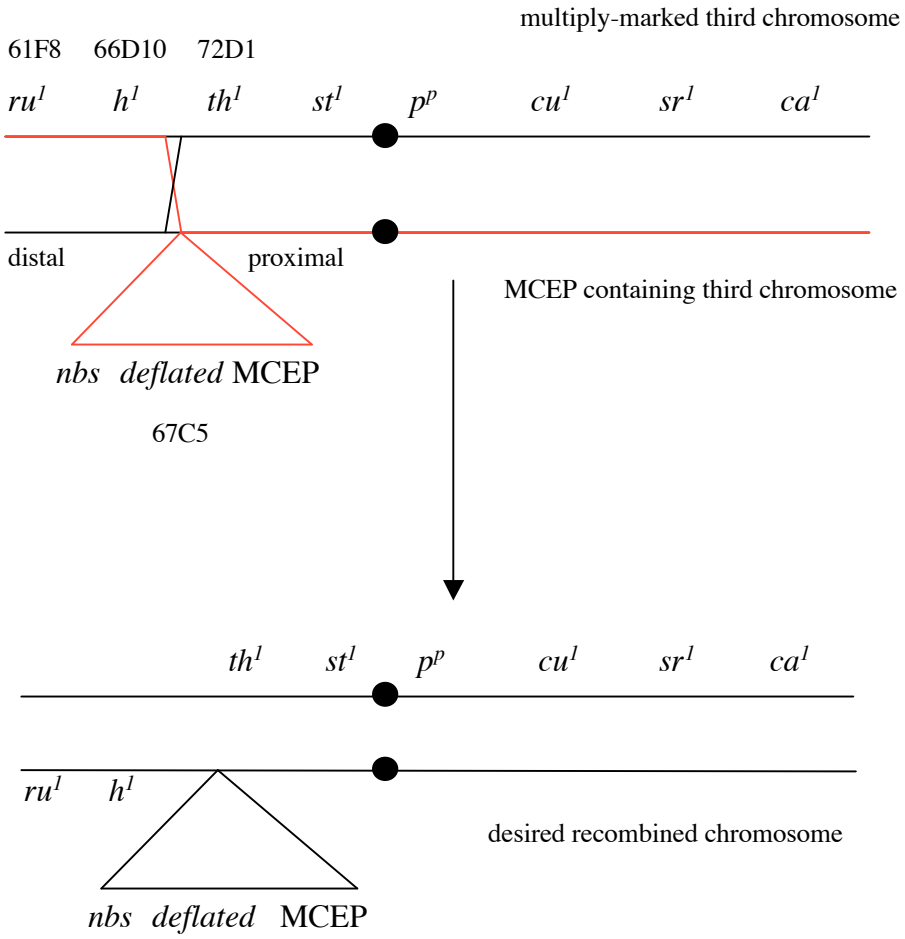

Figure 3.6 The selection of desired P-element induced male recombination events

Markers on both the multiply-marked chromosome and the MCEP insertion containing chromosome are shown (not drawn to scale, black circles represent centromeres). *deflated* and *nbs* are found at 67C5 between *hairy* and *thread*. MCEP is inserted in the *deflated* coding region and is proximal to the transcription sites of both *deflated* and *nbs*. The chromosomal positions of the recessive markers flanking 67C are shown. Any recombination events originating at MCEP and involving *deflated* and *nbs* will also involved *h* and *ru* as shown by the red line as they are also distal to MCEP. This will result in the desired recombined chromosome as shown.

3.4 Complementation analysis

To begin characterisation of the insertions and deletion alleles generated, all were balanced over *TM6B*. Sixteen of the insertions and the one deletion proved to be recessive lethal. The number of complementation groups represented by these seventeen alleles was determined by pairwise complementation analysis. Four distinct complementation groups were identified, denoted A-D (Figure 3.7).

During the course of the complementation analysis it was found that transheterozygote combinations of Group B alleles had a pupal abdominal phenotype, which led to the CG18176 being named *deflated* (see Section 4.4.2). The combinations that gave this abdominal phenotype involved MBEZ and any of the other alleles that fell into this group (indicated by an asterisk in Figure 3.7). As MBEZ demonstrated recessive lethality and also fell into complementation group D it was concluded that this chromosome carries two lesions that affect two different genes, *deflated* and another unknown gene. The recessive lethality is most likely due to disruption of the other gene, since the effect the MBEZ allele has on *deflated* function appears quite mild since development can progress to adulthood in a percentage of individuals when in *trans* to other *deflated* alleles (see Section 4.4.2).

3.5 Mapping the insertions and deletion at the molecular level

In order to understand the nature of the alleles more fully, all the alleles generated in Sections 3.2 and 3.3 were sequenced out from both ends of the P-element. As a first step, the orientation of the P-elements for each insertion or deletion was determined. This was achieved using PCR primers that were specific to either the 5′ or the 3′ ends of the P-element and an appropriate genomic primer for that particular insert or

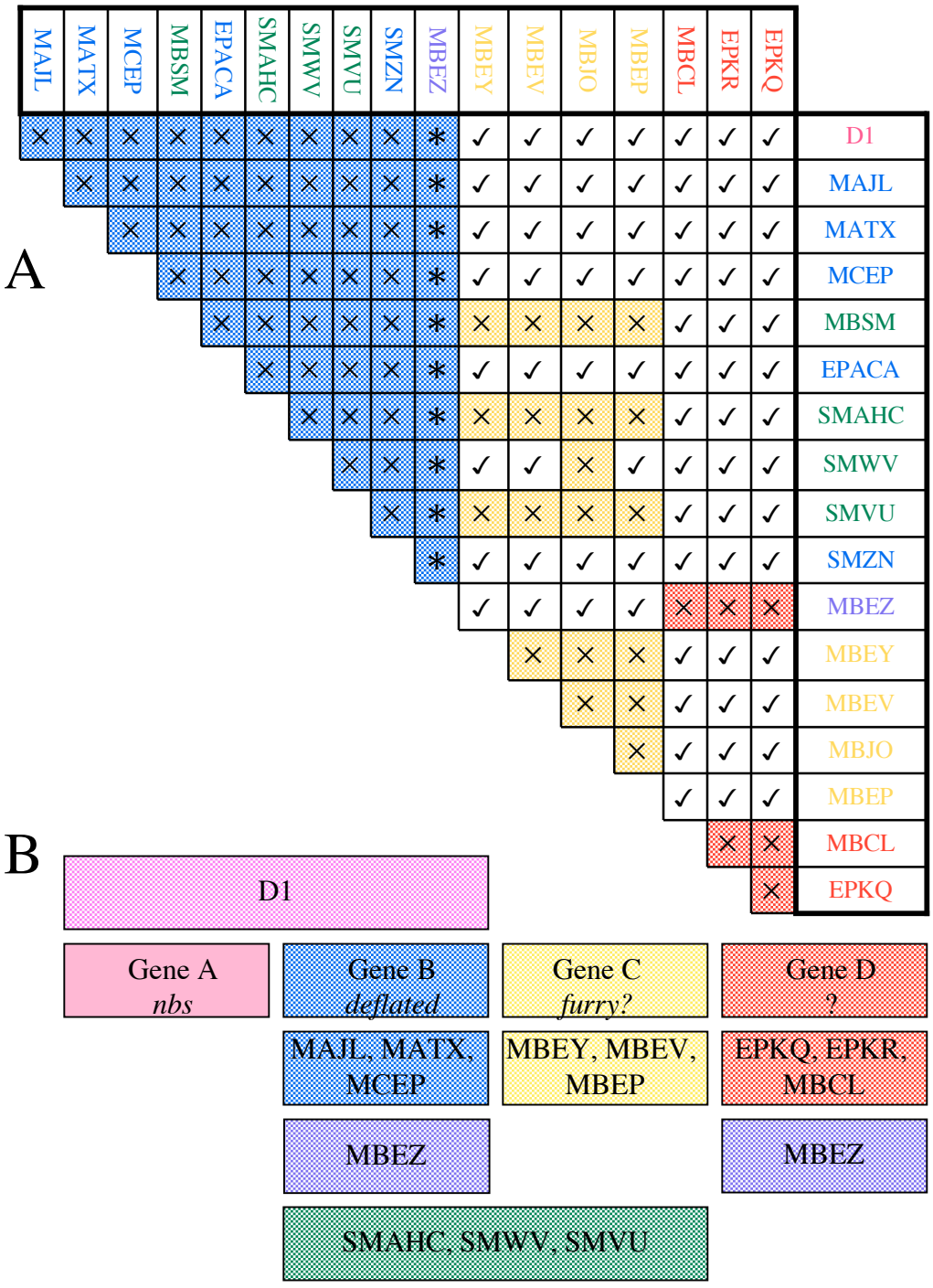

Figure 3.7 Complementation analysis of recessive lethal alleles.

(**A**) Pairwise crosses of each of the 17 recessive lethal alleles were performed to assess their ability to complement the homozygous lethality. Crosses which only produced progeny carrying the dominant TM6B marker *Humeral* failed to complement as shown by the cross (✕). Those alleles that did complement are shown by a tick (✓). Crosses involving MBEZ and other *deflated* alleles resulted in predominant lethality with few adult escapees as shown by the asterisk (see Section 4.2). (**B**) The four complementation groups identified in this study are shown. Group A (pink) corresponds to *nbs*, Group B (blue) corresponds to *deflated*, Group C (yellow) is likely to be *furry*, and Group D is an unidentified gene(s). Representative alleles of each group, plus alleles that belong to two groups are shown.

deletion. The PCR products generated were then used as templates for the sequencing reaction using either the 5′ or 3′ P-element primer to determine the genomic sequence flanking both ends of the P-element.

Determination of the DNA sequence was straightforward for most alleles. However, more than one PCR product was generated for some alleles, which indicated that the insertions were complicated and it was likely that there were two P-elements, one inserted within the other. This made sequence analysis very difficult because of the existence of multiple sequences generated by the one sequencing primer. Therefore, for these alleles (MAJL, MATX and MBEZ), only a rough breakpoint could be determined based on the size of the PCR product generated.

Other alleles, for example MCEP, did not produce products with the primer that was predicted to flank the other side of the P-element (primer 857, Table 2.1). In these situations, inverse PCR (Section 2.14.3) was then used to determine the breakpoint of these ends. For MCEP, it was found that the mobilisation of the P-element had resulted in a deletion (Figure 3.8 and 3.9). Using the assumption that other alleles may have also resulted in a similar deletion, PCR products that covered the assumed breakpoints were generated (using primer 759) and the DNA sequence could then be determined. A summary of the inserts and their breakpoints are shown in Figure 3.8.

Taken together these data showed that complementation Group C (yellow; Figures 3.7 and 3.8) was likely to be the gene *furry*, while complementation Group A (pink) corresponded to *nbs*, Group B (blue) to *deflated*, and Group D (red) to an unknown gene. The remainder of the insertions were clustered around the original EP(3)3301

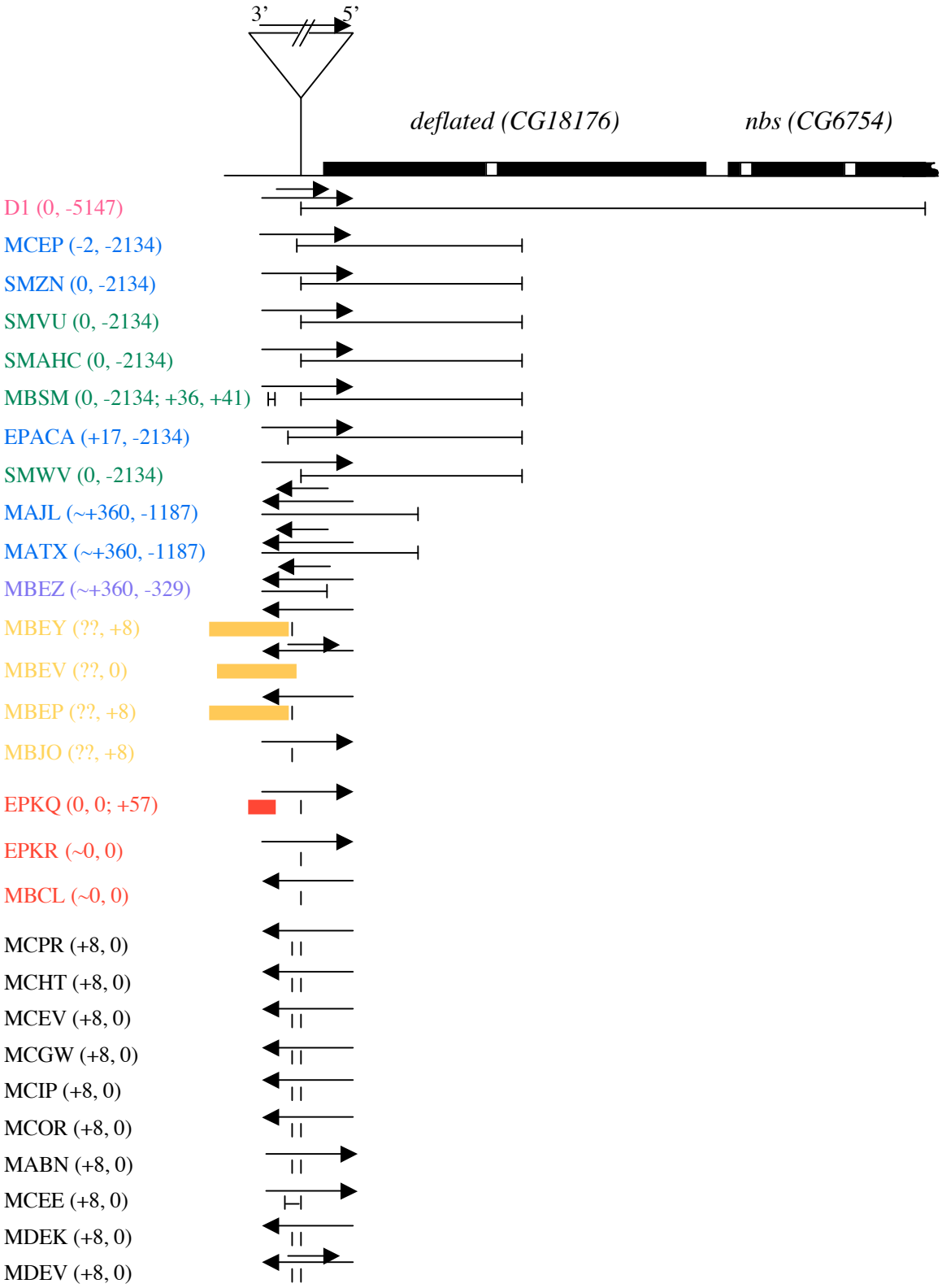
3'
5'
deflated (CG18176)
nbs (CG6754)
D1 (0, -5147)
MCEP (-2, -2134)
SMZN (0, -2134)
SMVU (0, -2134)
SMAHC (0, -2134)
MBSM (0, -2134; +36, +41)
EPACA (+17, -2134)
SMWV (0, -2134)
MAJL (~+360, -1187)
MATX (~+360, -1187)
MBEZ (~+360, -329)
MBEY (??, +8)
MBEV (??, 0)
MBEP (??, +8)
MBJO (??, +8)
EPKQ (0, 0; +57)
EPKR (~0, 0)
MBCL (~0, 0)
MCPR (+8, 0)
MCHT (+8, 0)
MCEV (+8, 0)
MCGW (+8, 0)
MCIP (+8, 0)
MCOR (+8, 0)
MABN (+8, 0)
MCEE (+8, 0)
MDEK (+8, 0)
MDEV (+8, 0)

Figure 3.8 Summary of P-element insertions and deletions.

Molecular analysis of all 27 local transpositions and the male recombination-induced D1 deletion are shown. Transposition events are coloured according to which complementation group they fall into as described in Figure 3.7. Black represents alleles that are homozygous viable, pink represents Group A (*nbs*), blue, Group B (*deflated*), yellow, Group C (possibly *furry*), and red, Group D (gene unidentified). Alleles that fall into two groups are coloured to represent this. The numbers in brackets indicate the position of the breakpoints for each end of the P-element. An exact number indicates the breakpoint has been determined by sequencing and is depicted by the vertical line. An approximate number indicates that the breakpoint has been determined by PCR only and is shown by an open line. The presence of question marks (??) indicates that the end of the P-element could not be found in the DNA sequence. The direction of the arrows indicate the orientation the P-element (the arrow points 5′). Two arrows indicates that there is a second P-element inserted within the first. The yellow or red boxes show where unrelated DNA sequence is found within the *deflated* genomic region. Yellow represents *furry* sequence, red unknown sequence.

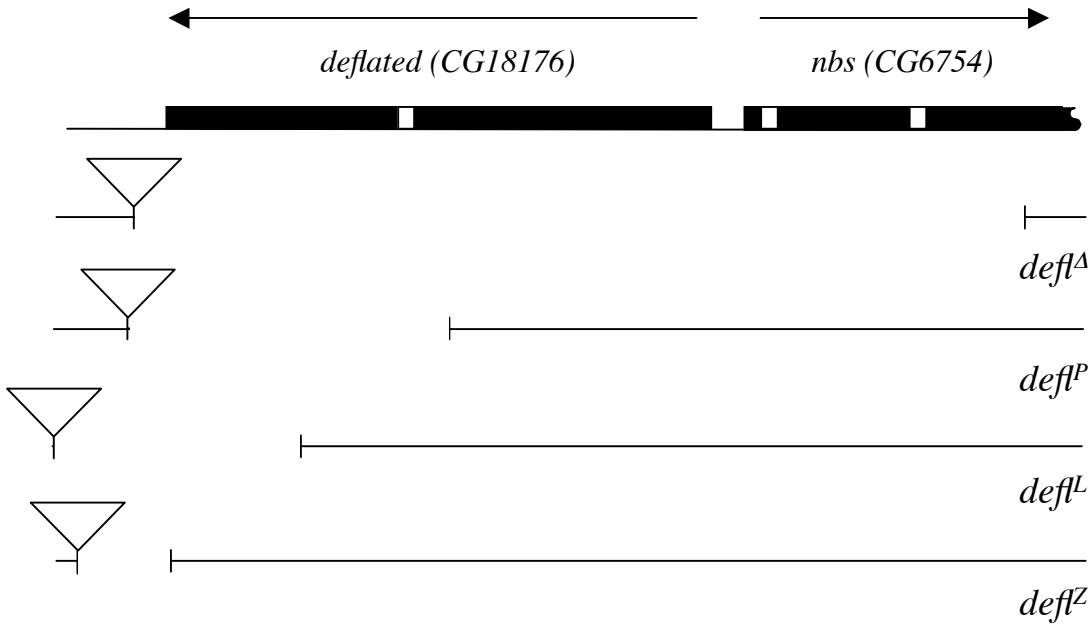

Figure 3.9 The *deflated* alleles used for further analysis

The four different *deflated* alleles were chosen because they represent the spectrum of deletions generated in the P-element mutagenesis. *defl*$^{\Delta}$ is a deletion of the entire *deflated* coding region and half of the *nbs* coding region (including the transcription start site). *defl*^{P} deletes half of the *deflated* coding region. *defl*^{L} deletes approximately one quarter and *defl*^{Z} only 45 bp of the *deflated* coding region. All alleles retain the P-element, depicted as the triangle. Note, absence of a line indicates deletion of DNA and lines indicate DNA still present in each of the alleles.

insertion site and were homozygous viable. The assignments of each of the complementation groups to specific genes were made as follows. D1 resulted in the deletion of the transcription start sites of both *nbs* and *deflated* and did not complement alleles from Group B. Alleles from Group B all resulted in deletions of the *deflated* coding region, therefore Group A comprises of alleles of *nbs* and Group B, alleles of *deflated*. Alleles in Group C were likely to be lesions in the *furry* gene, due to the finding of *furry* coding sequence juxtaposed with the *nbs* and *deflated* genomic region in MBEY, MBEV, and MBEP, which indicates that there may be a reciprocal disruption at the *furry* locus (see Discussion). While MBJO did not contain this extra sequence, its failure to complement alleles that do suggests that it is also likely to affect the *furry* locus. Mapping and sequencing of the *nbs* and *deflated* genomic region of three alleles from Group D did not allow for identification of the gene(s) that they affected, which indicated that this gene(s) is likely to be located elsewhere on the chromosome.

3.6 Discussion

In an attempt to generated alleles of *deflated* and *nbs,* two approaches mobilising a nearby P–element were employed. The first approach, local P-element mobilisation generated 27 local transpositions. Of these local transpositions, ten resulted in a partial deletion of the *deflated* coding region, while the remaining seventeen reinserted at or very close to the original P-element insertion site. The second approach used, P-element induced male recombination generated a small deletion of the *deflated* coding region and the transcription start site of *nbs*. Together these two approaches have generated a series of *deflated* alleles that can be used to examine the role that *deflated* plays in cell proliferation regulation.

3.6.1 The local transposition events recovered were non-random

Similar to previous reports, many of the P-element insertions recovered clustered around the original P-element insertion site and also showed clustering at other sites (Timakov et al., 2002; Tower et al., 1993). There are two major possible reasons for this non-randomness. Firstly, P-elements do transpose to hot spots within the genome and even in local transposition events there are favoured sites for P-element integration (Timakov et al., 2002). Secondly, it has been observed that P-element transpositions can occur pre-meiotically, resulting in clustering of identical insertion events in the offspring (Daniels and Chovnick, 1993).

It has been hypothesised that local transpositions occur at high frequency and cluster around the original P-element insertion because the transposase complex keeps the P-element close to the insertion site, thereby favouring local insertions (Zhang and Spradling, 1993). In addition, it is expected that hot spots may occur, also favouring insertion at these sites. These local hot spots are not necessarily the same as general genomic hot spots, as it is possible that the presence of a pre-existing P-element at a chromosomal site may influence the local chromatin structure, favouring further integration.

Previous P-element mobilisation studies have shown that favoured integration sites also depend upon the sex of the parent in which the mobilisation occurs (Timakov et al., 2002; Zhang and Spradling, 1993). This was observed in this study, with the male germline generating a higher frequency of mobilisation within a few kb of the original site and the female germline causing a clustering around the original insertion site. This

non-randomness may reflect expression patterns within each germline, with gene expression postulated to allow for an open chromatin configuration and therefore an increased frequency of P-element insertion (Timakov et al., 2002; Zhang and Spradling, 1993). Since insertions from complementation Groups B (*deflated*) and C (*furry*) all arose from male germlines, it may be expected that these genes are expressed in the male germline. This does not seem to be the case, at least for *deflated,* as developmental microarray data show that its expression is downregulated in adult males and since no data was available on *furry* expression in the male germline, no conclusions can be made (Arbeitman et al., 2002).

The second major reason why clustering may be observed in local P-element mobilisations was that the transposition event occurred pre-meiotically (Daniels and Chovnick, 1993). In the insertions recovered from this study it was difficult to rule out a clonal origin for some that appear identical to one another. It is clear that some identical insertions were not clones of each other, as they were raised under different experimental conditions and must therefore have originated independently. However, there are a number of insertions for which this cannot be known, as the transpositions occurred in mass matings. Therefore the insertions that may be clonal fall into four groups: MAJL and MATX; SMVU, SMWV, and SMZN; EPKQ and EPKR; and MCGW, MCHT, MCIP, MCPR, MCOR.

3.6.2 Only single local transpositions were recovered

Local transpositions frequently involve double inserts, where the original P-element insert is retained and a second new insertion occurs nearby (Daniels and Chovnick, 1993; Tower et al., 1993; Zhang and Spradling, 1993). This was not directly observed

in any of the P-element mobilisations recovered in this study. This could be because there were none generated. However, this seems unlikely considering that this is a common occurrence. It is more likely that double inserts did occur but were not recovered due to the nature of the PCR screen employed. The multiplex PCR screen was designed to identify mobilised elements within the *deflated* and *nbs* genomic region by the presence of a PCR band that, due to the conditions used, could not be much bigger than 2 kb. Therefore, for a double P-element insertion to be identified the two P-elements needed to be closer than 2 kb and not less than about 50 bp. The use of the PF2 primer on its own was intended to identify any double inserts, but again it would only do so if they were within 2 kb of each other. Sequencing of the insertion sites also did not identify double inserts. The average sequence run in these experiments was about 300 bp so it would also be unlikely to uncover double inserts unless they were within 300 bp of each other.

3.6.3 Many of the insertions and deletions arose from simple transpositions

Many of the insertions recovered were clustered around the original insertion site. Although the original low resolution mapping seemed to indicate that they may not have been the products of transposition as they appeared to have not moved, sequencing showed that they were in fact re-insertions. Firstly, all insertions were identified as a change in the size of the PCR product generated in the initial PCR multiplex PCR screen. Of those inserts that clustered around the original insertion, the initial PCR product was larger than 1.5 kb, but upon sequencing was found to not have changed chromosomal position. The reasons for this discrepancy is unknown, but it is possible that the transposition event first screened was complicated and was resolved between

the time of setting up the stock and subsequent DNA sequence analysis. The finding that many of the P-elements are in the opposite orientation to the original P-element proves that they are the products of transposition. Further evidence for transposition could also be seen when each complementation group was examined.

Those insertions that did not affect viability (black type in Figure 3.8) did not move chromosomal position. While a majority of the elements had switched orientation (12/17), all showed a duplication of the 8 bp of the very end of the P-element inverted repeat, indicating that each was an insertion into the very end of the original P-element. This has been reported previously (Carney et al., 2004). Since these insertions were not significantly different from the original, it was not surprising that they proved to be homozygous viable.

The three insertions that fell into complementation Group D (shown in red type in Figure 3.8) also remained in the same chromosomal position as EP(3)3301, yet did show signs of transposition. MBCL is inserted in the opposite orientation to EP(3)3301. EPKQ and EPKR were products of mobilisation of the MCEP insertion, which was found to delete over half of the *deflated* coding region. For these insertions to have arisen on a chromosome that has the *deflated* coding region intact (Figure 3.8), they must be the product of transposition from the MCEP chromosome onto the homologous chromosome, which would have an intact *deflated* locus. It has been reported that P–element transposition onto the homologue also shows preference for local transposition, but unlike this study, the preference was not immediately around the original insertion site, but rather within 50kb on either side (Tower and Kurapati, 1994). So while transposition onto the homologous chromosome is the most simple explanation for the

chromosome structure seen in EPKQ and EPKR, it is possible that more complicated event mays have occurred (see below).

3.6.4 Some of the P-element insertions and deletions arose from complex chromosomal rearrangements

Unlike the insertions that did not affect viability, many of the P-element insertions isolated belonging to three of the complementation groups show signs of more complex rearrangements, rather than a simple 'cut and paste' transposition.

Of insertions belonging to complementation Group B only three (of thirteen) showed an opposite orientation and therefore could have arisen by simple transposition. Interestingly, these three also showed nested P-element insertion, indicating at least two transposition events must have occur. The other ten lines from Group B retained the P–element close to and in the same orientation as EP(3)3301 and contain deletions from the P-element into the *deflated* coding region. These deletions could have arisen through two means, both of which required transposase activity on the P-element. The first way these deletions could have arisen is through an aborted attempt at transposition. It is thought that the 5′ end of the P-element is cut first by the transposase (Daniels and Chovnick, 1993). If the transposition is aborted then there is a double strand break that needs to be repaired. This could result in the loss or duplication of flanking DNA, which is similar to what occurs in P-element induced male recombination. In the case of the Group B deletions, this could have occurred since all deletions extend from the 5′ end of the P-element. The second alternative involves a mobilisation into the *deflated* coding region that also preserved the original P-element insertion. It has been observed in a number of studies that this chromosomal

arrangement can be resolved to a single copy of the P-element with deletion of the intervening DNA (Cooley et al., 1990; Timakov et al., 2002; Zhang and Spradling, 1993).

While Group B alleles appear to have arisen through rearrangement of the chromosome at the *deflated* locus, some alleles of Groups C and D appear to have arisen through rearrangements that involve other regions of the chromosome. Group C alleles are likely to be affecting the *furry* locus due to the finding of *furry* homologous sequence flanking the P-element inserted near the *deflated* locus. *furry* is a large gene found on chromosome 3L at position 67C3-4 (FlyBase), approximately 48 kb from EP(3)3301 and well within the region of local transposition (< 100 kb). Therefore, for *furry* sequence to be flanking the P–element situated near the *deflated* coding region, the chromosome must have undergone a rearrangement. One possibility is that a P-element locally transposed into the *furry* coding region and an inversion took place between this new P-element and the original P-element, thus bringing the *furry* sequence next to *deflated*. This scenario may also explain the finding that MBJO, which does not contain this flanking *furry* sequence, belongs to Group C. MBJO may represent the initial P-element mobilisation into *furry*, thus disrupting the coding region. One of the Group D alleles (EPKQ) also contains 57 bp of unidentified sequence near the P-element. Homology searches failed to identify where this sequence came from but it is possible that this sequence is from a gene elsewhere on the chromosome and its disruption has caused the homozygous lethality. Similar P-element induced rearrangements have also been reported where DNA from elsewhere on the chromosome was juxtaposed to the genomic region of interest (Carney et al., 2004).

3.6.5 Generation of *deflated* and *nbs* alleles

From the P-element mobilisation and P-element-induced male recombination approaches a number of *deflated* alleles were generated, one of which is also an allele of *nbs*. Four alleles (MBEZ, MAJL, MCEP and D1) were used in the following studies of *deflated*, and the deleted regions of each allele are summarised in Figure 3.9. They were chosen because they represented the spectrum of *deflated* alleles generated. MCEP was chosen over similar deletions because, unlike MBSM, SMAHC, SMWV and SMVU, it did not belong to complementation Group C. The four selected alleles (MBEZ, MAJL, MCEP, and D1) were renamed $defl^{Z}$, $defl^{L}$, $defl^{P}$, and $defl^{\Delta}$, respectively, and form a series of alleles that can be used to dissect *deflated* function as presented in the following chapters.

Chapter 4- *deflated* encodes a highly conserved, novel protein that is required for normal development

4.1 Introduction

Many cell proliferation regulators have been studied in *Drosophila* (Section 1.3). Like their mammalian counterparts, these proteins have conserved domains and motifs that are recognised by their regulators and targets. These domains and motifs include protein interaction sites (such as those mapped between E2f, Dp and Rbf) phosphorylation sites (such as those recognised by cdks or MAPKs) and modification sites (such as those recognised by ubiquitin ligases such as the APC/C). The presence of similar domains and motifs in proteins of unknown function can give clues as to the protein's function. However, these predictions do need to be tested experimentally to confirm their biological significance.

Many cell proliferation regulators have characteristic expression patterns at different stages of development. The transcription of *Cyclin E* and *string* are controlled by developmental cues and anticipates the progression through S-phase or M-phase, respectively (Section 1.3.3; Edgar et al., 1994; Jones et al., 2000). A large number of genes required for progression through the cell cycle are transcriptional targets of E2F and, as such, have an expression pattern that is almost identical to the pattern of cells in S-phase (Duronio et al., 1995; Royzman et al., 1997). Negative regulators, on the other hand, are expressed in anticipation of their role in arresting the cell cycle and are therefore expressed at certain stages of development, e.g. *dacapo* and *Rbf* (de Nooij et al., 1996; Du and Dyson, 1999).

All cell proliferation regulators are essential for development in *Drosophila* and the phenotypes displayed by mutants demonstrate the roles that these regulators play in controlling the different cell cycles throughout development (Section 1.3). Cyclin E is absolutely essential for S-phase entry and in its absence S-phase cannot occur (Knoblich et al., 1994). In the absence of E2f or Dp, transcription of target genes is negligible but S-phase can sometimes occur, albeit at a slower rate, resulting in reduced growth and development (Duronio et al., 1995; Royzman et al., 1997). Negative regulators are required to halt the cell cycle at appropriate times and in their absence development is either abnormal or does not occur (de Nooij et al., 1996; Du and Dyson, 1999; Sigrist and Lehner, 1997). For example, Cyclin A-cdk1 is required for preventing endocycles. In the absence of cdk1 (*cdc2*), cells that should be arrested in G2 endoreplicate, which results in abnormal abdominal phenotypes (Hayashi, 1996).

It was postulated that *deflated* was likely to be a novel cell proliferation regulator due to its high levels of co-expression with the S-phase genes *Dp* and *Ctf4* (Section 1.4.2). For this hypothesis to hold, the examination of the *deflated* protein, its expression patterns, and mutant phenotypes should show that *deflated* displays some of the characteristics of other cell proliferation regulators.

4.2 *deflated* encodes a highly conserved, novel protein

The predicted DEFLATED protein sequence was examined for any conserved domains or motifs that would indicate what DEFLATED's (DEFL) biochemical function could be and whether these function(s) are consistent with a role in regulating cell proliferation. While DEFLATED is a well conserved protein, with homologues in all metazoan species examined to date (Table 1.1), PHI-BLAST homology searches failed

to identify further related proteins, which indicates that the DEFLATED proteins do not belong to a readily identifiable larger protein family.

Pre-existing data on DEFLATED orthologues identified by protein sequence homology are quite scarce. Some have been assigned a gene ontology class of protein targeting (*Mus musculus* ; Okazaki et al., 2002) or of protein binding (*Homo sapiens*- NCBI database). Reports of mutagenesis of the zebrafish and *C. elegans* orthologues indicate that they are both essential for normal development. The zebrafish gene (*Dkfzp434b168*) was mutated during a genome wide insertional mutagenesis screen for genes essential for embryonic development (Golling et al., 2002). RNAi of the *C. elegans* orthologue (*2L877*) resulted in larval lethality (Kamath et al., 2003). However, no in depth analysis was performed on these mutant phenotypes in either study.

An homology alignment of a representation of orthologues shows that the DEFLATED proteins have a high degree of conservation, particularly in the N- and C-termini (Figure 4.1). The N-terminus has been identified as a HEAT repeat region, which is a subfamily of the ARM repeat superfamily. These domains are tandemly repeated sequences of approximately 50 amino acids that are found in many proteins of diverse function that mediate protein-protein interactions (Andrade et al., 2001). 3-D modelling of DEFLATED indicates that the HEAT repeats are most like Ran-binding proteins (Metaxia Vlassi, pers. comm.) so it is possible that DEFLATED binds Ran or a related small GTPase. A number of additional predicted protein domains and motifs were also identified (Figure 4.2). The evolutionary conservation, and therefore likeliness that these motifs are functional, was assessed by examining the multiple homology alignment (Figure 4.1). Motifs identified include a clathrin box (at a.a. 28-32), a cyclin

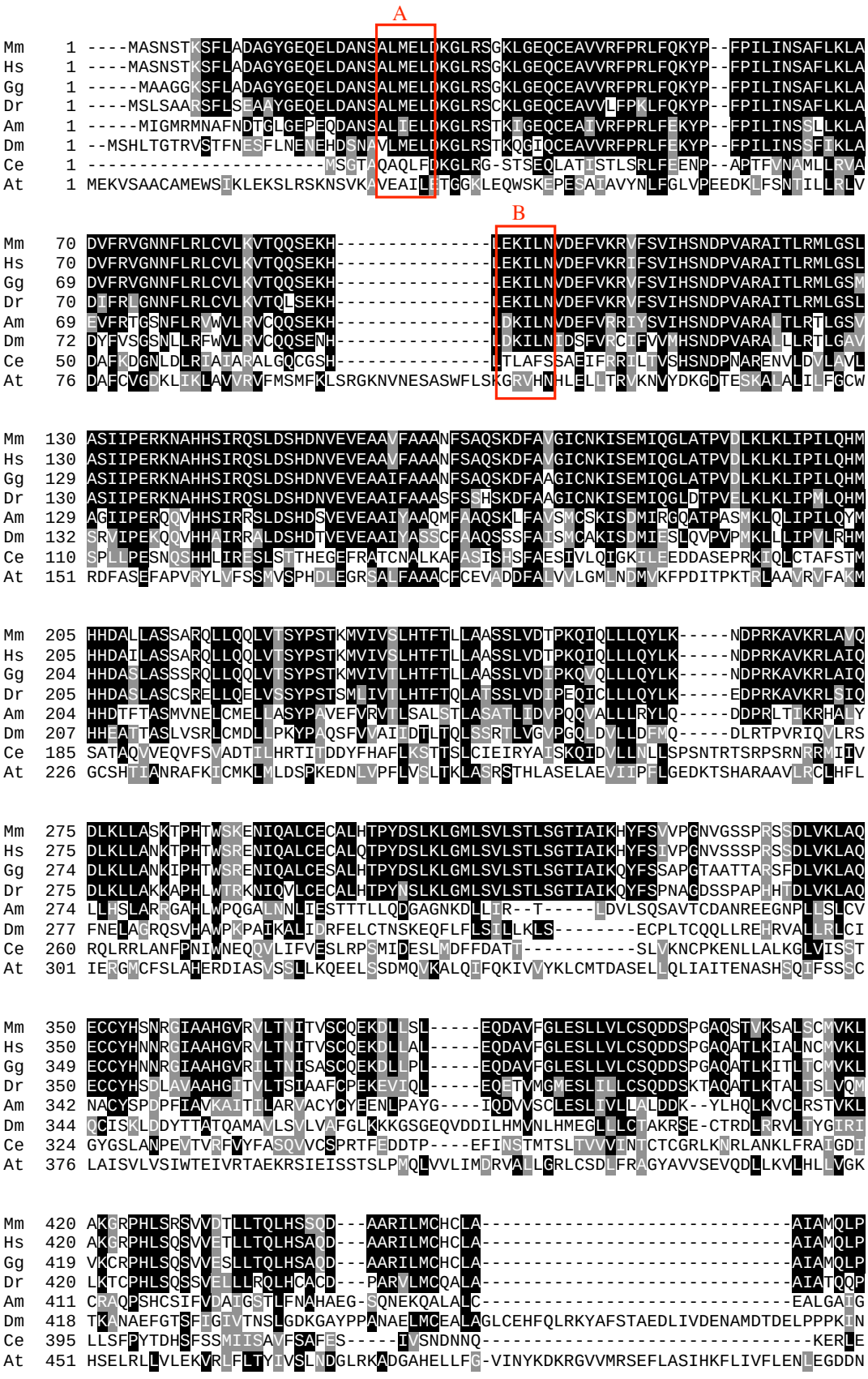
A
B
Mm 1 ----MASNSTKSFLADAGYGEQELDANSALMELDKGLRSGKLGEQCEAVVRFPRLFQKYP--FPILINSAFLKLA
Hs 1 ----MASNSTKSFLADAGYGEQELDANSALMELDKGLRSGKLGEQCEAVVRFPRLFQKYP--FPILINSAFLKLA
Gg 1 -----MAAGGKSFLADAGYGEQELDANSALMELDKGLRSGKLGEQCEAVVRFPRLFQKYP--FPILINSAFLKLA
Dr 1 ----MSLSAARSFLSEAAYGEQELDANSALMELDKGLRSCKLGEQCEAVVLFPKLFQKYP--FPILINSAFLKLA
Am 1 -----MIGMRMNAFNDTGLGEPEQDANSALIELDKGLRSTKIGEQCEAIVRFPRLFEKYP--FPILINSSLLKLA
Dm 1 --MSHLTGTRVSTFNESFLNENEHDSNAVLMELDKGLRSTKQGIQCEAVVRFPRLFEKYP--FPILINSSFIKLA
Ce 1 ----------------------MSGTAQAQLFDKGLRG-STSEQLATISTLSRLFEENP--APTFVNAMLLRVA
At 1 MEKVSAACAMEWSIKLEKSLRSKNSVKAVEAILETGGKLEQWSKEPESATAVYNLFGLVPEEDKLFSNTILLRLV
Mm 70 DVFRVGNNFLRLCVLKVTQQSEKH----------LEKILNVDEFVKRVFSVIHSNDPVARAITLRMLGSL
Hs 70 DVFRVGNNFLRLCVLKVTQQSEKH----------LEKILNVDEFVKRIFSVIHSNDPVARAITLRMLGSL
Gg 69 DVFRVGNNFLRLCVLKVTQQSEKH----------LEKILNVDEFVKRVFSVIHSNDPVARAITLRMLGSM
Dr 70 DIFRLGNNFLRLCVLKVTQLSEKH----------LEKILNVDEFVKRVFSVIHSNDPVARAITLRMLGSL
Am 69 EVFRTGSNFLRVWVLRVCQQSEKH----------LDKILNVDEFVRRIYSVIHSNDPVARALTLRTLGSV
Dm 72 DYFVSGSNLLRFWVLRVCQQSENH----------LDKILNIDSFVRCIFVVMHSNDPVARALLLRTLGAV
Ce 50 DAFKDGNLDLRIAIARALGQCGSH----------LTLAFSSAEIFRRILTVSHSNDPNARENVLDVLAVL
At 76 DAFCVGDKLIKLAVVRVFMSMFKLSRGKNVNESASWFLSKGRVHNHLELLTRVKNVYDKGDTESKALALILFGCW
Mm 130 ASIIPERKNAHHSIRQSLDSHDNVEVEAAVFAAANFSAQSKDFAVGICNKISEMIQGLATPVDLKLKLIPILQHM
Hs 130 ASIIPERKNAHHSIRQSLDSHDNVEVEAAVFAAANFSAQSKDFAVGICNKISEMIQGLATPVDLKLKLIPILQHM
Gg 129 ASIIPERKNAHHSIRQSLDSHDNVEVEAAIFAAANFSAQSKDFAAGICNKISEMIQGLATPVDLKLKLIPILQHM
Dr 130 ASIIPERKNAHHSIRQSLDSHDNVEVEAAIFAAASFSSHSKDFAAGICNKISEMIQGLDTPVELKLKLIPMLQHM
Am 129 AGIIPERQQVHHSIRRSLDSHDSVEVEAAIYAAQMFAAQSKLFAVSMCSKISDMIRGQATPASMKLQLIPILQYM
Dm 132 SRVIPEKQQVHHAIRRALDSHDTVEVEAAIYASSCFAAQSSSFAISMCAKISDMIESLQVPVPMKLLLIPVLRHM
Ce 110 SPLLPESNQSHHLIRESLSTTHEGEFRATCNALKAFASISHSFAESIVLQIGKILEEDDASEPRKIQLCTAFSTM
At 151 RDFASEFAPVRYLVFSSNVSPHDLEGRSALFAAACFCEVADDFALVVLGMLNDMVKFPDITPKTRLAAVRVFAKM
Mm 205 HHDALLASSARQLLQQLVTSYPSTKMVIVSLHTFTLLAASSLVDTPKQIQLLLQYLK-----NDPRKAVKRLAVQ
Hs 205 HHDAILASSARQLLQQLVTSYPSTKMVIVSLHTFTLLAASSLVDTPKQIQLLLQYLK-----NDPRKAVKRLAIQ
Gg 204 HHDASLASSSRQLLQQLVTSYPSTKMVIVTLHTFTLLAASSLVDIPKQVQLLLQYLK-----NDPRKAVKRLAIQ
Dr 205 HHDASLASCSRELLQELVSSYPSTSMLIVTLHTFTQLATSSLVDIPEQICLLLQYLK-----EDPRKAVKRLSIQ
Am 204 HHDTFTASMVNELCMELLASYPAVEFVRVTLSALSTLASATLIDVPQQVALLLRYLQ-----DDPRLTIKRHALY
Dm 207 HHEATTASLVSRLCMDLLPKYPAQSFVVAIIDTLTQLSSRTLVGVPGQLDVLLDFMQ-----DLRTPVRIQVLRS
Ce 185 SATAQVVEQVFSVADTILHRTITDDYFHAFLKSTTSLCIEIRYAISKQIDVLLNLLSPSNTRTSRPSRNRRMITV
At 226 GCSHTIANRAFKICMKLVLDSPKEDNLVPFLVSLIKLASRSTHLASELAEVIIPFLGEDKTSHARAAVLRCLHFL
Mm 275 DLKLLASKTPHTWSKENIQALCECALHTPYDSLKLGMLSVLSTLSGTIAIKHYFSVVPGNVGSSPRSSDLVKLAQ
Hs 275 DLKLLANKTPHTWSRENIQALCECALQTPYDSLKLGMLSVLSTLSGTIAIKHYFSIVPGNVSSSPRSSDLVKLAQ
Gg 274 DLKLLANKIPHTWSRENIQALCESALHTPYDSLKLGMLSVLSTLSGTIAIKQYFSSAPGTAATTARSFDLVKLAQ
Dr 275 DLKLLAKKAPHLWTRKNIQVLCECALHTPYNSLKLGMLSVLSTLSGTIAIKQYFSPNAGDSSPAPHHTDLVKLAQ
Am 274 LLHSLARRGAHLWPQGALNNLIESTTTLLQDGAGNKDLLIR--T-----LDVLSQSAVTCDANREEGNPLLSLCV
Dm 277 FNELACRQSVHAWPKPAIKALIDRFELCTNSKEQFLFLSILLKLS--------ECPLTCQQLLREHRVALLRLCI
Ce 260 RQLRRLANFPNIWNEQQVLIFVESLRPSMIDESLMDFFDATT----------SLVKNCPKENLLALKGLVISST
At 301 IERGWCFSLAHERDIASVSSLLKQEELSSDMQVKALQIFQKIVVYKLCMTDASELLQLIAITENASHSQIFSSSC
Mm 350 ECCYHSNRGIAAHGVRVLTNITVSCQEKDLLSL-----EQDAVFGLESLLVLCSQDDSPGAQSTVKSALSCMVKL
Hs 350 ECCYHNNRGIAAHGVRVLTNITVSCQEKDLLAL-----EQDAVFGLESLLVLCSQDDSPGAQATLKIALNCMVKL
Gg 349 ECCYHNNRGIAAHGVRILTNISASCQEKDLLPL-----EQDAVFGLESLLVLCSQDDSPGAQATLKITLTCMVKL
Dr 350 ECCYHSDLAVAAHGITVLTSIAAFCPEKEVIQL-----EQETVMGMESLILLCSQDDSKTAQATLKTALTSLVQM
Am 342 NACYSPDPFIAVKAITILARVACYCYEENLPAYG----IQDVVSCLESLIVLLALDDK--YLHQLKVCLRSTVKL
Dm 344 QCISKLDDYTTATQAMAVLSVLVAFGLKKKGSGEQVDDILHMVNLHMEGLLLCTAKRSE-CTRDLRRVLTYGIRI
Ce 324 GYGSLANPEVTVRFVYFASQVVCSPRTFEDDTP----EFINSTMTSLTVVVINTCTCGRLKNRLANKLFRAIGDI
At 376 LAISVLVSIWTEIVRTAEKRSIEISSTSLPMQLVVLIMDRVALLGRLCSDLFRAGYAVVSEVQDLLKVLHLLVGK
Mm 420 AKGRPHLSRSVVDTLLTQLHSSQD---AARILMCHCLA----------AIAMQLP
Hs 420 AKGRPHLSQSVVETLLTQLHSAQD---AARILMCHCLA----------AIAMQLP
Gg 419 VKCRPHLSQSVVESLLTQLHSAQD---AARILMCHCLA----------AIAMQLP
Dr 420 LKTCPHLSQSSVELLLRQLHCACD---PARVLMCQALA----------AIATQQP
Am 411 CRAQPSHCSIFVDAIGSTLFNAHAEG-SQNEKQALALC----------EALGAIG
Dm 418 TKANAEFGTSFIGIVTNSLGDKGAYPPANAELMCEALAGLCEHFQLRKYAFSTAEDLIVDENAMDTDELPPPKIN
Ce 395 LLSFPYTDHSFSSMIISAVFSAFES-----IVSNDNNQ----------KERLE
At 451 HSELRLLVLEKVRLFLTYIVSLNDGLRKADGAHELLFG-VINYKDKRGVVMRSEFLASIHKFLIVFLENLEGDDN

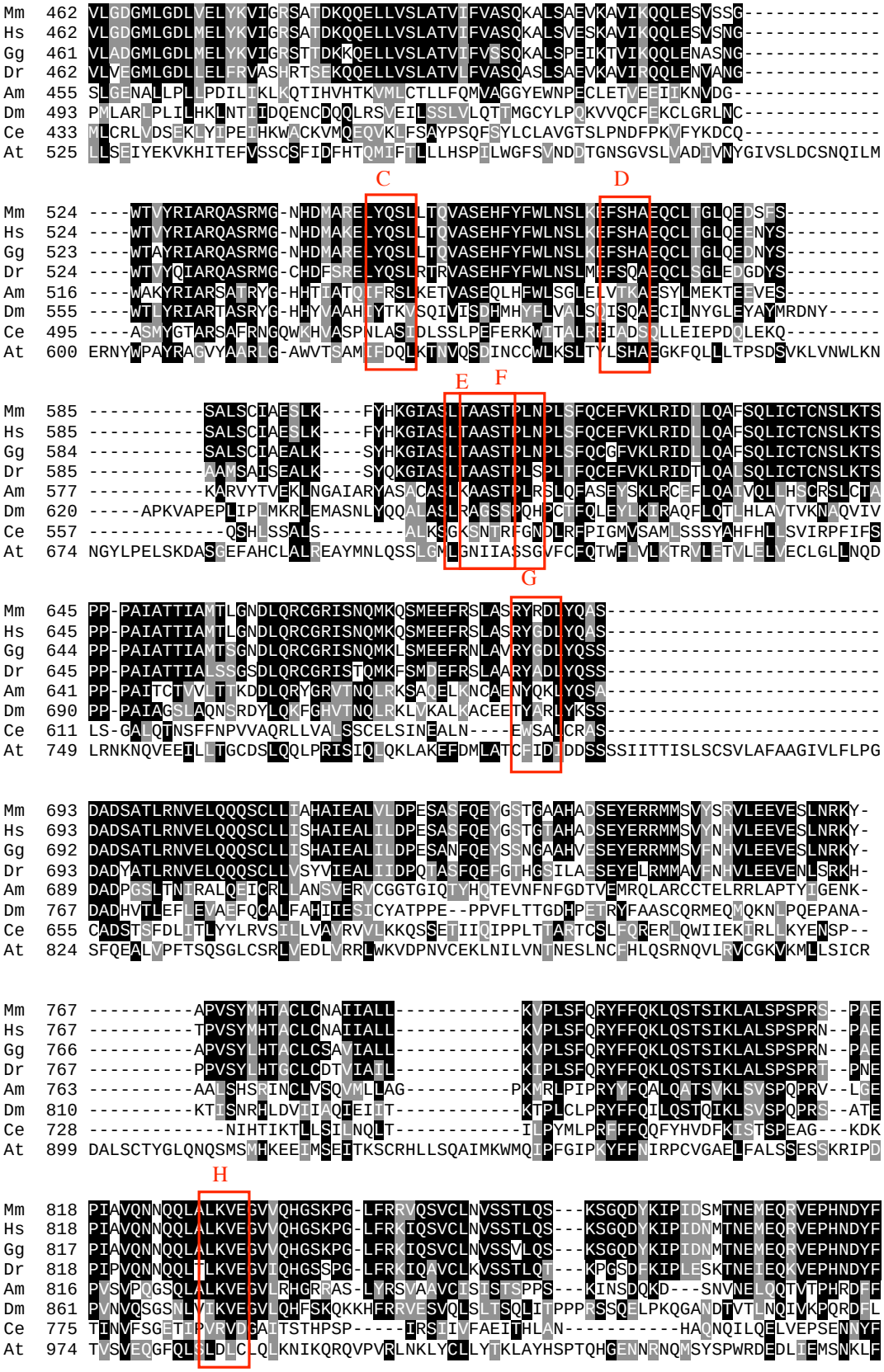
Mm 462 VLGDGMLGDLVELYKVIGRSATDKQQELLVSLATVIFVASQKALSAEVKAVIKQQLESVSSG
Hs 462 VLGDGMLGDLMELYKVIGRSATDKQQELLVSLATVIFVASQKALSVESKAVIKQQLESVSNG
Gg 461 VLADGMLGDLMELYKVIGRSTTDKKQELLVSLATVIFVSSQKALSPEIKTVIKQQLENASNG
Dr 462 VLVEGMLGDLLELFRVASHRTSEKQQELLVSLATVLFVASQASLSAEVKAVIRQQLENVANG
Am 455 SLGENALLPLLPDILIKLKQTIHVHTKVMLCTLLFQMVAGGYEWNPECLETVEEIIKNVDG
Dm 493 PMLARLPLILHKLNTIIDQENCDQQLRSVEILSSLVLQTIMGCYLPQKVVQCFEKCLGRLNC
Ce 433 MLCRLVDSEKLYIPEIHKWACKVMQEQVKLFSAYPSQFSYLCLAVGTSLPNDFPKVFYKDCQ
At 525 LLSEIYEKVKHITEFVSSCSFIDFHTQMIFTLLLHSPILWGFSVNDDTGNSGVSLVADIVNYGIVSLDCSNQILM
C
D
Mm 524 ----WTVYRIARQASRMG-NHDMARELYQSLLTQVASEHFYFWLNSLKEFSHAEQCLTGLQEDSES---------
Hs 524 ----WTVYRIARQASRMG-NHDMAKELYQSLLTQVASEHFYFWLNSLKEFSHAEQCLTGLQEENYS---------
Gg 523 ----WTAYRIARQASRMG-NHDMARELYQSLLTQVASEHFYFWLNSLKEFSHAEQCLTGLQEENYS---------
Dr 524 ----WTVYQIARQASRMG-CHDFSRELYQSLRTRVASEHFYFWLNSLMEFSQAEQCLSGLEDGDYS---------
Am 516 ----WAKYRIARSATRYG-HHTIATQIFRSLKETVASEQLHFWLSGLELVTKAESYLMEKTEEVES---------
Dm 555 ----WTLYRIARTASRYG-HHYVAAHLYTKVSQIVISDHMHYFLVALSQISQAECILNYGLEYAYMRDNY-----
Ce 495 ----ASMYGTARSAFRNGQWKHVASPNLASIDLSSLPEFERKWITALREIADSQLLEIEPDQLEKQ---------
At 600 ERNYWPAYRAGVYAARLG-AWVTSAMIFDQLKTNVQSDINCCWLKSLTYLSHAEGKFQLLLTPSDSVKLVNWLKN
E
F
Mm 585 ----------SALSCIAESLK----FYHKGIASLTAASTPLNPLSFQCEFVKLRIDLLQAFSQLICTCNSLKTS
Hs 585 ----------SALSCIAESLK----FYHKGIASLTAASTPLNPLSFQCEFVKLRIDLLQAFSQLICTCNSLKTS
Gg 584 ----------SALSCIAEALK----SYHKGIASLTAASTPLNPLSFQCGFVKLRIDLLQAFSQLICTCNSLKTS
Dr 585 ----------AAMSAISEALK----SYQKGIASLTAASTPLSPLTFQCEFVKLRIDTLQALSQLICTCNSLKTS
Am 577 ----------KARVYTVEKLNGAIARYASACASLKAASTPLRSLQFASEYSKLRCEFLQAIVQLLHSCRSLCTA
Dm 620 -----APKVAPEPLIPIMKRLEMASNLYQQALASLRAGSSPQHPCTFQLEYLKIRAQFLQTLHLAVTVKNAQVIV
Ce 557 ------------QSHLSSALS--------ALKSGKSNTRFGNDLRFPIGMVSAMLSSSYAHFHLLSVIRPFIFS
At 674 NGYLPELSKDASGEFAHCLALREAYMNLQSSLGMLGNIIASSGVFCFQTWFLVLKTRVLETVLELVECLGLLNQD
G
Mm 645 PP-PAIATTIAMTLGNDLQRCGRISNQMKQSMEEFRSLASRYRDLYQAS----------
Hs 645 PP-PAIATTIAMTLGNDLQRCGRISNQMKQSMEEFRSLASRYGDLYQAS----------
Gg 644 PP-PAIATTIAMTSGNDLQRCGRISNQMKLSMEEFRNLAVRYGDLYQSS----------
Dr 645 PP-PAIATTIALSSGSDLQRCGRISTQMKFSMDEFRSLAARYADLYQSS----------
Am 641 PP-PAITCTVVLTTKDDLQRYGRVTNQLRKSAQELKNCAENYQKLYQSA----------
Dm 690 PP-PAIAGSLAQNSRDYLQKFGHVTNQLRKLVKALKACEETYARLYKSS----------
Ce 611 LS-GALQTNSFFNPVVAQRLLVALSSCELSINEALN----EWSALCRAS----------
At 749 LRNKNQVEEILLTGCDSLQQLPRISIQLQKLAKEFDMLATCFIDIDDSSSSIITTISLSCSVLAFAAGIVLFLPG
Mm 693 DADSATLRNVELQQQSCLLIAHAIEALVLDPESASFQEYGSTGAAHADSEYERRMMSVYSRVLEEVESLNRKY-
Hs 693 DADSATLRNVELQQQSCLLISHAIEALILDPESASFQEYGSTGTAHADSEYERRMMSVYNHVLEEVESLNRKY-
Gg 692 DADSATLRNVELQQQSCLLISHAIEALILDPESANFQEYSSNGAAHVESEYERRMMSVFNHVLEEVESLNRKY-
Dr 693 DADYATLRNVELQQQSCLLVSYVIEALIIDPQTASFQEFGTHGSILAESEYELRMMAVFNHVLEEVENLSRKH-
Am 689 DADPGSLTNIRALQEICRLLANSVERVCGGTGIQTYHQTEVNFNFGDTVEMRQLARCCTELRRLAPTYIGENK-
Dm 767 DADHVTLEFLEVAEFQCALFAHIIESICYATPPE--PPVFLTTGDHPETRYFAASCQRMEQMQKNLPQEPANA-
Ce 655 CADSTSFDLITLYYLRVSILLVAVRVVLKKQSSETIIQIPPLTTARTCSLFQRERLQWIIEKIRLLKYENSP--
At 824 SFQEALVPFTSQSGLCSRLVEDLVRRLWKVDPNVCEKLNILVNINESLNCFHLQSRNQVLRVCGKVKMLLSICR
Mm 767 ----------APVSYMHTACLCNAIIALL-----------KVPLSFQRYFFQKLQSTSIKLALSPSPRS--PAE
Hs 767 ----------TPVSYMHTACLCNAIIALL-----------KVPLSFQRYFFQKLQSTSIKLALSPSPRN--PAE
Gg 766 ----------APVSYLHTACLCSAVIALL-----------KVPLSFQRYFFQKLQSTSIKLALSPSPRN--PAE
Dr 767 ----------PPVSYLHTGCLCDTVIATL-----------KIPLSFQRYFFQKLQSTSIKLALSPSPRT--PNE
Am 763 ----------AALSHSRINCLVSQVMLLAG----------PKMRLPIPRYYFQALQATSVKLSVSPQPRV--LGE
Dm 810 ----------KTISNRHLDVIIAQIEIIT-----------KTPLCLPRYFFQILQSTQIKLSVSPQPRS--ATE
Ce 728 ------------NIHTIKTLLSILNQLT-----------ILPYMLPRFFFQQFYHVDFKISTSPEAG---KDK
At 899 DALSCTYGLQNQSMSMHKEEIMSEITKSCRHLLSQAIMKWMQIPFGIPKYFFNIRPCVGAELFALSSESSKRIPD
H
Mm 818 PIAVQNNQQLALKVEGVVQHGSKPG-LFRRVQSVCLNVSSTLQS---KSGQDYKIPIDSMTNEMEQRVEPHNDYF
Hs 818 PIAVQNNQQLALKVEGVVQHGSKPG-LFRKIQSVCLNVSSTLQS---KSGQDYKIPIDNMTNEMEQRVEPHNDYF
Gg 817 PIAVQNNQQLALKVEGVVQHGSKPG-LFRKIQSVCLNVSSVLQS---KSGQDYKIPIDNMTNEMEQRVEPHNDYF
Dr 818 PIPVQNNQQLTLKVEGVIQHGSSPG-LFRKIQAVCLKVSSTLQT---KPGSDFKIPLESKTNEIEQKVEPHNDYF
Am 816 PVSVPQGSQLALKVEGVLRHGRRAS-LYRSVAAVCISISTSPPS---KINSDQKD---SNVNELQQTVTPHRDFF
Dm 861 PVNVQSGSNLVIKVEGVLQHFSKQKKHFRRVESVQLSLTSQLITPPPRSSQELPKQGANDTVTLNQIVKPQRDFL
Ce 775 TINVFSGETIPVRVDGAITSTHPSP-----IRSIIVFAEITHLAN----------HAQNQILQELVEPSENNYF
At 974 TVSVEQGFQLSLDLCLQLKNIKQRQVPVRLNKLYCLLYTKLAYHSPTQHGENNRNQMSYSPWRDEDLIEMSNKLF

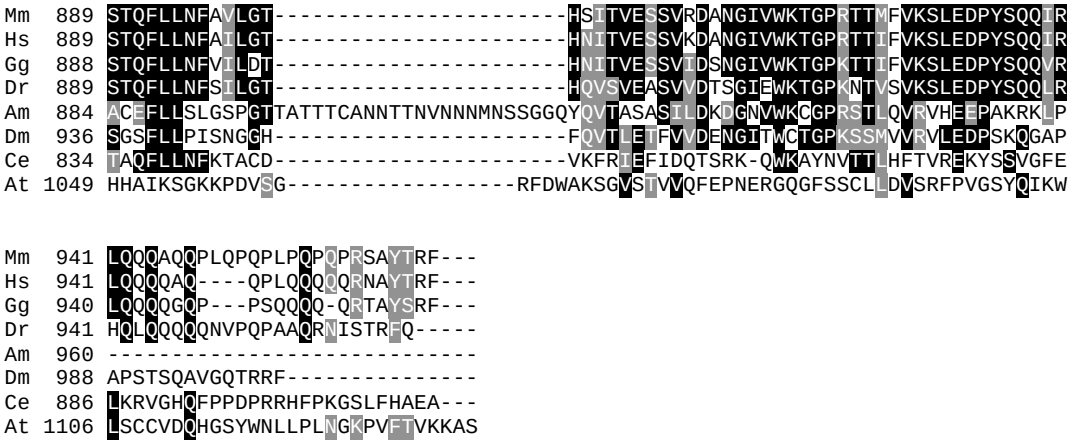

Figure 4.1 Homology alignment of DEFLATED orthologues.

The DEFLATED orthologues from mouse- *Mus musculus* (Mm), human- *Homo sapiens* (Hs), chicken- *Gallus gallus* (Gg), zebrafish- *Danio rerio* (Dr), bee- *Apis mellifera* (Am), fruitfly- *Drosophila melanogaster* (Dm), nemotode- *Caenorhabditis elegans* (Ce) and mustard cress- *Arabidopsis thaliana* (At) were used to generate an homology alignment using the ClustalW 1.8 program (BCM Search Launcher). Identical residues are shaded black and conserved residues are shaded grey. Red boxes indicate conserved motifs shown schematically in Figure 4.2.

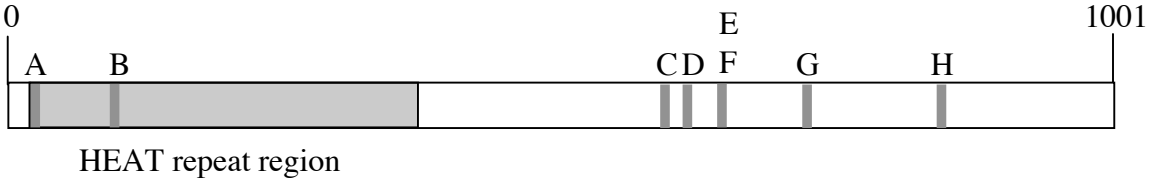

Figure 4.2 Schematic of conserved putative protein domains and motifs of DEFLATED.

(**A**) Clathrin box at amino acids (a.a.) 28-32. (**B**) Cyclin binding site at a.a. 98-102. (**C**) Adaptor protein complex interaction site at a.a. 577-580. (**D**) Chk2 phosphorylation site at a.a 600-602. (**E**) 14-3-3 binding site at a.a. 650-655. (**F**) Proline-directed (e.g. MAPK) phosphorylation site at a.a. 651-657. (**G**) Adaptor protein complex interaction site at a.a. 730-733. (**H**) SUMO modification site at a.a. 872-875. The N-terminus contains a well conserved HEAT repeat region (shaded grey).

binding site (at a.a. 98-102), two adaptor protein complex interaction sites (at a.a. 577-580 and 730-733), a Chk2 phosphorylation site (at a.a. 600-603), a 14-3-3 binding site (at a.a. 650-655), a proline-direct kinase (e.g. MAPK) phosphorylation site (at a.a. 651-657), and a SUMO modification site (at a.a. 872-875). Some of these motifs are quite simple and could have arisen by chance (e.g. cyclin binding site and SUMO modification site) and may only appear to be conserved because they are in conserved regions of the protein. However, others are highly conserved and are therefore more likely to be functional (e.g. 14-3-3 binding site).

4.3 Expression of *deflated* occurs in proliferating postblastoderm embryonic tissues

To examine the pattern of *deflated* expression throughout development, an RNA probe to the *deflated* coding region was generated and used for *in situ* hybridisation to wild type 0-15 hr embryos (Section 2.21). A sense RNA probe to the same region was used as a negative control. The final colour development of the alkaline phosphatase catalysed reaction was reproducibly slow, indicating that *deflated* mRNA was expressed at low levels. Despite the extended period of colour development, the sense probe control always displayed minimal colour development (Figure 4.3 K and L).

deflated mRNA expression was not detected in syncytial or cellularised embryos (Figure 4.3 A and B), implying there is no maternal contribution of *deflated* mRNA to the oocyte. *deflated* expression was first detectable postcellularisation in the epidermis (Figure 4.3 C) and expression continued in the epidermis throughout gastrulation, germband expansion and retraction (Figure 4.3 D-G). After germband retraction, expression was no longer detected in the epidermis but was detected in the brain, the

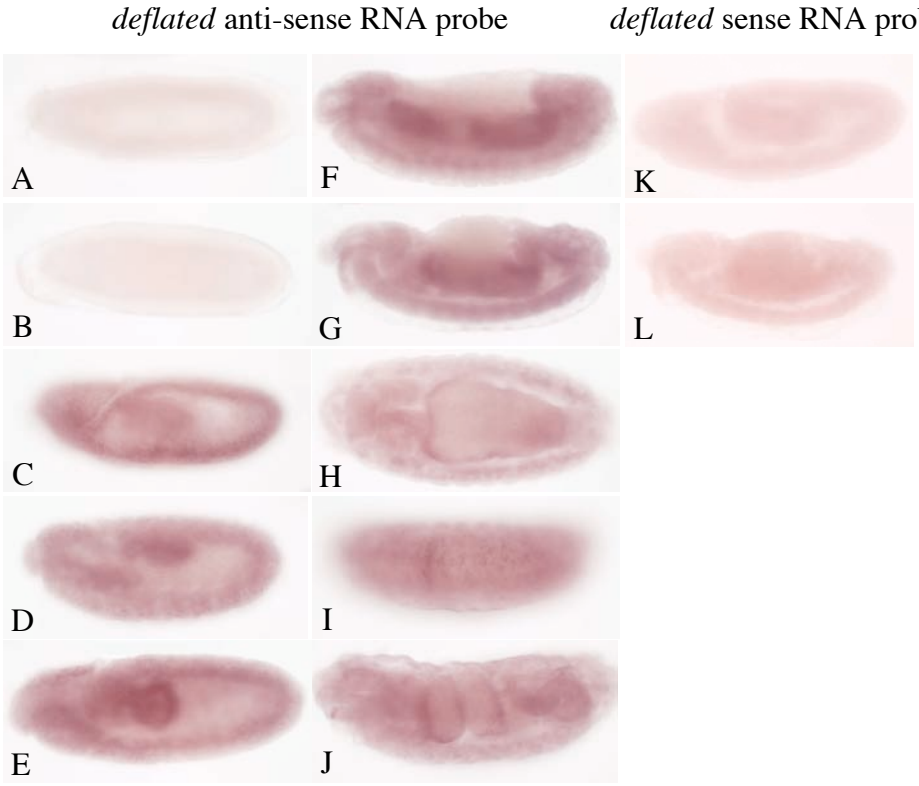

Figure 4.3 *deflated* mRNA is expressed in proliferating tissues in postblastoderm embryos.

(**A-J**) w^{1118} embryos were hybridised with an anti-sense RNA probe to *deflated*. (**A and B**) Expression of *deflated* mRNA is not detected in syncytial or cellularised embryos. (**C**) Expression is detected after cellularisation in the epidermis. (**E, F and G**) Later in development *deflated* expression is limited to the brain, (**F, G, H, and J**) gut, (**F and G**) CNS, and (**I**) PNS. (**K and L**) w^{1118} embryos hybridised with a sense probe processed in parallel detected no expression in similarly staged embryos.

central nervous system, the gut and the peripheral nervous system (Figure 4.3 F-I). At later stages, expression was only detected in the embryonic gut (Figure 4.3 J). The expression pattern of *deflated* mRNA in all these cells correlate with the pattern of developmentally controlled DNA replication during embryogenesis, therefore *deflated* is expressed in cells undergoing proliferation or endoreplication.

4.4 *deflated* mutant phenotype characterisation

4.4.1 Homozygous *deflated* mutants die as second instar larvae

In generating the *deflated* alleles it was observed that they resulted in lethality when homozygous (Section 3.4). To examine the lethality period in more detail, one of the lines (EPACA) that resulted in deletion of the same amount of *deflated* coding region as $defl^{P}$ was set up as a heterozygous stock over the balancer TM6B, α-IT::GFP. This balancer contains two dominant markers, *Tubby* and *GFP,* so heterozygous larvae can be readily distinguished from homozygous larvae. Eggs laid by *EPACA/TM6B,α-IT::GFP* mothers were collected and placed in an array on a fresh grape juice agar plate (Section 2.18). The plate was incubated at 25°C for 24 hr and the hatched larvae were scored and counted. Of the 130 eggs arrayed, 118 hatched (90%). Although this number is higher than the expected frequency of 75% (TM6B/TM6B individuals do not survive embryogenesis), it indicates that embryos deficient in zygotic *deflated* expression are capable of proper development.

Some of the larvae were collected to determine the post-embryonic stage at which the homozygotes died. These larvae were collected, examined, and put onto fresh grape juice agar plates at 24 hr intervals. The larval stage of the heterozygotes and homozygotes was noted at each collection by examination of their posterior spiracles

(Ashburner, 1989). Of the seven homozygotes, one was found dead as a first instar larva 48 hr after the beginning of the experiment. A further five were found dead as second instar larvae at 96 hr and the remaining homozygote alive was sluggish and no longer feeding. This larva was found dead as a second instar larva 24 hr later. Of the 39 heterozygotes followed none were found dead at any time interval in the 120 hr of the experiment. All the heterozygous larvae had moulted into third instars by 96 hr. These data show that larvae deficient in *deflated* grow more slowly than their heterozygous siblings and do not survive past the second instar stage.

Qualitative analysis of the other *deflated* alleles, $defl^{Z}$, $defl^{P}$, $defl^{L}$, and $defl^{\Delta}$ showed that the homozygous mutant larvae of these alleles also do not reach the third instar larval stage. Homozygous second instar larvae are commonly observed to wander out of the food, become sluggish, and die prior to moulting into third instar larvae. Consequently, all the *deflated* alleles result in lethality at a similar stage in development.

4.4.2 Transheterozygous *deflated* individuals show abnormal abdominal, wing, bristle, and eggshell phenotypes

During the complementation analysis described in chapter 3 (Section 3.4), it was noted that some transheterozygous combinations of *deflated* alleles allowed a percentage of individuals to develop into adulthood, with the remainder dying at the pupal stage. The crosses that produced these adult escapees always involved the $defl^{Z}$ allele in combination with another *deflated* allele. To examine why a proportion of the individuals were dying at the pupal stage, transheterozygous and wild type pharate pupae were dissected from their pupal cases. At the pharate stage of development wild type flies have formed all adult structures but have not yet eclosed (Figure 4.4 A and

B). In the transheterozygotes, the anterior of the fly formed normally but the abdomen had failed to form (Figure 4.4 C and D). This phenotype lead to naming the gene *deflated*. The severity of the malformation did vary from individual to individual, but in all cases between one and four of the anterior tergites formed while the posterior ones never did. Furthermore, the external genitals never formed in these individuals.

The transheterozygous adult escapees were also examined in detail. The number of adults that eclosed was noted in each of the crosses. The proportion of transheterozygote adult escapees of $defl^{Z}$ in combination with both $defl^{L}$ and $defl^{\Delta}$ was 18% of expected (21/252 and 7/84 transheterozygote adults / total adult progeny, respectively). $defl^{P}$ in combination with $defl^{Z}$ resulted in more transheterozygous individuals making it to adulthood, 60% of the expected number eclosed (38/164). The majority of the adult escapees were male: 100% of $defl^{L}/defl^{Z}$ (21/21), 70% of $defl^{\Delta}/defl^{Z}$ (5/7), and 80% of $defl^{P}/defl^{Z}$ (32/38).

The transheterozygous escaped adults were also examined for developmental defects. Wild type wings show five longitudinal veins that extend all the way to the wing margin (Figure 4.4 E). In wings from *deflated* transheterozygotes, the longitudinal vein L5 does not reach the margin of the wing (Figure 4.4 F). Another defect was observed in humeral bristle morphology. In wild type flies there are two slightly curved humeral bristles (Figure 4.4 G). Humeral bristles from *deflated* transheterozygotes are frequently bent at right angles (Figure 4.4 H). While these two defects are minor, they indicate that normal differentiation and morphogenesis may not occur properly in the absence of wild type *deflated* function.

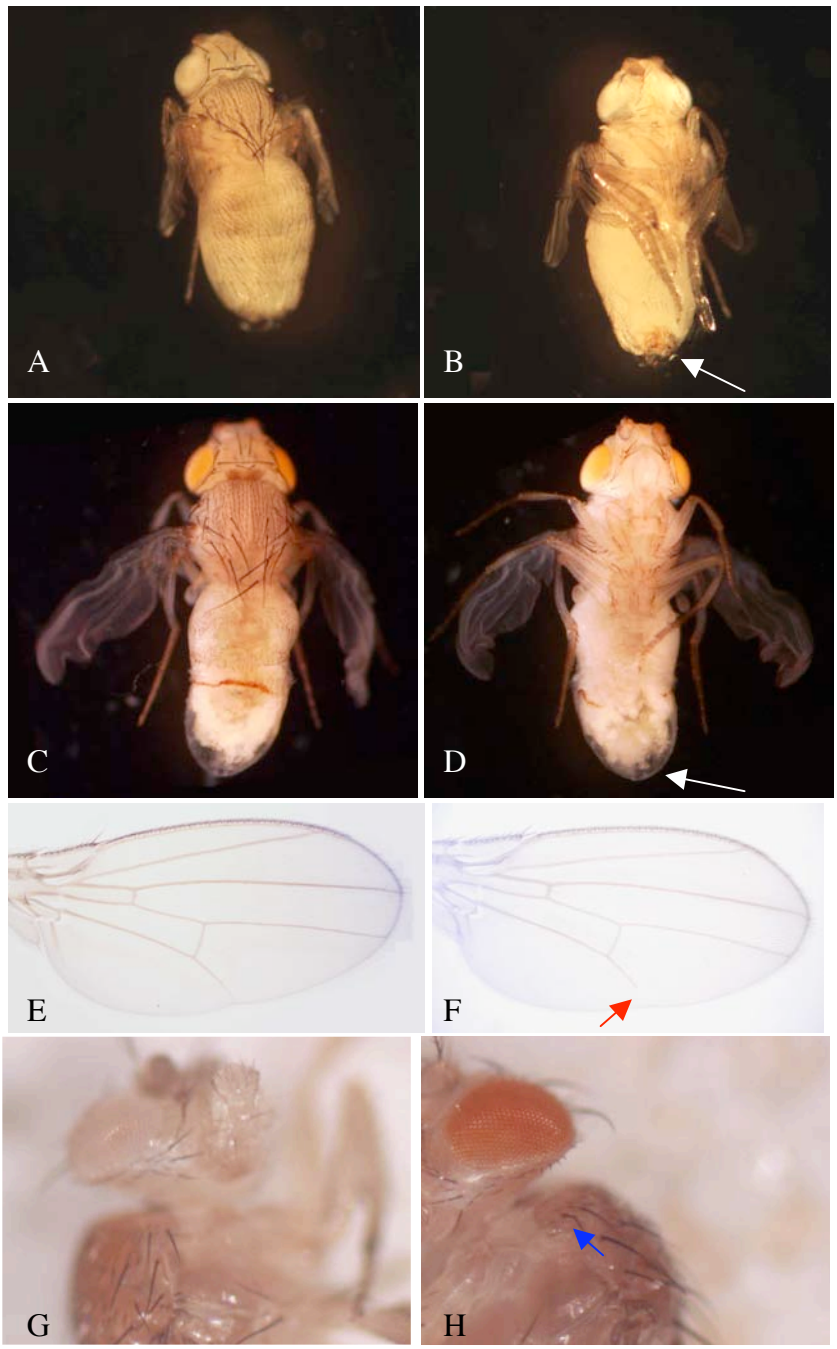

Figure 4.4 Phenotypes of *deflated* transheterozygotes.

(**A and B**) Wild type pharate adult showing normal tergite and external genital formation. (**C and D**) *defl*^{L}/*defl*^{Z} pharate adult showing abnormal abdominal development. In this particular case the formation of three anterior tergites occurred normally, but the posterior tergites did not develop. In all cases examined only between one and four of the abdominal segments ever formed and the external genitalia never formed (compare arrows in B and D). The differences seen in the wings between A and B and C and D is due to their preparation. The fly in A and B still has the transparent pupal cuticle intact holding the wings together, whereas the fly in C and D had this cuticle removed and the wings were free to spread out. (**E**) Wild type wing showing that all longitudinal veins reach the wing margin. (**F**) A *defl*^{P}/*defl*^{Z} wing showing that longitudinal vein L5 does not reach the wing margin (red arrow). (**G**) A wild type fly showing straight humeral bristles. (**H**) A *defl*^{P}/*defl*^{Z} showing a bent humeral bristle (blue arrow).

Attempts at establishing a stock from the transheterozygote adults proved unsuccessful. To explore this further, the fertility of the adult males and the few females was assessed by crossing them to wild type flies. Male transheterozygotes were able to produce offspring. Female transheterozygotes, on the other hand, showed reduced fertility. In these crosses, no larvae were observed in the vials. Females that had been crossed to wild type males were observed to lay eggs. Examination of these eggs revealed a high frequency of abnormal dorsal appendages and the chorion was thinner and more transparent than in wild type. The frequency of these defects were 40% from $defl^{P}/defl^{Z}$ mothers (224/557 eggs examined), 64% from $defl^{L}/defl^{Z}$ mothers (35/55, these numbers are comparatively lower because females escapees of this genotype were rare), and 7% from w^{1118} mothers (40/609; see Figure 4.5 for similar egg phenotypes from cDNA-rescued mothers). It is possible that the dorsal appendage and chorion defects are responsible for the infertility (Spradling, 1993). However, embryonic defects could not be ruled out as although a proportion of the eggs looked normal, the frequency of hatching was reduced (3% for $defl^{P}/defl^{Z}$ (4/121) compared to 87% for wild type (296/340)).

4.5 *deflated* homozygous lethality can be rescued by expression of wild type *deflated* cDNA

To ensure that the second instar lethality observed in homozygous *deflated* mutants was due to the small deletions in the *deflated* coding region and not to other lesions elsewhere on the chromosome, the ability of *deflated* cDNA to rescue the lethality was tested. The full length *deflated* cDNA (Berkely Drosophila Genome Project EST GH11567; Stapleton et al., 2002) was cloned into the P-element vector pUAST, downstream of the minimal Hsp70 promoter and Gal4 UAS elements present in this

vector (Section 2.16.1). Nine independent transgenic lines were generated by P-element transformation and the P[UAS-*defl*] transgenes were mapped to a chromosome by segregation analysis (Section 2.17). Four transgenes mapped to chromosome II and five transgenes mapped to chromosome III.

Three of the transgenes that mapped to the second chromosome (BA2, AV3 and BB1) were introduced into the $defl^{\Delta}$, $defl^{P}$, and $defl^{L}$ backgrounds. Stocks were established and, surprisingly, it was found that the cDNA was able to rescue the lethality in the absence of Gal4 induced expression. The level of rescue did depend on the transgenic line used, most likely reflecting differences in "leaky" expression of the cDNA in these transgenes modulated by chromosomal positioning (Table 4.1). $defl^{P}$ homozygous individuals were most easily rescued by cDNA expression. With P[UAS-*defl*]BB1, adults eclosed at the expected frequency and could be propagated as a healthy stock without the presence of the TM6B balancer. P[UAS-*defl*]BB1 could also rescue $defl^{L}$ homozygotes to adulthood, but at sub-mendelian ratios. P[UAS-*defl*]BB1 could not rescue $defl^{\Delta}$ homozygotes to adulthood. These individuals died as white pupae, most likely due to *nbs* loss of function caused by the deletion. Other *nbs* alleles also show lethality at the larval to pupal boundary (Yikang Rong, pers. comm.)

$defl^{L}/defl^{L}$ individuals partially rescued by P[UAS-*defl*] show both larval and adult phenotypes. Those partially rescued by P[UAS-*defl*]AV3 die at the larval/ pupal boundary and develop melanotic pseudotumours (Figure 4.5 B). Although the growth of these larvae did not appear to be any different from their heterozygous siblings, the imaginal discs were much smaller and almost unidentifiable in morphology and were very easily damaged during dissection (Figure 4.5 D and F).

Table 4.1 Rescue of *deflated* homozygous mutants by expression of wildtype *deflated* cDNA transgenes.

***defl* genotype**	***defl* cDNA transgene**[†]	**Lethal period**[§]
$defl^{L}/defl^{L}$	-	2nd instar larval
$defl^{P}/defl^{P}$	-	2nd instar larval
$defl^{\Delta}/defl^{\Delta}$	-	2nd instar larval
$defl^{L}/defl^{L}$	*P[UAS-defl]AV3*	3rd instar larval
$defl^{L}/defl^{L}$	*P[UAS-defl]BA2*	pupal
$defl^{P}/defl^{P}$	*P[UAS-defl]BA2*	pupal
$defl^{L}/defl^{L}$	*P[UAS-defl]BB1*	adult escapees, females infertile
$defl^{P}/defl^{P}$	*P[UAS-defl]BB1*	full rescue
$defl^{\Delta}/defl^{\Delta}$	*P[UAS-defl]BB1*	pupal

[†] All cDNA lines used contain the transgene on the 2nd chromosome.
[§] The lethal period is the stage at which the homozygous (non-tubby due to absence of TM6B) individuals die.

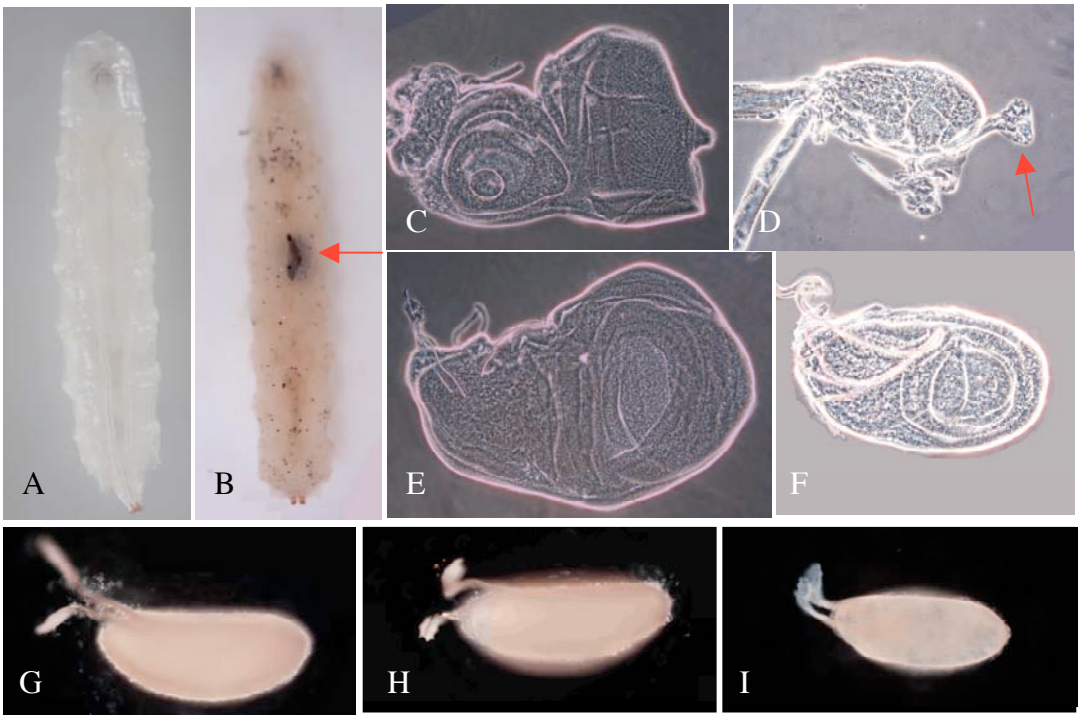

Figure 4.5 Phenotypes of *defl*^{L} homozygotes partially rescued by *deflated* cDNA expression.

(**A**) A wild type third instar larvae. (**B**) A *defl*^{L}/*defl*^{L} third instar larvae rescued by *P[UAS-defl]AV3* which displays a melanotic pseudotumour. (**C-F**) Third instar imaginal discs were dissected, fixed in 3.7% paraformaldeyde and mounted in 80% glycerol in PBS. All discs are at the same magnification. (**C and D**) Eye antennal imaginal discs orientated posterior to the right. (**E and F**) Wing imaginal disc. (**C and E**) Imaginal discs from *w*^{1118} third instar larvae. (**D and F**) Imaginal discs from *P[UAS-defl]AV3; defl*^{L}/*defl*^{L} third instar larvae. Larval tissue was kept intact at the anterior and posterior ends (red arrow indicates where the posterior end of the eye disc attaches to the optic lobe of the brain) in order to orientate the eye antennal disc correctly. (**G-I**) Phenotypes of eggs laid by *P[UAS-defl]BB1*;*defl*^{L}/*defl*^{L} mothers. (**G**) 16.8% (19/113) eggs laid had normal dorsal appendage formation and chorion thickness. (**H**) 38.9% (44/113) eggs had dorsal appendages that were shortened and looked like holly leaves. (**I**) 44.2% (50/113) of the eggs laid had abnormal dorsal appendages and thin chorions.

Like the transheterozygotes, escapee $defl^{L}/defl^{L}$ females rescued by P[UAS-*defl*]BB1 had reduced fertility due to dorsal appendage and chorion defects. Just fewer than 17% of the eggs laid by these mothers had normal morphology (Figure 4.5 G). Almost 39% had shortened dorsal appendages that looked more like holly leaves than long paddles (Figure 4.5 H). The majority (44%) were smaller, had thin chorions and dorsal appendages with holly leaf appearance or frayed edges (Figure 4.5 I).

4.6 Loss of wild type *deflated* results in defects in S- and M- phase entry

deflated is expressed in cells undergoing cell division and endoreplication and the phenotypes of mutants are consistent with it having a role in cell proliferation. However, the pleiotrophic nature of the phenotypes made assessment of *deflated's* precise role difficult. Evolutionary conserved co-expression with *Dp* and *Ctf4* suggests *deflated* plays a role in regulating S-phase. To assess the role of *deflated* in S-phase, second instar larval brains were dissected from wild type and mutant individuals and immunostained for bromodeoxyuridine (BrdU) incorporation. As homozygous *deflated* mutant larvae die before reaching the third instar larval stage, the second instar brains were chosed for examination of proliferation defects. Brains were dissected from active homozygous $defl^{L}$, $defl^{P}$, and w^{1118} second instar larvae and incubated with BrdU for 1 hr. BrdU is a nucleotide analogue that is incorporated into replicating DNA and is readily detected by immunofluorescence with the level of incorporation indicative of S-phase progression.

In these experiments, the pattern of S-phases detected in the second instar brains occurred in a random pattern (Figure 4.6 A), so each BrdU-positive focus was considered to be a single S-phase cell. The number of foci per brain was counted from

confocal images and this gave a measure of the number of cells in S-phase during the 1-hour labelling period. The 22 wild type, 21 $defl^{L}/defl^{L}$, and 21 $defl^{P}/defl^{P}$ brains examined displayed a wide range of BrdU-positive cells per brain (Figure 4.6 B). $defl^{L}$ homozygote brains showed the greatest range, with some brains having many more BrdU-positive cells than wild type brains but only having a slightly higher median, which was not statistically significant (p=0.3410, Mann-Whitney test). In comparison, $defl^{P}$ homozygote brains had a smaller range of BrdU-positive cells per brain and a smaller median than wild type, which was statistically significant (p=0.0241, Mann-Whitney test). Although preliminary, these data indicate that in the absence of wild type *deflated* protein cells in the brains are defective in regulating S-phase.

To examine whether the reduced S-phases observed in the $defl^{P}$ homozygous mutant brains led to a reduction in mitoses, brains were dissected from active homozygous $defl^{P}$, $defl^{L}$, and w^{1118} second instar larvae. After fixation, brains were immunostained with a phospho-histone H3 antibody to identify mitotic cells. Histone H3 is phosphorylated while chromosomes are condensed during mitosis and therefore anti-phospho-histone H3 provides a good marker for cells in mitosis. Sectioned confocal images were taken of 20 wild type, 20 $defl^{L}/defl^{L}$, and 19 $defl^{P}/defl^{P}$ brains to measure the total number of mitotic cells throughout the brain. These sectioned images were projected to form a single image so all mitotic cells could be quantified.

Like cells in S-phase, M-phase cells occurred in a random pattern in the second instar brains (Figure 4.6 C). Unlike S-phase, the range of M-phases in these brains was not as great, with the wild type brains showing the greatest variation in M-phase cells per brain. Furthermore, both mutant *deflated* genotypes showed a reduction in the median

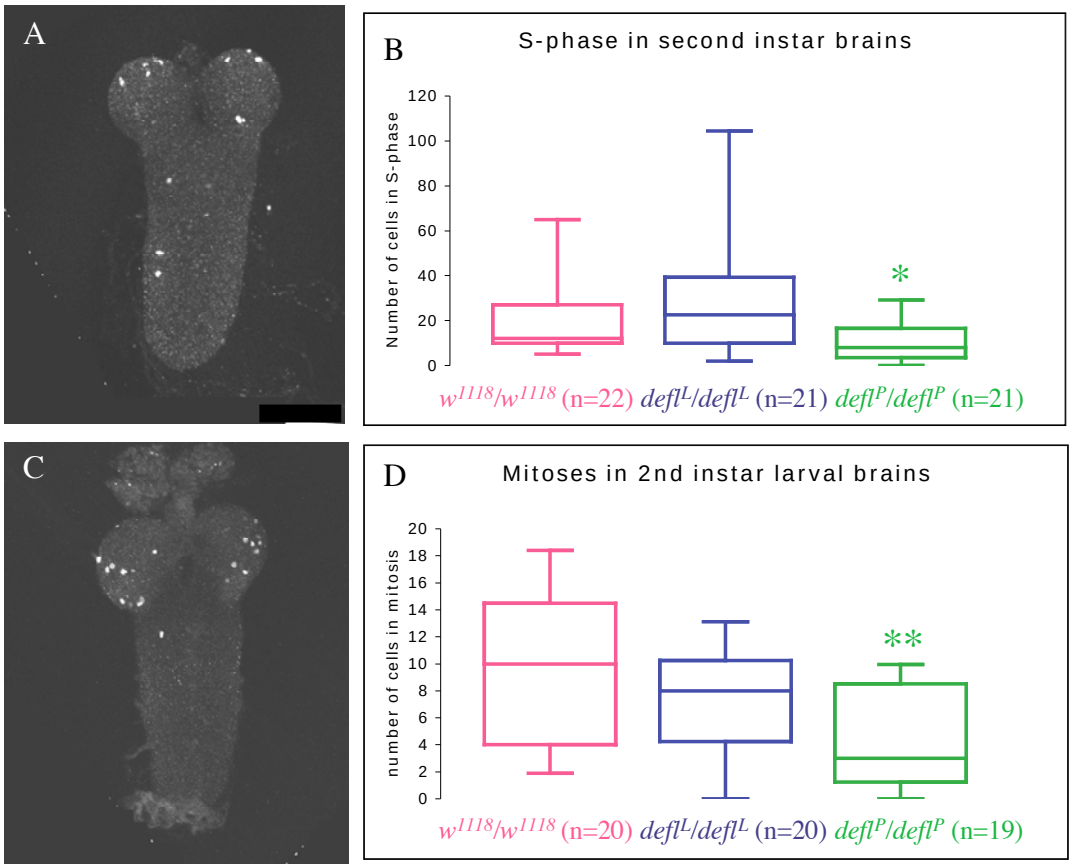

Figure 4.6 Cells in brains from homozygous *deflated* mutants show defects in cell cycle progression.

(**A**) Example of a second instar brain showing BrdU-positive cells detected by immunofluorescence. Brains were labelled with BrdU for 1 hr and detected with anti-BrdU antibody. (**B**) The number of BrdU-positive cells in 22 w^{1118}, 21 $defl^{L}/defl^{L}$, and 21 $defl^{P}/defl^{P}$ brains were counted and plotted as the number of foci per brain on box and whisker plots. The upper and lower ranges represent the 95th and 5th percentiles, the boxes the 75th and 25th percentiles and the line in the middle is the median. The median BrdU-positive cells $defl^{P}/defl^{P}$ brain differs significantly from wild type (*p=0.0241, Mann-Whitney test). The median for $defl^{L}/defl^{L}$ was not significantly different (p=0.3410, Mann-Whitney test). (**C**) Example of a second instar brain showing phospho-histone H3 positive mitotic cells. (**D**) The number of M-phase cells per brain were counted from 20 w^{1118}, 20 $defl^{L}/defl^{L}$, and 19 $defl^{P}/defl^{P}$ brains and plotted as for B. The difference in median of M-phase cells per brain was significant for $defl^{P}/defl^{P}$ when compared to the mean for wild type(**p=0.0056, Mann-Whitney test), whereas the median did not significantly differ for $defl^{L}/defl^{L}$ brains (p=0.2785, Mann-Whitney test).

of M-phases per brain compared to wild type. However, only the differences between wild type and $defl^{P}/defl^{P}$ brains were strongly significant (p=0.0056, compared with p=0.2785 for $defl^{L}/defl^{L}$, Mann-Whitney test). These preliminary studies indicate that cells in the $defl^{P}$ homozygous brain are not in M-phase as frequently as the cells in the wild type brain.

4.7 Discussion

Taken together, the RNA *in situ* hybridisation data and the phenotypes seen in *deflated* homozygotes, transheterozygotes, and cDNA-rescued homozygotes are mostly consistent with *deflated* having a role in the regulation of cell proliferation. The conserved protein motifs found in DEFLATED are also consistent with this role but indicate that the regulation affected by *deflated* may be indirectly acting to regulate the cell cycle.

4.7.1 DEFLATED contains conserved protein motifs found in proteins involved in diverse cellular processes

DEFLATED is highly conserved amongst metazoan species, thus implying that the cellular role it plays may be specific to multicellular organisms. This suggests that DEFLATED may be required for cell-cell communication or the coordination of cell proliferation with growth and differentiation. Amino acid conservation was highest in the N-terminus, which was identified has having multiple HEAT repeats. These repeats mediate protein-protein interactions and are found in many proteins, including those involved in cellular transport or cell signalling. Since 3-D modelling suggested that these repeats are most like those found in Ran binding proteins, it is possible that DEFLATED may also bind Ran and function within this pathway. Consistent with a

role for DEFLATED in regulating cell proliferation, the Ran pathway regulates nuclear import and export, mitotic spindle formation, nuclear envelope formation and cell cycle progression (Moore, 2001; Pemberton and Paschal, 2005).

Conserved motifs that were identified in DEFLATED included those found in proteins that are involved in regulating the cell cycle (a cyclin binding site and a Chk2 phosphorylation site), signalling cascades (proline directed kinase phosphorylation site), endocytosis (clathrin binding site and adaptor protein complex interaction sites), protein-protein interaction (14-3-3 binding site) and protein modification (SUMO modification site). Examined individually, these motifs do not provide an obvious function for *deflated.* Taken together, however, they suggest that *deflated* could be involved in a number of cellular processes. It is possible that some of these motifs are fortuitous, being only predicted by chance, and not biochemically functional. An examination of their physical interactions, through biochemical studies of DEFLATED or by yeast two hybrid analysis, would be required to establish their functionality.

4.7.2 When is *deflated* required throughout development?

Two sets of data provide insights into when *deflated* function is required throughout development. RNA *in situ* hybridisation showed that *deflated* is expressed in cells undergoing DNA replication in the post-blastoderm embryo. The lethality period of individuals lacking wild type *deflated* function and their rescue by minimal cDNA expression indicated that *deflated* is required at many stages throughout development.

Maternal mRNA expression of *deflated* was not detected, which indicates that there is either no maternal contribution, or that it is in the form of protein rather than RNA. This

indicates that *deflated* may not be required in the synchronous cell cycles of the syncytial and cellularised embryo. *deflated* expression was observed in the proliferating cells of the epidermis, and in the endoreplicating cells of the gut. *deflated* expression was found to no longer occur in the epidermis once proliferating cells arrest in G1 of cycle 17. Taken together, these expression patterns suggest that *deflated* is not required for cell proliferation *per se*. It may be required once cells have formed when there is developmental need for differential proliferation. Interestingly the pattern of *deflated* mRNA expression is very similar to those of E2F transcription targets such as *PCNA*, *Cyclin E,* and *RNR2* (Duronio et al., 1998; Royzman et al., 1997), suggesting that *deflated* may also be a target of E2F transcription. However, *deflated* or its orthologues have not yet been identified in microarray experiments designed to identify E2F targets (Dimova et al., 2003; Ishida et al., 2001; Muller et al., 2001; Ren et al., 2002; Young et al., 2003).

The expression levels of *deflated* detected in embryos were low, which suggests that *deflated* is only required at low levels at this stage of development. This is consistent with developmental microarray data, which showed that *deflated* expression was never outside a two-fold range in difference and that maximal expression occurred in late embryogenesis and during pupariation (Arbeitman et al., 2002). The low level requirement of *deflated* expression in embryos is also consistent with the cDNA rescue experiments, where it was found that sufficient expression of the P[*UAS-defl*] transgene occurred to allow full development in the absence of Gal4. These data also show that *deflated* is required post-embryonically for proper larval and imaginal disc growth and morphogenesis, as well as for adult abdominal, wing, bristle, and egg development.

4.7.3 Phenotypes of *deflated* mutants phenocopy *E2f/Dp/Rbf* mutants

The products of the *E2f1*, *Dp*, *Rbf*, and *Cyclin E* genes are all required to control entry into S-phase during development, including the endoreplication of larval and ovarian cells (Section 1.3). Individual flies lacking these gene products show pleiotrophic phenotypes due to their inability to correctly regulate S-phase. These phenotypes are very similar to those observed in *deflated* mutants. A majority of *Dp* homozygous mutants die as pupae with abdominal defects. *E2f1* homozygous mutants die at the third instar/pupal boundary, and both develop melanotic tumours (Royzman et al., 1997). *E2f1* homozygous individuals grow slowly and have small imaginal discs. Weak alleles and germline clones of both *Dp* and *E2f1* are female sterile due to chorion defects (Myster et al., 2000; Royzman et al., 1999; Royzman et al., 2002; Royzman et al., 1997). *Rbf* null mutants die as early larvae (Du, 2000) and weak alleles are female sterile (Bosco et al., 2001). *E2f2* mutants are viable but female sterile due to chorion defects that are very similar to what is seen in *deflated* mutants (Cayirlioglu et al., 2001; Frolov et al., 2001).

Homozygous *deflated* mutants die at the second instar larval stage. This lethality could be due to two different defects. *deflated* is likely to be required for endoreplication as its high expression in embryonic gut cells shows. Therefore, larvae fail to grow in the absence of proper endoreplication and subsequently die. Alternatively, death at the second instar larval stage may be due to defects occurring earlier in life that manifest their effects at a later stage. *deflated* mRNA is expressed in the proliferating nervous system, which suggests that it may be required for its correct development. If the correct number of neurons or their specification does not occur correctly it is possible that the effects will not be observed until later. The abnormal behaviour of the larvae

before death could support either alternative. If endoreplication of the salivary gland does not occur, the larvae cannot feed properly and will become sluggish. The abnormal larval behaviour of leaving the food and becoming sluggish could also be due to abnormal neural function. Therefore, further work will be required to distinguish between these alternatives.

Other *deflated* larval phenotypes could also be consistent with a role for *deflated* in regulating cell proliferation. Small and malformed imaginal discs occur in $defl^{L}$ homozygotes that are partially rescued by the *deflated* cDNA transgenic line AV3. This disc phenotype is very likely due to an inability of the cells to proliferate. These third instar larvae also show the formation of melanotic pseudotumours. Pseudotumours form from haemocytes produced in response to abnormal cells, including those cells that display abnormal development (Sparrow, 1978). Therefore the presence of melanotic tumours in *deflated*, *E2f1*, and *Dp* mutant larvae indicate that abnormal development has occurred. In the case of *E2f1*, these tumours are suppressed by loss of *E2f2* (Frolov et al., 2001), which suggests that the causative factor is E2f2 activity in the absence of E2f1.

The E2f-Dp-Rbf network also has roles in controlling endoreplication and chorion gene amplification in follicle cells during oogenesis. When follicle cells fail to undergo the correct number of endocycles and gene amplification cycles, they cannot produce enough chorion, as seen in *Dp*, *E2f1,* and *E2f2* loss of function mutants, or they produce too much chorion as seen in *Rbf* loss of function and *E2f1* gain of function mutants (Bosco et al., 2001; Royzman et al., 1999). The fact that *deflated* mutant females lay

eggs with a thin chorion implies that wild type *deflated* has a positive role in the regulation of endoreplication and gene amplification.

4.7.4 *deflated* mutants phenocopy other cell proliferation regulators

A number of *deflated* phenotypes observed are less like mutants of the *E2f/Dp/Rbf* pathway and more like those observed for other cell proliferation regulators, including genes that regulate M-phase or signal to the cell cycle.

Abdominal defects were observed in *Dp* mutants but they are also observed in *myc*, *cdc2*, and *esg* mutants (Section 1.3.4). Mutant individuals have abnormal abdomens, which do form all tergites and adult cuticle but are small, malformed and lack hairs, bristles, and pigment (Fung et al., 2002; Hayashi et al., 1993; Stern et al., 1993). These mutant phenotypes are slightly different from those seen in *deflated* transheterozygotes (Figure 4.4), but are likely to arise from similar cellular defects.

The abdomen is the last adult structure to form during fly development (Fristrom and Fristrom, 1993; Madhavan and Madhavan, 1980). Like all cells that form the adult structures, the cells that are to become the abdomen are determined during embryogenesis. These cells are known as abdominal histoblast nests and they do not begin to proliferate or differentiate until the pupal stage. During the larval stages these groups of cells are arrested in G2. The abnormal abdomens observed in *myc*, *cdc2,* and *esg* mutants are caused by loss of the G2 arrest allowing entry into an endocycle program. This causes a shortage of cells when the abdominal cells differentiate, resulting in the defects observed. Unlike *deflated* mutants, *myc, cdc2* and *esg* mutants develop normal external genitalia, since the most posterior segment arises from the

genital imaginal disc and thus would not undergo improper endoreplication because imaginal disc cells do not arrest in an extended G2.

One explanation for the abdominal phenotype in the *deflated* mutants is an inability of the histoblast nest cells to correctly maintain a G2 arrest. Alternatively, the posterior segments are unable to differentiate. The absence of genitals suggests that the genital imaginal disc does not proliferate or differentiate properly. Taken together, all the phenotypic data suggest that the defects observed are due to the failure to meet a minimum threshold of functional DEFLATED protein. In some cases function may be sufficient for larval growth but not imaginal disc proliferation. In other cases sufficient function may be present to allow for development almost to adulthood, but is titrated out prior to development of the abdomen and genitals. In others, adults can develop but females do not have enough functional protein to make normal eggs.

4.7.5 The wing and bristle defect observed in *deflated* transheterozygotes suggest defects in cell signalling or the cytoskeleton

Adult transheterozygotes that eclose are almost normal in their morphology, except for having minor wing and bristle defects. The shortened L5 vein and the bent humeral bristles are difficult to explain by defects in cell proliferation and may indicate defects in cell signalling or cytoskeletal regulation, respectively. Wing vein differentiation and development is under the control of many signalling pathways including Dpp, EGFR, Hedgehog, Notch, and Wingless (de Celis, 2003). Therefore, the defect in L5 length in *deflated* transheterozygotes may result from a defect in the ability to signal that these cells should differentiate into veins. Bristle growth is due to growth of actin filaments pushing the plasma membrane out. This growth is also controlled by the microtubule

cytoskeleton (Fei et al., 2002; Tilney et al., 2004). Therefore, the bent bristle defect seen in the *deflated* transheterozygotes could be due to a misregulation of normal cytoskeletal growth. Whether these defects are direct of indirect consequences of reduced DEFLATED function will require further investigation.

4.7.6 A role for *deflated* in regulating S- and M- phase?

The phenotypes observed in *deflated* mutants are very similar to those seen in *E2f1*, *Dp* and *Rbf* mutants, which suggests a role for *deflated* in S-phase regulation. Working on the assumption that these phenotypes map to the *deflated* locus, it was found that brains from homozygous $defl^{P}$ larvae showed a significant decrease in the number of cells in S-phase compared to wild type, which indicates that they were not entering S-phase at the same rate. Brains from $defl^{L}$ homozygous individuals did show slightly more S-phases per brain than wild type, which indicates that the cells were either entering S-phase inappropriately or they had a prolonged S-phase. The latter is unlikely as the intensity of labelling was approximately the same for all the genotypes tested. If the rate of DNA synthesis was reduced then the amount of BrdU incorporated would also be reduced, resulting in weaker staining. These data show that the $defl^{L}$ and $defl^{P}$ alleles can be distinguished at the cellular level.

Unlike S-phases, brains from individuals homozygous for either $defl^{L}$ or $defl^{P}$ mutation contained less M-phases than wild type. For $defl^{P}$ it could be argued that the decrease in S-phase cells would mean that cells that had failed to complete DNA replication and consequently may not be able to enter M-phase. However, one interpretation could be that as the differences in M-phases per brain are greater than the differences in S-phases (as compared to wild type) it is possible that the $defl^{P}$ allele is also affecting M-phase

entry in addition to S-phase entry. On the other hand, *defl*^{L} seems to cause inappropriate entry into S-phase in a small number of brains, but a slight decrease of cells in M-phase in all brains, which suggests that this allele may also have a defect in M-phase entry.

However, *deflated's* role seems to be broader than that implied by the co-expression correlation (Stuart et al, 2003). While *deflated* mutant phenotypes do phenocopy those of the Dp-E2f-Rbf S-phase regulatory network, loss of wild type function may affect the ability of cells in the brain to enter both S- and M-phase independently. The protein sequence is also suggestive of a broader role, as although DEFLATED contains motifs that are found in other cell cycle proteins, it also contains motifs that are found in cell signalling and transport. The minor wing and bristle defects observed in adult *deflated* transheterozygotes are also suggestive of a broader role. From these data it appears that *deflated* may have a role in regulating cell proliferation and possibly in cell signalling.